



# UNIVERSITA' DEGLI STUDI DI VERONA

*DEPARTMENT OF BIOTECHNOLOGY*

*GRADUATE SCHOOL OF NATURAL AND ENGINEERING  
SCIENCES*

*DOCTORAL PROGRAM IN BIOTECHNOLOGY*

CYCLE XXXVI

TITLE OF THE DOCTORAL THESIS

**Investigation of the potential of new microorganisms and  
their derivatives as novel biostimulants**

S.S.D. BIO/19

Coordinator: Professor Matteo Ballottari

Tutor: Prof.ssa Silvia Lampis

Co-Tutor: Prof.ssa Giovanna Felis




Industrial Supervisor: Juan Fernando Mejia

Doctoral Student: Dott.ssa Ilaria Lebano

This work is licensed under a Creative Commons Attribution- Non Commercial- No Derivs 3.0 Unported License, Italy.

To read a copy of the licence, visit the web page:

<http://creativecommons.org/licenses/by-nc-nd/3.0/>

-  **Attribution** — You must give appropriate credit, provide a link to the license, and indicate if changes were made. You may do so in any reasonable manner, but not in any way that suggests the licensor endorses you or your use.
-  **Non Commercial** — You may not use the material for commercial purposes.
-  **No Derivatives** — If you remix, transform, or build upon the material, you may not distribute the modified material.

*Investigation of the potential of new microorganisms and  
their derivatives as novel biostimulants*

Ilaria Lebano

PhD thesis

Verona, 4 April 2024

*Il vero coraggio è come un aquilone:  
il vento contrario lo solleva più in alto.*

-Jean Antoine Petit-Senn

## **Ringraziamenti**

Desidero esprimere la mia profonda gratitudine a tutte le persone che hanno contribuito al completamento di questo percorso accademico e di ricerca.

Innanzitutto, desidero ringraziare la mia stimata tutor, la Professoressa Silvia Lampis, e co-tutor, la Professoressa Giovanna Felis, per la loro guida sagace e il loro incoraggiamento costante. Le loro competenze e il loro supporto hanno non solo notevolmente arricchito il mio percorso di dottorato, ma anche trasformato l'esperienza in qualcosa di stimolante e arricchente.

Un ringraziamento speciale va a tutti i colleghi della mia azienda, incluso il nostro direttore di ricerca Alberto Piaggese e il mio tutor Juan Fernando Mejia, per aver creduto in me e per avermi aiutato a intraprendere questo percorso. Ho apprezzato profondamente il vostro tempo, le critiche costruttive e l'interesse dimostrato nel mio lavoro di ricerca.

Non posso trascurare di esprimere la mia gratitudine ai miei stimati colleghi di laboratorio, con i quali ho condiviso sfide e successi. Il vostro spirito collaborativo ha arricchito e reso più stimolante questa esperienza.

Un grazie sentito va a mia madre e mia sorella, per il loro sostegno incondizionato e per avermi sempre incoraggiato, anche nei momenti più impegnativi.

In un toccante omaggio, dedico questo risultato alla memoria della Prof.ssa Carrì, la mia mentore, figura fondamentale nel mio percorso accademico e personale. I suoi insegnamenti sono stati il faro guida di tutto questo percorso.

Infine, dedico questo traguardo al mio amato marito, che con amore, sacrificio, comprensione e pazienza ha reso possibile ogni mio passo. Questo successo è frutto della nostra collaborazione, e la nostra unione è stata la chiave di ogni conquista.

Grazie di cuore a tutti coloro che hanno reso possibile questo viaggio.  
La vostra presenza e il vostro sostegno hanno reso questa impresa non solo accademica, ma anche umanamente significativa.

*Ilaria Lebano*

Lanciano, 12/2023

## **Acknowledgements**

I would like to express my deep gratitude to all the people who have contributed to the completion of this academic and research journey.

First and foremost, I would like to thank my esteemed supervisor, Professor Silvia Lampis, and co-supervisor, Professor Giovanna Felis, for their insightful guidance, constant encouragement, and infinite patience. Their expertise and support have not only significantly enriched my doctoral journey but also transformed the experience into something stimulating and enriching.

A special thanks goes to all my colleagues at work, including my director Alberto Piaggese and my mentor Juan Fernando Mejia, for believing in me and helping me on this journey. I deeply appreciate their time, constructive feedback and interest in my research.

I cannot overlook expressing my gratitude to my esteemed laboratory colleagues with whom I have shared challenges and successes. Your collaborative spirit has enriched and made this journey more stimulating.

A heartfelt thanks go to my family, especially my mother and sister, for their unwavering support and always encouraging me, even in the most challenging moments.

In a touching tribute, I dedicate this achievement to the memory of Professor Maria Teresa Carri, my mentor, a key figure in my academic and personal journey. Her teachings have been the guiding beacon in this journey.

Finally, I dedicate this achievement to my beloved husband, who with love, sacrifice, understanding, and patience has made every step of my journey possible. This success is the result of our collaboration, and our union has been the key to every accomplishment.

From the bottom of my heart, I thank all those who have made this experience possible. Your presence and support have made this endeavour not only academic but also significantly relevant on a human level.

*Ilaria Lebano*

Lanciano, 12/2023

## **Sommario**

Il continuo aumento della popolazione mondiale, unito alla crescente domanda di cibo, ha spinto i sistemi agricoli tradizionali a dipendere fortemente dai fertilizzanti chimici per migliorare la resa delle produzioni. Le preoccupazioni legate all'esaurimento delle riserve di petrolio necessarie per la sintesi di fertilizzanti inorganici, al dilavamento dei fertilizzanti chimici azotati nel terreno, alla diminuzione della fertilità del suolo e ai cambiamenti climatici hanno spinto le organizzazioni mondiali a promuovere pratiche più sostenibili. L'Organizzazione delle Nazioni Unite per l'Alimentazione e l'Agricoltura (FAO), il Green Deal della Commissione Europea e varie istituzioni accademiche come l'Accademia Nazionale delle Scienze, stanno promuovendo l'adozione di strumenti innovativi e sostenibili per integrare i metodi agricoli esistenti e garantire l'approvvigionamento alimentare globale.

Tra le soluzioni proposte ci sono i biostimolanti vegetali (PBS), considerati strumenti innovativi ed complementari per affrontare le sfide agricole attuali e future. I PBS, che possono includere sostanze biologiche (BS) e/o batteri benefici, offrono un approccio sostenibile per migliorare il rendimento delle colture, la loro produttività e resistenza agli stress ambientali.

In questo contesto di crescente interesse per i PBS microbici, una sfida importante è l'identificazione di candidati microbici efficaci e idonei per lo sviluppo di prodotti commerciali.

Questo progetto di dottorato mira a stabilire un flusso di lavoro sistematico e graduale per selezionare i candidati microbici più promettenti come agenti attivi nello sviluppo di PBS. L'efficacia di questo processo è stata valutata utilizzando un pool di 17 ceppi batterici isolati da diverse colture.

In dettaglio, questo processo di selezione include criteri critici, tra cui i) identificazione microbica, ii) considerazioni di biosicurezza relativamente alle specie microbiche oggetto dello studio, iii)



conformità di queste con la normativa dei biostimolanti, iv) valutazione dell'attività antagonista microbica e v) valutazione dei tratti di promozione della crescita delle piante. I ceppi ritenuti idonei per questa prima valutazione e con significativi tratti di promozione per la crescita delle piante, sono stati sottoposti a ulteriori test sulla pianta modello *A. thaliana* e sul peperone (*C. annuum*) come coltura agronomica rappresentativa. L'obiettivo è stato quello di convalidare i risultati osservati *in vitro* sulla promozione di crescita delle piante e procedere con la selezione finale dei migliori ceppi microbici.

Durante questa esplorazione, è stata esaminata anche la compatibilità tra i ceppi microbici selezionati e le comuni sostanze biologiche tipicamente utilizzate nelle formulazioni dei PBS, con l'obiettivo di sfruttare, oltre al potenziale microbico, le sinergie risultanti dalla combinazione dei due componenti.

Fondamentale per l'attuazione del flusso di lavoro sopra descritto è stata l'esplorazione e l'adozione della MALDI-TOF MS come tecnologia veloce e affidabile per supportare la fase di identificazione microbica. Inoltre, l'applicabilità di questo strumento è stato ulteriormente esplorato da uno studio parallelo che esaminava l'uso dell'analisi proteomica accoppiata a metodi statistici per prevedere ed esplorare differenze tra ceppi strettamente correlati e il suo potenziale applicativo in grandi dataset microbici.

In conclusione, integrando metodi robusti e affidabili di identificazione, tipizzazione microbica, criteri multifunzionali che affrontano gli aspetti di biosicurezza e regolamentari, valutazione dei tratti di promozione della crescita delle piante e esplorazione delle potenziali sinergie microbiche, l'approccio proposto in questo studio mira non solo a semplificare il processo di sviluppo dei PBS, ma anche a facilitare la messa in commercio di soluzioni efficaci e sostenibili.

Keywords: Biosicurezza, Biostimolanti vegetali, Candidati microbici, Conformità normativa, Identificazione, MALDI-TOF MS, Potenziamento del rendimento delle colture, Sostenibilità agricola, Tipizzazione.

## **Abstract**

The continuously growing global population, coupled with an increasing demand for food, has driven traditional agricultural systems to depend heavily on chemical fertilizers to improve yields. Concerns about the depletion of petroleum reserves needed to produce inorganic fertilizers, the runoff of chemical nitrogen fertilizers into the soil, declining soil fertility, and climate change have prompted global organizations to promote more sustainable practices. The Food and Agriculture Organization of the United Nations (FAO), the European Commission's Green Deal, and various academic institutions such as the National Academy of Sciences are promoting the adoption of innovative and sustainable tools to complement existing agricultural methods and secure global food supply.

Among these solutions are plant biostimulants (PBS), which are gaining traction as innovative and complementary tools to address current and future agricultural challenges. PBS, which can include biological substances (BSs) and/or beneficial microorganisms, offer a sustainable and environmentally friendly approach to improving crop yield, productivity, quality, and tolerance to abiotic stresses.

Although interest in microbial PBS is growing, one major challenge is identifying effective and suitable microbial candidates for commercial products. This PhD project aims to establish a systematic and stepwise workflow to select the most promising microbial candidates to promote plants as active agents for PBS development. The effectiveness of this process was evaluated using a pool of 17 bacterial strains isolated from various cultures. In more detail, this comprehensive process includes critical criteria, such as i) initial identification, ii) biosafety considerations, iii) PBS regulatory compliance, iv) evaluation of antagonistic activity, and v) evaluation of plant growth-promoting traits. Strains found suitable for this first evaluation, exhibiting significant plant growth-promoting (PGP) traits, underwent further testing on the model plant *A. thaliana* and pepper

(*C. annuum*) as a representative crop. This aimed to validate the results observed *in vitro* on plant growth promotion and proceed with the final selection of the best microbial strains. During this exploration, the compatibility between the selected microbial strains and common BSs typically used in PBS formulations was also examined, with the goal of leveraging, besides the potential of the selected candidates, the synergies resulting from the combination of the two components.

Critical for implementing the above-described workflow has been the exploration and the adoption of MALDI-TOF MS as a fast and reliable technology to support the microbial identification step. In addition, the applicability of this tool was further investigated by a parallel study examining the use of proteomic analysis coupled with statistical methods to predict and explore differences between closely related strains and its potential application in large microbial datasets.

In conclusion, by incorporating robust and reliable microbial identification and typing methods, multifaceted criteria that address biosafety and regulatory aspects, evaluation of plant growth-promoting traits, and exploration of potential synergies to enhance microbial activity, the approach proposed in this study aims not only to simplify the PBS development process but also to facilitate the release of effective and sustainable solutions.

Keywords: Agricultural sustainability, Biosafety, Crop yield enhancement, Identification, MALDI-TOF MS, Microbial candidates, Plant biostimulants, Regulatory compliance, Typing.



## Contents

List of Figures .....	xiv
List of Tables.....	xvi
Acronyms .....	xviii
<b>Chapter 1.....</b>	<b>1</b>
<b>Introduction .....</b>	<b>1</b>
References .....	6
<b>Chapter 2.....</b>	<b>8</b>
<b>MALDI-TOF as a powerful tool for identifying and differentiating closely related microorganisms: the strange case of three reference strains of <i>Paenibacillus polymyxa</i>.....</b>	<b>8</b>
2.1 Abstract .....	9
2.2 Introduction .....	10
2.3 Results .....	12
2.3.1 MALDI-TOF MS identification results .....	12
2.3.2 Mass data statistical analysis results and in-house database implementation with DSM 292 and DSM 365 profiles. ....	14
2.3.3 16S rRNA sequence retrieving from genomes and comparison .....	20
2.3.4 Genome comparison results .....	20
2.3.5 Phenotypical test (API) and fatty acids cellular composition results ...	21
2.4 Discussion.....	24
2.5 Methods .....	29
2.5.1 Strain culture condition .....	29
2.5.2 MALDI-TOF MS analysis: sample preparation and identification .....	30
2.5.3 Statistical analysis of mass spectra .....	31
2.5.4 16S rRNA sequence analysis.....	33
2.5.5 Comparative genomics.....	34
2.5.6 Phenotypical test and fatty acids cellular composition profiles .....	34
References .....	35
Supplementary material .....	41
<b>Chapter 3.....</b>	<b>50</b>

<b>A Systematic Framework for the Selection of Plant-Growth Promoting Microbial Candidates in Biostimulant Development: from Identification to <i>in vitro</i> Evaluation</b> .....	<b>50</b>
3.1 Abstract .....	51
3.2 Introduction .....	51
3.3 Methods .....	55
3.3.1 Bacteria and culture conditions .....	55
3.3.2 Microbial culture identification and data processing by MALDI-TOF MS .....	55
3.3.3 Identification of bacterial isolates by 16S rDNA .....	57
3.3.4 Identification with additional markers ( <i>gapA</i> , <i>pgk</i> , <i>uvrA</i> , <i>purH</i> ).....	57
3.3.5 Bioinformatic analysis of 16S rRNA and protein-coding genetic markers .....	58
3.3.6 Comparative genomics .....	58
3.3.7 Biosafety evaluation and bio-pesticide databases assessment.....	59
3.3.8 Kinetic studies .....	59
3.3.9 <i>In vitro</i> bacterial antagonism evaluation .....	60
3.3.10 Bacterial antagonism evaluation on <i>S. lycopersicum</i> .....	62
3.3.11 Strains characterisation for plant growth-promoting activities .....	62
3.3.12 Statistical analysis .....	66
3.4 Results .....	67
3.4.1 Bacterial cultures identification by MALDI-TOF MS .....	67
3.4.2 Bacterial culture identifications by genetic analysis.....	67
3.4.3 Biosafety evaluation and bio-pesticide databases assessment.....	69
3.4.4 Kinetic performance.....	70
3.4.5 <i>In vitro</i> bacterial antagonism evaluation .....	70
3.4.6 Bacterial antagonism evaluation on <i>S. lycopersicum</i> .....	70
3.4.7 Screening for PGP activities.....	71
3.5 Discussion.....	73
References .....	87
<b>Chapter 4.....</b>	<b>99</b>
<b>Unraveling the Potential of Synergistic Interactions in Microbial Biostimulants.....</b>	<b>99</b>
4.1 Abstract .....	100
4.2 Introduction .....	101
4.3 Methods .....	104
4.3.2 Effects of BSs on microbial growth <i>in vitro</i> .....	104



4.3.3	<i>In vitro</i> treatment on <i>A. thaliana</i> .....	105
4.3.4	Plant Assay Treatment Data Collection .....	106
4.3.6	Statistical analyses .....	107
4.4	Results .....	108
4.4.1	Microbial growth assessment through impedance flow cytometry ....	108
4.4.2	<i>In vitro</i> compatibility with BSs .....	109
4.4.3	<i>In vitro</i> treatment on <i>A. thaliana</i> .....	111
4.4.4	Greenhouse experiment on pepper .....	112
4.5	Discussion.....	117
	References .....	121
	<b>Chapter 5</b> .....	<b>125</b>
	<b>Conclusions</b> .....	<b>125</b>

## List of Figures

- Figure 2.1.** Graphical representation of *P. polymyxa* identification by MALDI Biotyper Software. The colour of the peaks reflects the degree of matching of (a) ATCC 842<sup>T</sup>, (b) (c) DSM 292, and (d) (e) DSM 365 with the reference MSPs (green = full match, yellow = partial match and red = mismatched) reported in the lower part of the graphs (blue spectra). ..... 133
- Figure 2.2.** (a) Pseudo-gel like view of ATCC 842<sup>T</sup> (red), DSM 292 (green) and DSM 365 (blue) mass spectra (15 replicates per class) displayed on a rainbow scale. The peak intensity is reported on y-axis in arbitrary units; 2-D PCA (b) and Loadings of 2D-PCA (c) plots of ATCC 842<sup>T</sup> (red), DSM 292 (green) and DSM 365 (blue). ..... 166
- Figure 2.3.** Average spectra of the most characteristic peaks among *P. polymyxa* strains. Intensities of characteristic peaks in ATCC 842<sup>T</sup> (red), DSM 292 (green) and DSM 365 (blue) are shown on y-axis and expressed in arbitrary intensity units. .... 177
- Figure 2.4.** 2D scatter plots of characteristic peaks for ATCC 842<sup>T</sup> (red), DSM 292 (green) and DSM 365 (blue) selected by QC and SNN classification models. (a) Scatter plots of peaks 2,944 and 3,314 Da (selected by the QC model) and (b) 5,504 and 9,492 Da (selected by the SNN model). The intensities of peaks were expressed in arbitrary intensity units and served as y-axis. The ellipses represent the 95% confidence intervals of peak intensity for each strain. .... 177
- Figure 3.1.** PCA of the seventeen bacterial cultures. .... 83
- Figure 3.2.** Antagonistic activity results of bacterial cultures against *R. solani* V1, *F. culmorum* V2, *B. cinerea* V3 (A) and *X. campestris* V4 (B) in vitro and PIRG (%) interpretation (A): PIRG ≤ 50%: low, 50% < PIRG ≤ 60%: medium, 60% < PIRG ≤ 75%: high, PIRG > 75%: very high. Drop method interpretation (B): inhibition zone > to 25 mm: very strong (++++), inhibition zone from 15 to 25 mm: strong (+++), inhibition zone from 7 to 15 mm: moderate (++) , inhibition zone < 7 mm: weak activity (+) and inhibition zone = 0: no activity (-). Error bars show standard deviation. Data were subjected to analysis of variance (ANOVA) (n=3). Different letters indicate significant differences among treatments according to LSD's test ( $\alpha = 0.05$ ). .... 84
- Figure 3.3.** P-solubilization assay on solid medium (A); P-solubilization liquid assay (B); CMC degrading Index (C), IAA production (D), Protease assay (E) and Biofilm production (F) in TSB and SBOG after 48 hours at 30°C. Error bars show standard deviation. Data were subjected to analysis of variance (ANOVA) (n=3). Different letters indicate significant differences among treatments according to LSD's test ( $\alpha = 0.05$ ). .... 85
- Figure 3.4.** A) Frequency growth distribution of the eight strains tested in LGI, NFM, and SYP solid media after 24 h incubation at 30°C; B) Strains 11, 12 and 13 growth on LGI, NFM, and SYP solid media in Petri-dish plates after 34h incubation at 30°C; C) Interaction of strains and media on OD600nm\_MAX in LGI, NFM, SYP, and TSB liquid media after 24 h incubation at 30°C; D) Ammonia production as NH<sub>4</sub>Cl ( $\mu$ M) release by strains 11, 12, and 13 in LGI, NFM, and SYP liquid media after 24h incubation at 30°C in a low oxygen atmosphere (O<sub>2</sub> < 0.1%). Error bars show standard deviation. Data were subjected to analysis of variance (ANOVA) (n=3). Different letters indicate significant differences among treatments according to LSD's test ( $\alpha = 0.05$ ). .... 86
- Figure 4.1.** Kinetic curves of strains 11, 12, and 13 in TSB medium for 24 hours. Cell viability at each time point (0, 4, 8, and 24 hours) was determined by plate counts (CFU/ml) and by IFC (ICC) using the BactoBox® device. .... 109

**Figure 4.2.** Effect of BSs 1, 2, and 3 on the growth of strains 11 (A), 12 (B), and 13 (C) after 6 h of incubation. Positive control: inoculated TSB without BSs (0 ppm). Vertical bars denote 0.95 confidence intervals. Two-way ANOVA with Fisher's LSD test was performed for data analysis. Different letters represent significant differences between treatments ( $p < 0.05$ ). Fluorescence microscopy of strain 11 inoculated with BS 1 (D) and strains 12 (E) and 13 (F) inoculated with BS 3. Green cells indicate living cells. Scale bar 1000  $\mu\text{m}$ .....112

**Figure 4.3.** Effect of BSs 1, 2, and 3 (A, B, C) and strains 11, 12 and 13 (D, E, F) on *A. thaliana*. Shoot biomass (A; D), total root length (B; E), and root area (C; F) were evaluated 7 days after treatments. Mean and standard error values from 20 replicates are represented for each treatment. Different letters represent significant differences between treatments according to the Student-Newman-Keuls (SNK) test ( $p < 0.05$ ). .....113

**Figure 4.4.** Effect of combination of strain 13 with BS 3 on *A. thaliana*. Image acquisition took by EPSON scanner 14 days post-inoculation (I). Shoot biomass (II, A), total root length (II, B), and root surface area (II, C) were evaluated 7 days after treatments. Mean and standard error values from 20 replicates are represented for each treatment. Different letters represent significant differences between treatments according to Student-Newman-Keuls (SNK) test ( $p < 0.05$ ).....114

**Figure 4.5.** Plant growth-promoting effects of strains 11, 12, and 13 under greenhouse conditions (positive control: plant biostimulant B3-2642). Shoot biomass (A), shoot height (B), and root weight (C) were evaluated 14 days after the third treatment. Mean and standard error values for fifteen replicates are represented for each treatment. Different letters indicate significant differences according to Duncan's test ( $p < 0.05$ ).....115

**Figure S 2.1.** Vegetative cells and endospore observation of (a) ATCC 842<sup>T</sup>, (b) DSM 292 and (c) DSM 365. The strains were grown at 28°C on M220 medium supplemented with MnSO<sub>4</sub> for 48 hours. Samples were examined by Axio Scope.A1 microscope (Zeiss) with objective oil len 100X. Pictures were made with Axio Cam MRc Zeiss using the Axiovision Rel 4.8. software. Scale bars represent 5  $\mu\text{m}$ .....41

**Figure S 2.2.** Three- and two-dimensional principal component analysis and respective loadings plots of *P. polymyxa* ATCC 842<sup>T</sup> (red), DSM 292 (green), and DSM 365 (blue) strains.....41

**Figure S 2.3.** Average spectra view of *P. polymyxa* ATCC 842<sup>T</sup> (red), DSM 292 (green) and DSM 365 (blue) generated through ClinProTools Software (v 3.0; Bruker Daltonics, Bremen, Germany) and processed following the standard data preparation workflow (baseline subtraction, normalisation, recalibration, average peak list calculation, and peak calculation).....42

## List of Tables

<b>Table 2.1.</b> List of characteristic mass peaks selected according to the p-value ( $\leq 0.05$ ) obtained through W/KW analysis. Changes in peak average intensity between classes are reported as a heatmap of $\log_2$ fold change.....	18
<b>Table 2.2.</b> Performance of classification models of ATCC 842 <sup>T</sup> , DSM 292 and DSM 365. Accuracy, sensitivity and specificity are reported as a percentage. Each of the parameters was calculated as follows: Accuracy= TP + TN / TP + TN +FP+ FN; Sensitivity= TP/ TP + FN; Specificity= TN/ TN + FP. TP, true positive; FN, false negatives; TN, true negatives; FP, false positives (FP). .....	19
<b>Table 2.3.</b> List of discriminative peaks according to QC and SNN CMs. ....	19
<b>Table 2.4.</b> Comparison of main differing features in the phenotypical characterisation and fatty acids cellular composition of ATCC 842 <sup>T</sup> , DSM 292 and DSM 365. "W" = weak; "-" = very weak; "o" = no kit; range colour reaction in API ZYM kit = 0-5 where 3,4 and 5 can be considered positive results. Fatty acid values are expressed as a percentage of the total sum. "ND" = not detected.....	23
<b>Table 3.1.</b> Bacterial culture identification (ID) results by MALDI-TOF MS and genetic analysis. Bacterial cultures previously identified by MALDI-TOF MS with high reliability (log score $\geq 2.3$ ) and not further genetically investigated (NA:Not Analysed) are reported in grey. ....	80
<b>Table 3.2.</b> List of <i>B. licheniformis</i> and <i>B.subtilis</i> Plant Protection Products (PPP) active substances reported in the EU Pesticide database [34], EPA database [35] and BPDB [36]. Regulatory Status: NA: Not Approved (according to the EC Regulation 1107/200); Pe: Pending (according to the EC Regulation 1107/200).....	82
<b>Table 3.3.</b> Kinetic performance evaluation for all strains in four media according to COMB_value (A). Kinetic performance comparison of all strains calculated as COMB value in TSB medium (B). Data were subjected to analysis of variance (ANOVA) (n=3). Different letters indicate significant differences among treatments according to LSD's test ( $\alpha = 0.05$ ).....	82
<b>Table 3.4.</b> Quantification of aerial pellicle biofilm produced by strains 12 and 13 by the means of the dry weight in TSB and SBOG growth media. Data were subjected to analysis of variance (ANOVA) (n=3). Different letters indicate significant differences among treatments according to LSD's test ( $\alpha = 0.05$ ).....	86
<b>Table S 2.1.</b> Identification results for ATCC 842 <sup>T</sup> , DSM 365, and DSM 292, using MBT Compass Library (v. 11.0.0.0). (Log)score values 2.00 - 3.00 indicate high-confidence identifications (green), 1.70 - 1.99 suggest low-confidence (yellow), and 0.00 - 1.69 (red) imply unfeasible organism identification. ....	43
<b>Table S 2.2.</b> Comparison of DSM 365 and DSM 292 mass spectra with the type strain profile <i>P. polymyxa</i> DSM 36 <sup>T</sup> DSM 2 in MBT Compass Library (v. 11.0.0.0). (Log)score values 2.00 - 3.00 indicate high-confidence identifications (green), 1.70 - 1.99 suggest low-confidence (yellow), and 0.00 - 1.69 (red) imply unfeasible organism identification.....	44
<b>Table S 2.3.</b> Identification results for DSM 365 and DSM 292 compared to their own MSPs and reference spectra in MBT Compass Library (v. 11.0.0.0). (Log)score values 2.00 - 3.00 indicate high-confidence identifications (highlighted in green), 1.70 - 1.99 suggest low-confidence (highlighted in yellow), and 0.00 - 1.69 (in red) imply unfeasible organism identification.....	46

<b>Table S 2.4.</b> Morphological and biochemical characterization of ATCC 842 <sup>T</sup> , DSM 292 and DSM 365.....	47
<b>Table S 2.5.</b> Results of API 20E system (Biomérieux) recorded after 48 hours post-incubation at 28°C.....	47
<b>Table S 2.6.</b> Results of API 50 CHB system (Biomérieux) recorded after 48 hours post-incubation at 28°C.....	48
<b>Table S 2.7.</b> Results of API 20 NE system (Biomérieux) recorded after 48 hours post-incubation at 28°C.....	49
<b>Table S 2.8.</b> Results of API ZYM system (Biomérieux) recorded after 6 hours post-incubation at 37°C.....	49
<b>Table S 3.1.</b> MALDI-TOF MS identification results for strains 12 and 13, based on the top match from MBT Compass Library. (Log)score values reported in yellow indicated a likely genus identification (scores between 1.7 and 2.0) and those reported in red indicate an uncertain identification (score of less than 1.7). <i>B. brevis</i> NCBI identifier: 1393.....	88

## **Acronyms**

**2,3-BDO** 2,3- Butanediol

**ABSA** American Biological Safety Association

**ACC** 1-aminocyclopropane-1-carboxylic acid

**ACN** Acetonitrile

**AD** Anderson-Darling

**ANI** Average Nucleotide Identity

**Ar** reference Absorbance

**ARA** Ethylene Reduction Assay

**ATCC** American Type Culture Collection

**BNM** Basal Nutritive Media

**BPDB** Bio-Pesticides DataBase

**BSL** Biosafety Level

**BSs** Biological Substances

**BTS** Bruker Bacterial Test Standard

**CAGR** Compound Annual Growth Rate

**CAS** Chrome azurol S

**CMC** Carboxymethyl Cellulose

**CMs** Classification Models

**DSMZ** Deutsche Sammlung von Mikroorganismen und Zellkulturen

**EPA** United States Environmental Protection Agency

**EPS** Exo-polysaccharides

**EU** European

**FA** Formic Acid

**FAO** Food and Agriculture Organization of the United Nations

**FIB** Flow Impedance Buffer

**GA** Genetic Algorithm

**GIC** Growth Inhibition Category

**GRAS** Generally Recognized As Safe

**GTDB** Genome Taxonomy Database

**HCCA** alpha-cyano-4-hydroxycinnamic acid

**HDTMA** Hexadecyltrimethyl Ammonium Bromide

**IAA** Indole-3-Acetic Acid

**ICC** Intact Cell Concentration

**ID** Identification

**IFC** Impedence Flow Cytometry

**ISR** Immune Systemic Resistance

**K** Potassium

**LB** Luria Bertani

**MALDI-TOF MS** Matrix-assisted laser desorption ionisation time-of-flight Mass Spectrometry

**MPBS** Microbial Plant Biostimulant

**MSP** Main Spectrum Profile

**NA** Not Analyzed

**NB** Nutrient Broth

**NYB** Nutrient Yeast Broth

**OD** Optical Density

**P** Phosphate

**PBS** Plant Biostimulant

**PCA** Principal Component Analysis

**PDA** Potato Dextrose Agar

**PGI** Percentage of Growth Inhibition

**PGP** Plant Growth-Promoting

**PGPB** Plant Growth-Promoting Bacteria

**PGPR** Plant Growth-Promoting Rhizobacteria

**PIPES** Piperazine-1,4-bis(2-ethanesulfonic acid)

**PSI** Phosphate Solubilization Index

**PSI** P-solubilization Index

**QC** Quick Classifier

**RG** Risk Group

**RL** Root Length

**RSA** Root Surface Area

**SFW** Shoot Fresh Weight

**SNK** Student-Newman-Keuls

**SNN** Supervised Neural Network

**SU** Siderophore Units

**TFA** Trifluoroacetic Acid

**TSA** Tryptic Soy Agar

**TSB** Tryptic Soy Broth

**UTC** Untreated Control



**VP** Voges-Proskauer

**W/KW** Wilcoxon/Kruskal Wallis

**Zn** Zinc



# **Chapter 1**

---

## **Introduction**

As the world's population has grown and the demand for food has increased, traditional agricultural practices have relied heavily on chemical fertilisers to increase crop yields. However, concerns about depleting petroleum reserves, environmental impacts, declining soil fertility and the impending menace of climate change have prompted global organisations such as the Food and Agriculture Organization of the United Nations (FAO) and the European Commission, in conjunction with academic institutions, to encourage for the development and adoption of sustainable agricultural practices.

In response to these needs, there is a growing emphasis on the central role of plant biostimulants (PBSs) as innovative tools to address current and future agricultural challenges. Plant biostimulants, encompassing biological substances (BSs) and beneficial microorganisms, offer sustainable approaches to enhance crop yield, productivity, quality, and tolerance to abiotic stresses ([Regulation (EU) 1/1009] [1]).

Microbial Plant Biostimulants are a promising category within the realm of plant biostimulants. They harness the potential of beneficial microorganisms, such as bacteria and fungi, to enhance plant growth and improve crop performance.

These microorganisms can exert beneficial effects through various mechanisms, including facilitating nutrient uptake, enhancing stress tolerance, and promoting root growth and development [2]. By utilising the natural interactions between plants and microorganisms, Microbial PBSs provide a sustainable and eco-friendly method for enhancing agricultural productivity.

Such beneficial microorganisms, include species that form symbiotic relationships with plant roots (such as rhizobia, mycorrhizal fungi, actinomycetes, and diazotrophic bacteria), aid in nutrient mineralization and availability and generate plant growth-regulating hormones.

Many of these organisms occur naturally in the soil, although in certain circumstances, it can be advantageous to bolster their populations through inoculation or by implementing diverse agricultural management practices aimed at augmenting their abundance and activity.

Several factors can affect the effectiveness of microbial inoculants as biostimulants, such as plant root exudates, chemical fertilizers, pesticides, types of soils and environmental conditions [3].

Genera like *Bacillus* sp., *Pseudomonas* sp., *Azotobacter* sp., *Azospirillum* sp., *Gluconoacetobacter* sp. are well recognized beneficial microorganisms able to promote plant growth through the following mechanisms: nitrogen fixation, solubilization of inorganic phosphate, iron-chelating agents, secondary metabolites and phytohormones production. Nitrogen fixation and phosphorus solubilization are extensively studied traits, given the critical roles of nitrogen and phosphorus as the primary and secondary elements essential for plant growth [4].

Nitrogen is an essential element for all living organisms, including plants, as it constitutes key components such as amino acids, nucleic acids, proteins, and energy currency (ATP, GTP, ADP), among others, making it a fundamental building block of cells. Certain diazotrophic bacteria, such as *Azospirillum* sp., have the ability to convert atmospheric nitrogen into ammonia, a form that plants can readily utilize. *Azospirillum*, particularly species like *A. brasilense* and *A. lipoferum*, has been extensively studied as a microbial inoculant for nitrogen fixation, with reported significant increases in nitrogen content in various crops such as sugarcane and wheat [5].

In addition to nitrogen, phosphorus is another crucial plant nutrient. It is typically found in limited quantities in agricultural soils, with only about 1 mg/kg<sup>-1</sup> accessible in forms such as dihydrogen phosphate and hydrogen phosphate [3]. Phosphorus exists in both inorganic and organic forms, with the inorganic form being sparingly soluble due to soil interactions, while the organic form constitutes a significant portion of total phosphorus. The low availability of phosphorus in agricultural systems presents a significant challenge, which can be addressed by phosphorus-solubilizing microorganisms. These microorganisms achieve phosphorus solubilization through the production of organic acids or phosphatase and phytase enzymes, transforming insoluble phosphorus into soluble forms that plants can readily absorb from the soil. Notably, prominent rhizospheric bacteria

known for their ability to solubilize insoluble phosphorus belong to the *Bacillus* sp and *Pseudomonas* sp genera [6].

While activities such as nitrogen fixation, phosphorus solubilization, and others are crucial considerations in selecting effective microbial inoculants, it's equally important to acknowledge that some of these microbes have been associated with human and/or animal infections. For example, microorganisms like *Klebsiella* sp. [7], *Enterobacter* sp. [8, 9], and *Stenotrophomonas* sp. [3] have been identified as potent microbial inoculants but are also capable of causing opportunistic infections in humans.

This underscores an important consideration: the development of a robust and reliable microbial biostimulant must equally prioritize the safety aspects of the microbial species under study. This balanced approach is essential in the development of future agricultural products, ensuring that biological efficacy is harmonized with safety considerations. By carefully evaluating the potential risks associated with microbial inoculants and implementing stringent safety assessments, the agricultural industry can foster the creation of innovative and sustainable biostimulants that effectively enhance crop productivity while upholding human and environmental safety standards.

In this regard, effective identification and typing methods play a crucial role. Techniques such as matrix-assisted laser desorption ionization time-of-flight mass spectrometry (MALDI-TOF MS) have gained prominence for their rapid and accurate identification of microbial strains, accelerating the development and use of microbial plant biostimulants. Such a technology allows obtaining a mass fingerprint profile for the analysed strain, enriched in highly abundant ribosomal proteins, which is compared with reference protein spectra contained in a database to assign an identification result.

The spectrum of molecular weights utilized for bacterial species identification relies on the inherent ribosomal proteins and spans from 2 to 20,000 Da, providing a strong signal-to-noise ratio with minimal disruption from microbial culture conditions [10].

The primary advantage of MALDI-TOF MS is its significantly reduced identification time, taking only a few minutes compared to the 24–48 hours required by other methods, including biochemical culture-based or molecular approaches. This time-saving aspect is particularly crucial for expediting the identification and selection of potential candidates for a microbial plant biostimulant development, thereby accelerating the go-to-market phase of the final product.

Nevertheless, it's important to consider some limitations of the MALDI-TOF MS technique, such as its challenge in distinguishing between closely related species. This limitation can be effectively addressed by leveraging statistical tools capable of identifying discriminative biomarkers to enhance the resolution level of the database [11-13].

All the aspects mentioned above, from the identification and screening to the selection of promising microorganisms for the development of a microbial biostimulant, will be covered and discussed in the three chapters of this thesis. The purpose of this work is indeed to analyze and investigate the most relevant aspects in the development process of a microbial plant biostimulant but also to facilitate the release of effective and sustainable solutions by means of a systematic and holistic approach.

## References

- [1] EU. Regulation 2019/1009 of the European Parliament and of the Council of 5 June 2019 laying down rules on the making available on the market of EU fertilising products and amending Regulations (EC) No 1069/2009 and (EC) No 1107/2009 and repealing Regulation (EC) No 2003/2003. *Off J Eur Union* (2019)
- [2] Ortiz, A. and E. Sansinenea. The role of beneficial microorganisms in soil quality and plant health. *Sustainability* **14**, 5358 (2022)
- [3] Kumari, M., Swarupa, P., Kesari, K. K., & Kumar, A. Microbial inoculants as plant biostimulants: A review on risk status. *Life* **13**, 12 (2022)
- [4] Sinha, D. and P. K. Tandon, An overview of nitrogen, phosphorus and potassium: Key players of nutrition process in plants. *Sustainable solutions for elemental deficiency and excess in crop plants*, 85-117 (2020)
- [5] Calvo, P., et al. Agricultural uses of plant biostimulants. *Plant and Soil* **383**, 3-41 (2014).
- [6] Rodríguez, H. and R. Fraga. Phosphate solubilizing bacteria and their role in plant growth promotion. *Biotechnology Advances* **17**, 319-339 (1999)
- [7] Sapre, S., Gontia-Mishra, I., & Tiwari, S. Klebsiella sp. confers enhanced tolerance to salinity and plant growth promotion in oat seedlings (*Avena sativa*). *Microbiological Research* **206**, 25-32 (2018)
- [8] Shahid, M., Hameed, S., Imran, A., Ali, S., & van Elsas, J. D. Root colonization and growth promotion of sunflower (*Helianthus annuus* L.) by phosphate solubilizing *Enterobacter* sp. Fs-11. *World Journal of Microbiology and Biotechnology* **28**, 2749-2758 (2012)
- [9] Borham, A., Belal, E., & Metwaly, M. Phosphate solubilization by *Enterobacter cloacae* and its impact on growth and yield of wheat plants. *Journal of Sustainable Agricultural Sciences* **43**, 89-103 (2017)
- [10] Suarez, S., Ferroni, A., Lotz, A., et al. Ribosomal proteins as biomarkers for bacterial identification by mass spectrometry in the clinical microbiology laboratory. *Journal of Microbiological Methods* **94**, 390-396 (2013)
- [11] Pérez-Sancho, M., Vela, A. I., Horcajo, P., et al. Rapid differentiation of *Staphylococcus aureus* subspecies based on MALDI-TOF MS profiles. *Journal of Veterinary Diagnostic Investigation* **30**, 813-820 (2018)
- [12] Gekenidis, M.-T., Studer, P., Wüthrich, S., Brunisholz, R., & Drissner, D. Beyond the matrix-assisted laser desorption ionization (MALDI) biotyping workflow: in search of



microorganism-specific tryptic peptides enabling discrimination of subspecies. *Applied and Environmental Microbiology* **80**, 4234-4241 (2014)

[13] Huang, C.-H., & Huang, L. Rapid species- and subspecies-specific level classification and identification of *Lactobacillus casei* group members using MALDI Biotyper combined with ClinProTools. *Journal of Dairy Science* **101**, 979-991 (2018)

## Chapter 2

---

### **MALDI-TOF as a powerful tool for identifying and differentiating closely related microorganisms: the strange case of three reference strains of *Paenibacillus polymyxa***

*The work described in this chapter is taken from: I. Lebano, F. Fracchetti, M. Li Vigni, J.F. Mejia, G. Felis, S. Lampis; MALDI-TOF as a powerful tool for identifying and differentiating closely related microorganisms: the strange case of three reference strains of Paenibacillus polymyxa. Scientific Reports 14, 2585 (2024). doi: 10.1038/s41598-023-50010-w.*

## Contributions

I.L., G.F., J.F.M. and S.L. conceived and designed the research; I.L. carried out experiments, analysed data, drafted the manuscript and prepared figures; F.F. performed molecular analyses and analysed sequencing data; M.L.V. contributed to the MALDI-TOF data analysis; S.L. and G.F. reviewed and contributed to the writing of the final manuscript. All authors read and approved the manuscript.

## Article location

doi: 10.1038/s41598-023-50010-w

## Supplementary material

The supplementary material of this article is available at <https://www.ncbi.nlm.nih.gov/pmc/articles/PMC10831075/#MOESM1:~:text=Supplementary%20Information>.

## 2.1 Abstract

### Background

Accurate identification and typing of microbes are crucial steps in gaining an awareness of the biological heterogeneity and reliability of microbial material within any proprietary or public collection. *Paenibacillus polymyxa* is a bacterial species of great agricultural and industrial importance due to its plant growth-promoting activities and production of several relevant secondary metabolites. In recent years, Matrix-assisted laser desorption ionisation time-of-flight Mass Spectrometry (MALDI-TOF MS) has been widely used as an alternative rapid tool for identifying, typing, and differentiating closely related strains.

### Results

In this study, we investigated the diversity of three *Paenibacillus polymyxa* strains. The mass spectra of ATCC 842<sup>T</sup>, DSM 292, and DSM 365 were obtained, analysed, and compared to select discriminant peaks using ClinProTools software and generate classification models. MALDI-TOF MS analysis showed inconsistent results in identifying DSM 292 and DSM 365 as belonging to *P. polimixa* species, and comparative analysis of mass spectra revealed the presence of highly discriminatory biomarkers among the three strains. 16S rRNA

sequencing and Average Nucleotide Identity (ANI) confirmed the discrepancies found in the proteomic analysis.

## **Conclusions**

The case study presented here suggests the enormous potential of the proteomic-based approach, combined with statistical tools, to predict and explore differences between closely related strains in large microbial datasets.

## **2.2 Introduction**

*Paenibacillus* is a ubiquitous genus consisting of 280 bacterial species able to colonise different environmental niches, having great relevance in the industrial and agricultural fields [1-2].

*Paenibacillus polymyxa* is the type species of the genus *Paenibacillus* [3-4]. Members of such species are undoubtedly the most studied and characterised because of their beneficial properties and ability to produce an extensive repertoire of industrially relevant secondary metabolites [5-6]. Indeed, many *Paenibacillus polymyxa* have been reviewed for their plant growth promotion activity through phosphorus solubilization [2], nitrogen fixation [7-8], siderophores, phytohormones production, and organic matter degradation [9].

Among the secondary metabolites of *P. polymyxa* with biotechnological and medical applicability, there are antimicrobial compounds (e.g., polymyxins and fusaricidins) [10], exo-polysaccharides (EPS) [11], hydrolytic enzymes (e.g., amylases, pectinases, cellulases, hemicellulases) [510] and 2,3- Butanediol (2,3-BDO). This last valuable compound has a vast range of applications in the chemical, pharmaceutical, and food industries as a precursor or additive of many manufacturing processes [12-14].

One of the most efficient producers of 2,3-BDO optically active isomers is *Paenibacillus polymyxa* DSM 365 [15-16], a generally recognised safe (GRAS) microorganism. This strain was isolated from garden soil [17], and the genome was sequenced completely [16]. Genome annotation disclosed several traits related to biostimulant activity (e.g., nitrogen fixation, siderophores and EPS biosynthesis) [16]. Moreover, the strain was also described as a biocontrol agent

able to induce the Immune Systemic Resistance (ISR) of tobacco plants against the pathogen *Phytophthora parasitica* [18].

Besides *P. polymyxa* DSM 365, another *P. polymyxa* strain having relevant biotechnological potential is DSM 292, a platform for heterologous protein production [19]. Indeed, the low proteolytic activity would make it an ideal host for the high-yield and stable production of enzymes [20] [19].

Since DSM 365 and DSM 292 are microbial cultures available in public collections and present relevant biotechnological and industrial applications, a thorough investigation of their biodiversity is particularly interesting.

Matrix-assisted laser/desorption ionisation time-of-flight mass spectrometry (MALDI-TOF MS) is a technology that has widely been introduced in many laboratories as a high-throughput, cost-effective, fast, and reliable tool to identify, classify and typing unknown microorganisms. It allows obtaining a mass fingerprint profile for each unknown strain that is matched against the reference spectra in the instrument database to assign an identity.

In this study, we tested MALDI-TOF MS analysis integrated with statistical tools to explore the biodiversity among DSM 365, DSM 292, and the type strain of the species ATCC 842<sup>T</sup>. In addition, 16S rRNA sequence analysis and Average Nucleotide Identity (ANI) were performed to assess and verify MALDI-TOF MS results. Phenotypical test and fatty acids cellular composition analysis were also performed to assess putative differences among the three strains here taken into consideration. This work represents, in our opinion, an interesting case study that highlights the potential of the proposed complementary typing approach to improve the identification resolution of very closed related strains in any proprietary or public culture collection, making it possible to enrich any *in-house* reference database. This approach to biodiversity screening could precede genomic analyses as a kind of predictive tool, able to point to interesting discrepancies that need to be investigated further with a targeted, in-depth approach.

## 2.3 Results

### 2.3.1 MALDI-TOF MS identification results

In this study, the identification of ATCC 842<sup>T</sup>, DSM 292, and DSM 365 with the BDAL library through the MBT Compass (Bruker Daltonik GmbH, Bremen, Germany) software did not provide the expected results. More specifically, the identification of DSM 292 and DSM 365 did not reach the minimum log(score) for a high match with the reference spectra in the database; thus for 8 out of 15 of DSM 292 and 14 out of 15 of DSM 365 signal replicates the identification was confirmed only at the genus level, with a log(score) ranging from 1.71 – 1.84 and 1.72 – 1.99, respectively. Conversely, regarding ATCC 842<sup>T</sup>, 13 out of 15 signal replicates were correctly identified as *P. polymyxa* DSM 36<sup>T</sup> (reference spectrum DSM 36T DSM\_2) with a log(score) ranging from 2.01 - 2.25 (**Table S 2.1**). Furthermore, it was noticed that both the profiles of the DSM 292 and the DSM 365 were even more different from the reference spectrum of the type strain DSM 36<sup>T</sup> since, for most replicates, it was not reported among the closest classification results, and the matching resulted in not reliable identification. Indeed, the identification (log)score for DSM 365 and DSM 292 compared to DSM 36<sup>T</sup> DSM\_2 ranged from 1.52 – 1.92 and 1.05 – 1.85 (**Table S 2.2**).

The matching degree between each analysed strain and the reference Main Spectrum Profile (MSP) is reported in **Figure 2.1**.

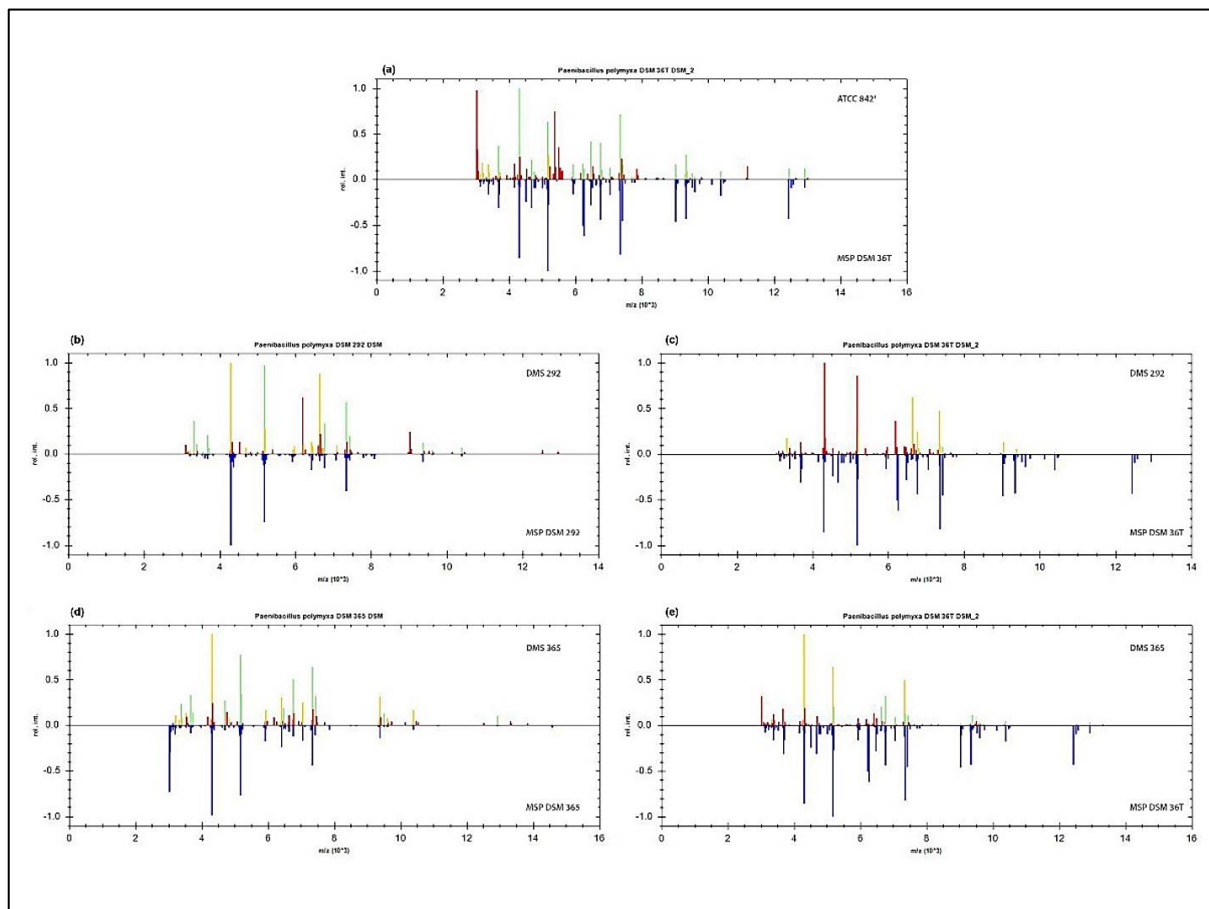


**Figure 2.1.** Graphical representation of *P. polymyxa* identification by MALDI Biotyper Software. The colour of the peaks reflects the degree of matching of (a) ATCC 842<sup>T</sup>, (b) (c) DSM 292, and (d) (e) DSM 365 with the reference MSPs (green = full match, yellow = partial match and red = mismatched) reported in the lower part of the graphs (blue spectra).

### 2.3.2 Mass data statistical analysis results and in-house database implementation with DSM 292 and DSM 365 profiles.

Given the preliminary results obtained in the identification step, the mass spectra of the DSM 292 and 365 were compared with the mass profile of ATCC 842<sup>T</sup> to assess whether there were consistent differences and discriminative biomarkers in their mass fingerprint that could explain the mismatch with the type strain. All the 15 raw mass spectra for each strain were loaded into the ClinProTools software (v 3.0; Bruker Daltonics, Bremen, Germany) and processed following the standard data preparation workflow (baseline subtraction, normalisation, recalibration, average peak list calculation and peak calculation). A pseudo-gel-like view of the processed spectra loaded per class is reported in **Figure 2.2 a**. Moreover, the average spectra view of all three classes is reported in **Figure S 2.3**. As a first step, Principal Component Analysis (PCA) was performed to get more information about the data set variability and clustering of the three *Paenibacillus* strains. The two-dimensional representation of the scores (PC1 vs. PC2, **Figure 2.2 b** and **Figure S 2.2**) showed that the three *P. polymyxa* strains grouped differently. The loadings plot (PC1 vs PC2, **Figure 2.2 c** and **Figure S 2.2**) offers a visualisation of the peaks that influence this clustering the most, indicating that the three strains showed spectral differences in their mass fingerprint. Moreover, the study suggested that the peaks influencing this clustering could be potential discriminating markers.

Subsequently, after the visual comparison of *P. polymyxa* mass spectra, the selection of peaks showing a significant difference in the average intensity among ATCC 842<sup>T</sup>, DSM 292 and DSM 365 was made according to the p-values ( $\leq 0.05$ ) obtained through Wilcoxon/Kruskal Wallis (W/KW) analysis since the p-value for AD test was less than equal to 0.05 (**Table 2.1**). The selected masses were confirmed to be very informative in discriminating the three *P. polymyxa* strains since the p-value was  $< 0.000001$  for all. Moreover, such biomarkers strongly affected the clustering in the PCA (**Figure 2.2 c**). Peaks describing the fingerprint of each strain the most were identified by measuring their change in intensity average ( $\log_2$  fold change) as reported in **Table 2.1**. Results showed that high expression levels of peaks m/z 2,400, 2,685, 6,525, and the region from m/z



5,505 to 5,954 strongly described the fingerprint of ATCC 842<sup>T</sup>. Similarly, low-intensity levels of m/z 6,413 and 7,336 were good descriptors of such a profile. Low intensities of m/z 2,959 and 2,987 and high intensities of m/z 3,089 and 7,076 described the DSM 292 profile well. Furthermore, high expression levels of m/z 4,179, 4,748, 9,492 and 13,305 were indicative of the profile of DSM 365. Some discriminant characteristics of the selection (m/z 2,874, 2,944, 3,314, 5,374, 6,181, 6,631, 6,656) proved to be good descriptors of all three classes simultaneously, as their intensity values were quite distinct. The average intensities of the above mentioned peaks are reported in **Figure 2.3**.

Classification models (CMs) were generated by ClinProTools software using Quick Classifier (QC) [21], Supervised Neural Network (SNN) [21] and Genetic Algorithm (GA) [21-22] to obtain systematic and objective strain discrimination according to a defined list of discriminative biomarkers selected by the algorithm. The performance of all classification models was calculated to choose the best able to discriminate the three *P. polymyxa* strains simultaneously. According to the results reported in **Table 2.2**, GA\_KNN algorithms with 1, 3 and 5 nearest neighbor settings showed very high discriminating power (100% accuracy) for ATCC 842<sup>T</sup> and DSM 365 classes but not for DSM 292. The only multiclass models able to correctly assign and classify an independent data set into one out of three classes were SNN and QC, with a cross-validation value of 100%. Informative features selected by such multiclass classification models are reported in **Table 2.3**. Such peaks showed different expression patterns and high discriminatory power, as shown in 2D scatter plots reporting strain distributions according to peak intensity (**Figure 2.4**).

Given the successful performance of multiclass models in classifying and recognising the three strains of *P. polymyxa*, the independent signal sets tested in cross-validation were used to generate new MSPs for DSM 292 and DSM 365 inside the *in-house* reference library.

After implementing the library with the newly generated MSPs for DSM 292 and DSM 365, the identification results of the fifteen spectra showed improvement. These results exhibited a higher agreement in terms of log(score) with the

internally generated MSPs compared to the reference profiles in the MBT Compass library (**Table S 2.3**).

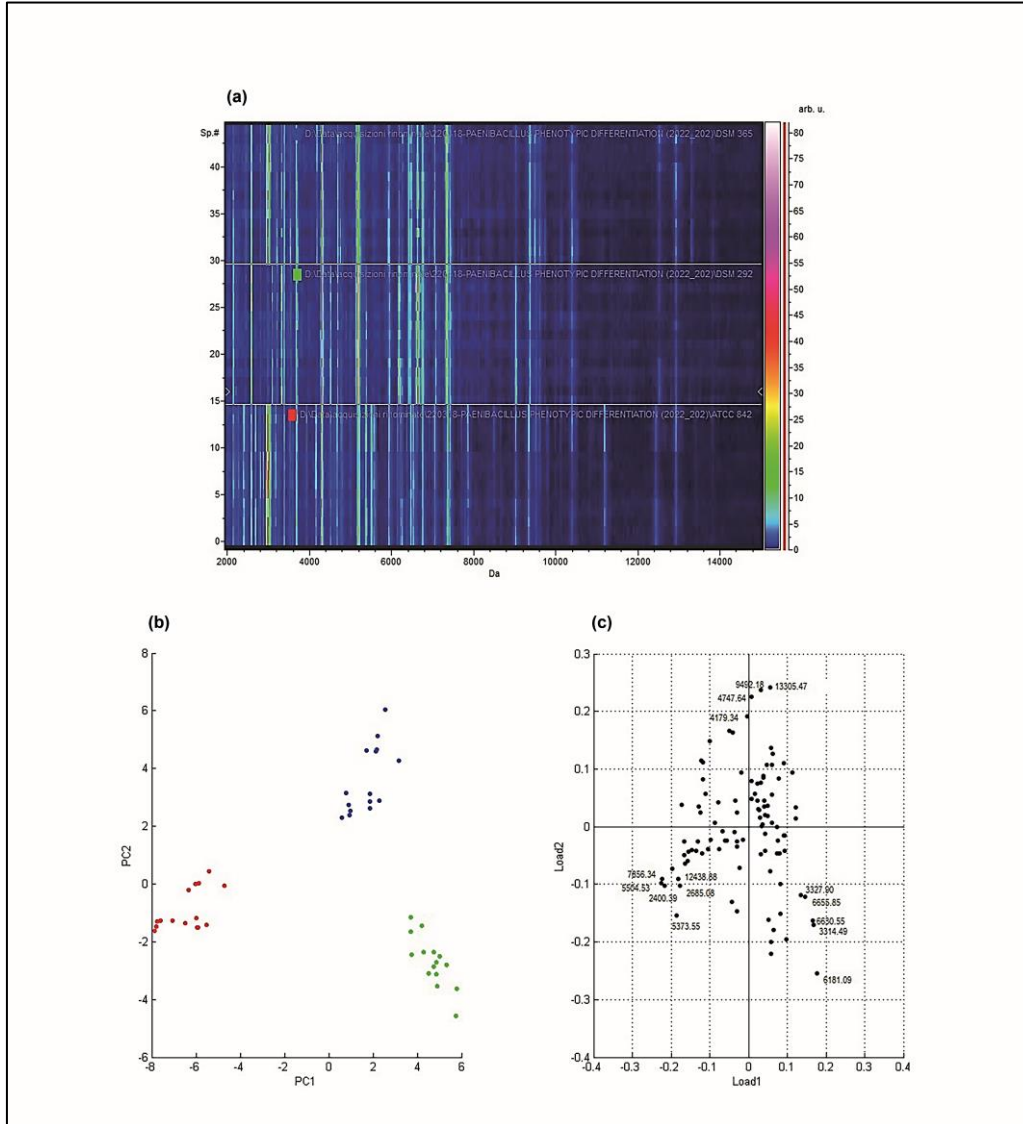


**Figure 2.2.** (a) Pseudo-gel like view of ATCC 842<sup>T</sup> (red), DSM 292 (green) and DSM 365 (blue) mass spectra (15 replicates per class) displayed on a rainbow scale. The peak intensity is reported on y-axis in arbitrary units; 2-D PCA (b) and Loadings of 2D-PCA (c) plots of ATCC 842<sup>T</sup> (red), DSM 292 (green) and DSM 365 (blue).

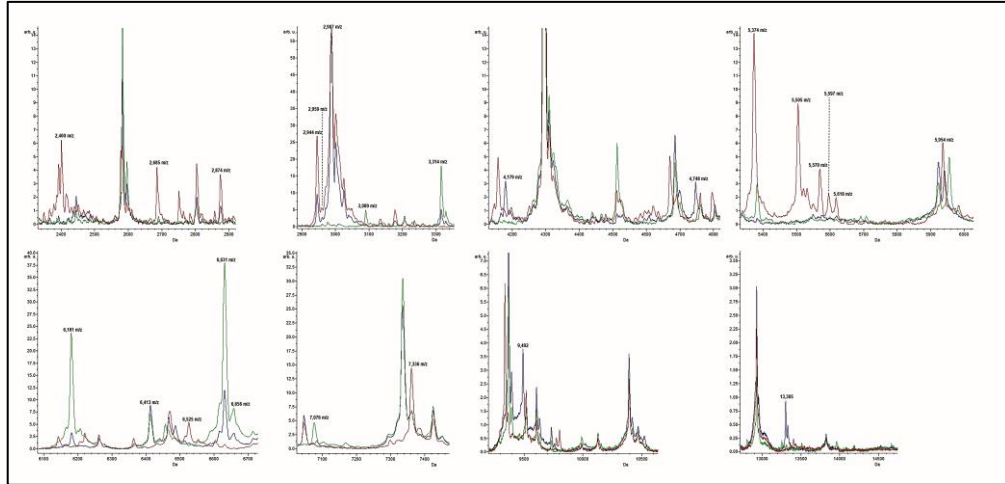


**Figure 2.3.** Average spectra of the most characteristic peaks among *P. polymyxa* strains. Intensities of characteristic peaks in ATCC 842<sup>T</sup> (red), DSM 292 (green) and DSM 365 (blue) are shown on y-axes and expressed in arbitrary intensity units.

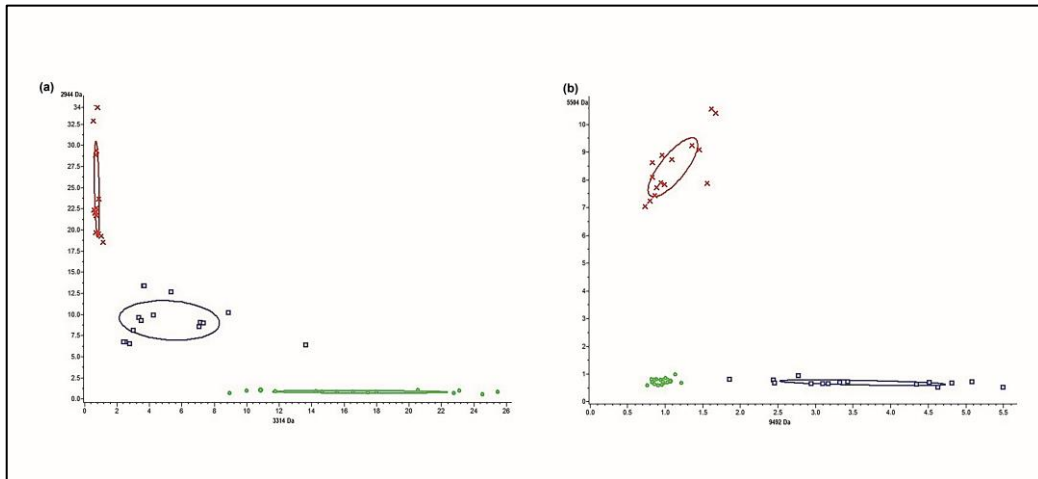


**Figure 2.4.** 2D scatter plots of characteristic peaks for ATCC 842<sup>T</sup> (red), DSM 292 (green) and DSM 365 (blue) selected by QC and SNN classification models. **(a)** Scatter plots of peaks 2,944 and 3,314 Da (selected by the QC model) and **(b)** 5,504 and 9,492 Da (selected by the SNN model). The intensities of peaks were expressed in arbitrary intensity units and served as y-axes. The ellipses represent the 95% confidence intervals of peak intensity for each strain.

**Table 2.1** List of characteristic mass peaks selected according to the p-value ( $\leq 0.05$ ) obtained through W/KW analysis. Changes in peak average intensity between classes are reported as a heatmap of  $\log_2$  fold change.

Mass	PW/KW	PAD	Average of peak intensity $\pm$ stdev			Log <sub>2</sub> fold change			
			ATCC 842 <sup>T</sup>	DSM 292	DSM 365	ATCC 842 <sup>T</sup> vs 292	ATCC 842 <sup>T</sup> vs 365	DSM 292 vs 365	DSM 365 vs 292
2,400	< 0.000001	< 0.000001	6.72 $\pm$ 3.08	0.70 $\pm$ 0.14	0.88 $\pm$ 0.26	3.3	2.9	-0.3	0.3
2,685	< 0.000001	< 0.000001	4.71 $\pm$ 1.30	0.92 $\pm$ 0.19	0.68 $\pm$ 0.15	2.4	2.8	0.4	-0.4
2,874	< 0.000001	0.000629	4.22 $\pm$ 1.16	0.82 $\pm$ 0.18	1.93 $\pm$ 0.42	2.4	1.1	-1.2	1.2
2,944	< 0.000001	0.000211	27.6 $\pm$ 6.31	0.93 $\pm$ 0.16	10.3 $\pm$ 2.60	4.9	1.4	-3.5	3.5
2,959	< 0.000001	0.002880	6.25 $\pm$ 1.80	1.18 $\pm$ 0.23	3.51 $\pm$ 0.39	2.4	0.8	-1.6	1.6
2,987	< 0.000001	0.000003	59.6 $\pm$ 12.12	1.99 $\pm$ 0.50	58.5 $\pm$ 15.52	4.9	0	-4.9	4.9
3,089	< 0.000001	< 0.000001	1.61 $\pm$ 0.26	5.44 $\pm$ 2.42	1.34 $\pm$ 0.24	-1.8	0.3	2	-2
3,314	< 0.000001	0.000003	0.86 $\pm$ 0.17	18.9 $\pm$ 5.99	5.82 $\pm$ 3.43	-4.5	-2.8	1.7	-1.7
4,179	< 0.000001	0.000017	1.70 $\pm$ 0.29	0.93 $\pm$ 0.22	3.75 $\pm$ 1.15	0.9	-1.1	-2	2
4,748	< 0.000001	< 0.000001	1.56 $\pm$ 0.29	0.89 $\pm$ 0.15	3.65 $\pm$ 1.51	0.8	-1.2	-2	2
5,374	< 0.000001	< 0.000001	14.6 $\pm$ 4.95	3.41 $\pm$ 0.91	0.86 $\pm$ 0.19	2.1	4.1	2	-2
5,505	< 0.000001	< 0.000001	9.39 $\pm$ 1.18	0.81 $\pm$ 0.12	0.76 $\pm$ 0.11	3.5	3.6	0.1	-0.1
5,570	< 0.000001	< 0.000001	4.47 $\pm$ 0.91	0.87 $\pm$ 0.09	1.21 $\pm$ 0.14	2.4	1.9	-0.5	0.5
5,597	< 0.000001	< 0.000001	2.74 $\pm$ 0.37	1.00 $\pm$ 0.18	1.04 $\pm$ 0.12	1.5	1.4	-0.1	0.1
5,618	< 0.000001	0.00000106	2.33 $\pm$ 0.35	0.86 $\pm$ 0.17	1.07 $\pm$ 0.18	1.4	1.1	-0.3	0.3
5,954	< 0.000001	0.0000052	1.86 $\pm$ 0.26	5.41 $\pm$ 0.95	2.45 $\pm$ 0.66	-1.5	-0.4	1.1	-1.1
6,181	< 0.000001	< 0.000001	1.15 $\pm$ 0.20	24.3 $\pm$ 7.51	3.73 $\pm$ 0.92	-4.4	-1.7	2.7	-2.7
6,413	< 0.000001	0.0000508	1.14 $\pm$ 0.26	7.59 $\pm$ 1.14	9.34 $\pm$ 2.21	-2.7	-3	-0.3	0.3
6,525	< 0.000001	< 0.000001	5.79 $\pm$ 0.98	1.49 $\pm$ 0.29	1.78 $\pm$ 0.22	2	1.7	-0.3	0.3
6,631	< 0.000001	0.0000173	1.30 $\pm$ 0.74	38.6 $\pm$ 95	12.4 $\pm$ 6.52	-4.9	-3.3	1.6	-1.6
6,656	< 0.000001	0.000211	0.73 $\pm$ 0.15	8.78 $\pm$ 2.61	3.74 $\pm$ 1.64	-3.6	-2.4	1.2	-1.2
7,076	< 0.000001	< 0.000001	1.70 $\pm$ 0.27	5.05 $\pm$ 0.88	1.47 $\pm$ 0.31	-1.6	0.2	1.8	-1.8
7,336	< 0.000001	< 0.000001	3.41 $\pm$ 0.81	31.0 $\pm$ 3.75	26.0 $\pm$ 4.32	-3.2	-2.9	0.3	-0.3
9,492	< 0.000001	< 0.000001	1.23 $\pm$ 0.37	1.06 $\pm$ 0.14	4.03 $\pm$ 1.23	0.2	-1.7	-1.9	1.9
13,305	< 0.000001	< 0.000001	0.23 $\pm$ 0.05	0.34 $\pm$ 0.08	1.1 $\pm$ 0.38	-0.6	-2.3	-1.7	1.7

**Table 2.2.** Performance of classification models of ATCC 842<sup>T</sup>, DSM 292 and DSM 365. Accuracy, sensitivity and specificity are reported as a percentage. Each of the parameters was calculated as follows: Accuracy= TP + TN / TP + TN +FP+ FN; Sensitivity= TP/ TP + FN; Specificity= TN/ TN + FP. TP, true positive; FN, false negatives; TN, true negatives; FP, false positives (FP).

Strain	Model	Selected	Accuracy	Sensitivity	Specificity
ATCC 842 <sup>T</sup>	GA_KNN1	30	100	100	100
	GA_KNN3	8	100	100	100
	GA_KNN5	5	100	100	100
	GA_KNN7	4	45.90	38.10	50
	SNN	3	100	100	100
	QC	4	100	100	100
DSM 292	GA_KNN1	30	90.16	70	100
	GA_KNN3	8	98.36	95	100
	GA_KNN5	5	95.08	85	100
	GA_KNN7	4	58.34	0	100
	SNN	3	100	100	100
	QC	4	100	100	100
DSM 365	GA_KNN1	30	100	100	100
	GA_KNN3	8	100	100	100
	GA_KNN5	5	100	100	100
	GA_KNN7	4	100	100	100
	SNN	3	100	100	100
	QC	4	100	100	100

**Table 2.3.** List of discriminative peaks according to QC and SNN CMs.

CMs	Mass	PW/KW	PAD	Average of peak intensity $\pm$ stdev		
				ATCC 842 <sup>T</sup>	DSM 292	DSM 365
QC	2,944	< 0.000001	0.000211	27.55 $\pm$ 6.31	0.93 $\pm$ 0.16	10.34 $\pm$ 2.6
	2,959	< 0.000001	0.002700	8.08 $\pm$ 2.35	1.52 $\pm$ 0.29	4.50 $\pm$ 0.50
	2,874	< 0.000001	0.000528	5.45 $\pm$ 1.52	1.05 $\pm$ 0.22	2.47 $\pm$ 0.53
	3,314	< 0.000001	0.0000035	0.86 $\pm$ 0.17	18.87 $\pm$ 5.99	5.82 $\pm$ 3.43
SNN	5,505	< 0.000001	< 0.000001	9.39 $\pm$ 1.18	0.81 $\pm$ 0.12	0.76 $\pm$ 0.11
	7,076	< 0.000001	< 0.000001	2.19 $\pm$ 0.35	6.48 $\pm$ 1.13	1.89 $\pm$ 0.41
	9,492	< 0.000001	< 0.000001	1.23 $\pm$ 0.37	1.06 $\pm$ 0.14	4.03 1.23

### 2.3.3 16S rRNA sequence retrieving from genomes and comparison

The identification of the strain ATCC 842<sup>T</sup> (= DSM 36<sup>T</sup>), DSM 292, and DSM 365 by comparison of the assembled Sanger sequence in EzBioCloud confirmed, as expected, the identification of the strain ATCC 842<sup>T</sup> as *P. polymyxa*. Contrarily the best hit resulting after the analysis of the 16S rRNA sequence of the strains DSM 292 (1372 bp) and DSM 365 (1385 bp) was *Paenibacillus peoriae*, with respectively 99.78 % and 99.85%) in the case of the sequence from the strain DSM 365 the second-best hit was *Paenibacillus ottowi* (99.56%), both the species belonging to the *P. polymyxa* group. The species *P. polymyxa* is, therefore, respectively, the second and third-best hit with a % similarity of 99.42 and 99.27. Remarkably, when the Sanger sequence obtained from the strain DSM 292 is compared with the most similar 16S rRNA locus sequence retrieved from the genome (OXKC02000021.1), the similarity percentage is 99.93%. Analogously, the comparison of the sequence of the most similar 16S rRNA locus sequence retrieved from the genome of the strain DSM 365 (JAKVDC010000038.1, contig 38) showed 99.92% similarity.

### 2.3.4 Genome comparison results

The relatedness of the strains by means of a whole-genome approach was defined by calculating the Average Nucleotide Identity (ANI) with the OrthoANI algorithm and setting 95-96% as the threshold to propose new species [23]. The ANI values of the strain DSM 365 and DSM 292 clearly separate these two strains from ATCC 842<sup>T</sup>, the type strain of *P. polymyxa* species, as they resulted in 90.12 and 89.99, respectively. Based on this result, the strains DSM 365 and DSM 292 are distinguishable from the type strains, and they can be suggested as references of a cluster of *P. polymyxa* strains different from the *P. polymyxa sensu stricto*. Remarkably, the ANI value resulting from the comparison of the strains DSM 365 and DSM 292 was close to the threshold, i.e., 95.40; therefore, it was not possible to clearly support the presence of a third emerging cluster nucleus within the *P. polymyxa* species.

The presence of remarkable genes and/or biosynthetic pathways were searched by BLASTn in the three previously reported genomes in order to enlighten differences in the presence of Butanediol Dehydrogenase (GenBank Acc. No.: JMIQ01000019: 17969.19021)14 and Polymyxin Synthetase (EU371992.1:22102-41040)38.

Considering peculiar genes and biosynthetic pathways, it was possible to evidence that the strain DSM 365 is the only strain among the three compared here to harbour the Butanediol Dehydrogenase gene. A genetic locus with different nucleotide similarity was found in both the other two strains: the most related gene in the strain DSM 292 was annotated as Sorbitol Dehydrogenase (GenBank Acc. No. OXKC02000003.1:428721-429773, locus\_tag "PPOLYM\_01857"), with only 96.39% nucleotide similarity. In the genome of the strain ATCC 842<sup>T</sup>, which is not annotated, it was not possible to find any predicted function, but a 100% coverage region with only 94.11% nucleotide similarity was found, suggesting that region (CAIGJZ010000013.1:3117-4169) does not code for Butanediol Dehydrogenase gene.

Concerning Polymyxin Synthetase, it was not possible to find the complete query in only one contig of the three genome strains, suggesting it was not completely assembled. More *in-silico* or *in-vivo* analyses are required to evaluate this genetic function.

### **2.3.5 Phenotypical test (API) and fatty acids cellular composition results**

Comparison results about substrate utilisation revealed that the strains differed for some traits (**Table 2.4**). In particular, both *P. polymyxa* DSM 292 and DSM 365 showed different behaviour in acetylmethylcarbinol production [24] according to the Voges-Proskauer (VP) assay compared to the type strain *P. polymyxa* ATCC 842<sup>T</sup>. Additionally, *P. polymyxa* DSM 292 was positive in malate assimilation, rhamnose, and  $\alpha$ -methyl-d-mannoside utilisation and weak in tween 80 degradation compared to ATCC 842<sup>T</sup> and DSM 365. Further differences can also be observed in growth temperature and tolerance to 5% of NaCl. More

specifically, DSM 365 grew at higher temperatures (35°C), and DSM 292 resulted in being not tolerant of 5% of NaCl.

Regarding the production of enzymes, colourimetric reactions of different intensities were recorded in the API ZYM kit. Differences in colour reactions might reveal potential differences in the enzyme production profiles of the three strains. Among the positive recordings, DSM 365 showed the highest intensity reaction for  $\beta$ -Galactosidase (**Table S 2.8**). The entire list of substrate utilisation and details about morphological description (including cell pictures) can be found in **Figure S 2.1, Table S 2.4, Table S 2.5, Table S 2.6, Table S 2.7, Table S 2.8**.

The comparison of fatty acids profiles (**Table 2.4**) revealed that all three strains have 15:0 anteiso, 16:00, 15:00 iso, 17:0 anteiso, 16:0 iso and 17:0 iso as major cellular fatty acids. Moreover, the fatty acid 16:1 w11c was the one that differed the most among the three strains.



**Table 2.4.** Comparison of main differing features in the phenotypical characterisation and fatty acids cellular composition of ATCC 842<sup>T</sup>, DSM 292 and DSM 365. "W" = weak; "-" = very weak; "o" = no kit; range colour reaction in API ZYM kit = 0-5 where 3,4 and 5 can be considered positive results. Fatty acid values are expressed as a percentage of the total sum. "ND" = not detected

Kit name	Feature	ATCC 842 <sup>T</sup>	DSM 292	DSM 365
o	5% NaCl	W	-	W
o	35°C	W	W	+
o	TWEEN 80	W	-	+
API 20 E	Voges-Proskauer (VP)	W	+	+
API 50 CHB	Rhamnose	-	+	-
API 50 CHB	$\alpha$ -methyl-d-mannoside	-	+	-
API 20 NE	Malate assimilation	-	+	-
API ZYM	Alcaline Phosphatase	0.5	0.5	1
API ZYM	Leucine-Arylamidase	0	1	0
API ZYM	Chymotrypsin	0.5	0	0
API ZYM	Acid Phosphatase	0.5	0	0
API ZYM	Naphthol-AS-BI-	0.5	1	0.5
API ZYM	$\alpha$ -Galactosidase	1	1	2
API ZYM	$\beta$ -Galactosidase	3	4	5
API ZYM	$\beta$ -Glucosidase	0	0.5	0.5
Fatty acid		ATCC 842 <sup>T</sup>	DSM 365	DSM 292
	15:0 anteiso	46.7	61.3	61.6
	16:00	11.5	6.3	6.9
	15:0 iso	8.6	6.9	7.1
	17:0 anteiso	8.3	7.2	9
	16:0 iso	8.1	7	5.3
	17:0 iso	5.5	2.9	3.8
	16:1 w11c	4.1	2.4	0.9
	14:00	2.1	1.4	1.4
	14:0 iso	1.7	1.3	1
	15:00	0.8	1.8	1.9
	17:1 iso w11c	0.6	0.4	0.2
	16:1 ISO w10c	0.5	0.5	ND
	17:00	0.4	0.2	0.3
	17:1 w6c	0.3	ND	0.7

## 2.4 Discussion

MALDI-TOF MS has been widely introduced and applied in the last few years as an identification technique and an alternative rapid approach for typing and discriminating microbial strains at the subspecies level [25-27]. Such a technology allows obtaining a mass fingerprint profile for the analysed strain, enriched in highly abundant ribosomal proteins, which is compared with reference protein spectra contained in a database to assign an identification result.

Although ribosomal proteins are strongly conserved in the bacterial species, they may present modest variation at the microbial strain level [28]. Several authors proposed using the MALDI-TOF MS typing method coupled with statistical tools to classify and improve the identification and differentiation of phylogenetically closely related species [27,29-31]. Indeed, adopting such an approach allows for identifying a certain number of discriminative and reproducible biomarkers with a specificity at the subspecies level [32].

In this study, we exploited the potential of unsupervised classification methods coupled with proteomic fingerprinting analysis to explore the diversity of three strains belonging to *P. polymyxa*. *P. polymyxa* is one of the most extensively described and discussed species due to its wide applicability in the biotechnological and agricultural fields [2]. This is evidenced by an increasing number of patents and genome sequencing projects in recent years. A search for patents using the genus *Paenibacillus* or the species *polymyxa* as query words returns 6,428 and 2,477 results, respectively (<https://worldwide.espacenet.com>). To date, the number of *P. polymyxa* genome sequencing projects available on NCBI and the Genome Taxonomy Database (GTDB) are 93 and 95 (<https://gtdb.ecogenomic.org/>), respectively. The increasing number of genome sequencing projects may reflect the need to retrieve functional information from the genetic code and even solve the intrinsic taxonomic complexity of the *Paenibacillus* genus and *polymyxa* species [233].

In addition, several works based on MALDI-TOF MS analysis have interested the genus *Paenibacillus* in recent years. Most of them focused on the identification, detection and typing of strains associated with pathogenicity potential and food

spoilage [34-35], production of antimicrobial compounds [36] and interaction with the plant [37].

The number and quality of reference spectra within the instrument database can greatly influence the success rate of identification using the proteomic approach [38]. The current Bruker Daltonics database contains 251 MSPs of *Paenibacillus* and ten profiles of *P. polymyxa*. These include the reference spectra of *P. polymyxa* ATCC 842<sup>T</sup>, DSM 365 and DSM 292.

In this study, the preliminary identification of the purchased *P. polymyxa* cultures with the manufacturer's database was inconclusive for *P. polymyxa* DSM 365 and DSM 292. In fact, the matching with their reference spectra did not reach the minimum log(score) required for a reliable identification at the species level. It is possible that the mass spectra of the two bacterial strains included in the database are still not sufficiently reproducible and should be updated with two new versions. Similarly, the strain ATCC 842<sup>T</sup> matched best to a more recent version of the DSM 36T reference spectrum (DSM 36T DSM\_2) (**Figure 2.1**). We also noticed marked differences when comparing the profiles of the DSM 365 and the DSM 292 with the reference spectrum of the DSM 36T type strain in the database. These findings led us to further investigate the observed divergence by comparing their mass fingerprints. Subsequent statistical analyses confirmed the observed differences and revealed different discriminating biomarkers among the three *Paenibacillus polymyxa*. The mass distribution of the *P. polymyxa* strains by PCA clearly showed three distinct clusters, most influenced by different markers whose expression pattern was characteristic of each of the strains. According to the gel view observation (**Figure 2.2**) and the list of discriminatory peaks selected in the W/KW analysis, ATCC 842<sup>T</sup> showed several biomarkers with higher intensity than DSM 365 and DSM 292 (**Table 2.1**). In addition, we noticed that peak  $m/z$  2,987 (**Table 2.1**) was consistently expressed in both profiles of ATCC 842<sup>T</sup> and DSM 365 but was remarkably low in DSM 292. This finding suggested that even very low-intensity signals can act as critical discriminators in mass comparisons. Some of these peaks ( $m/z$  2,400,  $m/z$  2,685,  $m/z$  2,987; **Figure 2.3**) fall in a variable region of the mass spectrum below  $m/z$  3,000 that is correlated with no ribosomal peptides, metabolites and lipopeptides production, known antimicrobial

compounds produced by several microbial species, including *P. polymyxa* [39-41]. Several authors have investigated such a region in the mass spectra of *P. polymyxa* by MALDI-TOF MS to detect and characterise lipopeptides, antibiotics or volatile compounds [42-44]. Interestingly, peaks  $m/z$  2,400 and 2,685 were strongly present in the spectrum of ATCC 842<sup>T</sup> but almost absent in DSM 292 and DSM 365. These results may reveal a different pattern of secondary metabolite production among the three strains. Based on this assumption, we believe that analysis and comparison focused on the low-mass region ( $m/z$  500-3,000) could potentially reveal additional differences, better supporting the description of biodiversity and even strain differentiation [39,45].

Moreover, considering the nature of our investigation into closely related species classification, it is worth noting that the analysis of the lower  $m/z$  range (up to  $m/z$  2,000) not only pertains to small peptides, as initially discussed, but also encompasses lipids. While our study primarily employed proteomics and genomics approaches, it is crucial to acknowledge that there exists a third option, namely MALDI lipidomics, which can offer valuable insights into the composition and variations of lipids within the studied strains [46-47]. This additional dimension of analysis could provide further support for the reliable classification of closely related species and enhance the comprehensiveness of our findings.

On the other hand, the presence of discriminant peaks in the region above  $m/z$  3,000 supported the consistency of the discriminant biomarkers that emerged from the statistical analysis of *P. polymyxa* mass spectra. Indeed, the core region of the fingerprint profile is less variable and is associated with highly abundant ribosomal subunit proteins, small-acid soluble proteins and conserved protein domains [48-49]. We found several peaks in this region that showed significant differences in the average intensity between the fingerprint profiles of the three *P. polymyxa* strains (**Figure 2.3, Table 2.1**). For example, the region from  $m/z$  5,505 to  $m/z$  5,618 proved to be very informative as it was characterised by high-intensity ATCC 842<sup>T</sup> spectrum signals.

From the list of informative peaks, we identified  $m/z$  2,944,  $m/z$  2,874 and  $m/z$  3,314 as potentially good descriptors of all classes simultaneously (**Table 2.1**).

Our assumption was then confirmed by the peak selection of the QC model (**Table 2.3**). On the other hand, we found that the SNN classification model behaved differently by selecting a list of three markers, each of which was highly informative for one of the three classes (**Table 2.3**). The reproducibility of the observed discriminative biomarkers and, consequently, the reliability of such classification models was definitively confirmed by the simultaneous discrimination of all three strains observed with the external dataset. According to these results, we believe that both models should be applied to classify and predict the future identification of new *P. polymyxa* strains.

MALDI-TOF MS identification is often considered culture-independent and relies heavily on signals derived from ribosomal proteins, which constitute a substantial portion of the spectra. However, it's important to note that less abundant proteins or signals can also play a crucial role in achieving strain-level differentiation [50-51]. These less abundant signals may not necessarily be of ribosomal origin, and the culture conditions, such as the culture medium, can indeed influence their abundance. In our study, the mass spectra analyzed were obtained by cultivating the three strains in the same growth medium and environment. While this approach was essential for the direct comparison of the strains, we acknowledge that it may introduce certain limitations. The uniform culture conditions might not fully represent the potential variations that could occur in different conditions. To address this aspect, it will be necessary in future research to repeat the discriminative analysis in the presence of different growth media or environmental conditions. This approach will help clarify the origin of the discriminative peaks and confirm which ones are indeed attributable to minor alterations in ribosomal protein genes.

The relationship between the three strains was further investigated using the ANI calculation in order to assess and verify the MALDI-TOF MS results obtained. Currently, comparative analysis of fully sequenced microbial genomes is the most successful tool for exploring and assessing molecular differences between microbial strains [52]. Several papers have reported the use of such an approach to distinguish closely related microorganisms through rigorous workflow procedures, including genome sequencing, contigs assembly, annotation, and

typing of the compared sequences [53-54]. Complementing the MALDI-TOF MS data with the genome sequence comparison of the three strains, we realised that the observed differences in their mass fingerprint profiles were also reflected in the genetic differences between the three strains. Indeed, from a genetic point of view, both *P. polymyxa* DSM 365 and DSM 292 are clearly distinguishable from ATCC 842<sup>T</sup>, e.g., considering ANI. Otherwise, there were less remarkable differences in the taxonomic relatedness of DSM 292 and DSM 365, as the ANI value was close to the threshold. Similarly, based on the fold change values, we found that both strains shared closer mean intensity values for most of the more significant markers than the ATCC 842<sup>T</sup>. Indeed, when comparing DSM 292 and DSM 365 with ATCC 842<sup>T</sup>, only four and five peaks respectively had a fold change as log<sub>2</sub> between 0 and 1 (as absolute values). On the contrary, the comparison between DSM 292 and DSM 365 resulted in nine discriminant peaks having a fold change as log<sub>2</sub> between 0 and 1 (as absolute values).

We also noted a more remarkable discriminatory power and sensitivity of the MALDI-TOF MS-based system compared to other phenotypic typing approaches used in this work. Analysis of substrate utilisation and comparison of fatty acid profiles did not reveal desirable features for a comprehensive description of intraspecific diversity. Indeed, all strains shared similar morphological and biochemical traits with few exceptions (**Table 2.4**, **Table S 2.4**, **Table S 2.5**, **Table S 2.6**, **Table S 2.7**, **Table S 2.8**). Regarding substrate utilisation, we found that ATCC 842<sup>T</sup> and DSM 292, unlike DSM 365, were unable to utilise rhamnose,  $\alpha$ -methyl-d-mannoside and malate. In addition, according to the semiquantitative enzymatic analysis, naphthol-AS-BI-Phosphohydrolase and  $\beta$ -Galactosidase activities appeared to be different in all three strains. Although such positive results, these results should be considered as preliminary and should be confirmed by specific quantitative enzymatic assays.

All these results provide new insights into the genomic diversity of these *P. polymyxa* strains. They could set the stage for a more comprehensive genomic study involving a larger number of strains. The classification of *P. polymyxa*, according to the framework of the GTDB, could help to select the representative strains according to genome phylogeny and intra-specific clustering.

Furthermore, we expect that future investigations on new bacterial isolates by MALDI-TOF MS analysis and classification algorithms can help to enrich *P. polymyxa* clusters, thus improving the richness and identification resolution of the *in-house* database.

In conclusion, the MALDI-TOF MS analysis performed in this study revealed disagreement in the identification assignment of DSM 365 and DSM 292 to the *P. polymyxa* species, along with notable differences in their mass spectra compared to ATCC 842<sup>T</sup>. These disagreements were corroborated by genetic analyses, reinforcing the consistency of the proteomic findings. Although this evidence was obtained for a limited set of strains, we believe that MALDI-TOF MS analysis, coupled with statistical tools, has considerable potential to study and compare large microbial datasets. Genome sequencing and comparison can be challenging, requiring highly skilled personnel and costly when dealing with large microbial data collections [55]. The application of such an approach could precede genomic analyses as a kind of predictive tool, helping to gain a greater awareness of the biodiversity contained in any microbial collection and highlighting interesting discrepancies between closely related strains that need to be investigated further with a targeted, in-depth approach. The predictive potential of this tool would allow time-consuming and costly efforts to be avoided if there are no factual assumptions that justify further comparative investigations.

## 2.5 Methods

### 2.5.1 Strain culture condition

For the present study, three bacterial strains belonging to *Paenibacillus polymyxa* species were studied: ATCC 842<sup>T</sup>, DSM 292 and DSM 365. *Paenibacillus polymyxa* ATCC 842<sup>T</sup> (= DSM 36<sup>T</sup>; =KCTC 3858<sup>T</sup>), the type strain of *P. polymyxa* and family *Paenibacillaceae*, was purchased from the American Type Culture Collection (ATCC). *P. polymyxa* DSM 292 (= CCM 1609; LMG 6320) and *P. polymyxa* DSM 365 were acquired from Deutsche Sammlung von Mikroorganismen und Zellkulturen (DSMZ), Braunschweig, Germany. All bacterial cultures were recovered from lyophilised vials onto Tryptic Soy Agar (TSA; Sigma Aldrich, United Kingdom) and grew at least for 24 hours at 30°C.

Next, single colonies were streaked on fresh TSA plates, incubated at 30°C for 16 hours, and identified by 16S rRNA and MALDI-TOF MS before further investigation studies.

### **2.5.2 MALDI-TOF MS analysis: sample preparation and identification**

Prior MALDI-TOF MS measurements, bacterial samples were processed according to the manufacturer's instruction, following the extraction method. Briefly, for each bacterial culture ~0.1 mg of cell material was directly transferred from a single colony to 1.5 ml tubes containing 300 µL sterile water. Following that, the bacterial samples were dissolved and then inactivated by the addition of 900 µL of absolute ethanol solution, with thorough mixing.

The bacterial samples were then centrifuged at 15,000 rpm for two minutes, and the obtained pellets were dried at room temperature for one hour and treated with an equal volume (approximately 25 µL) of 70% formic acid (FA) and acetonitrile (ACN) to extract proteins for acquisition of mass spectra.

For the analysis, one µL of supernatant was spotted on the MSP 96 polished steel target plate (3 biological and five technical replicates, totalising 15 spots per strain), air-dried and overlaid with 1 µL of 4HCCA matrix solution (10 mg/ml of alpha-cyano-4-hydroxycinnamic acid dissolved in a solution of 50% ACN and 2.5% trifluoroacetic acid [TFA], Sigma-Aldrich, Milan, Italy) to permit sample ionization [56].

The mass spectrum profile of each strain was acquired by Bruker Microflex™ LT MALDI-TOF mass spectrometer (Bruker Daltonics, Bremen, Germany) equipped with a 60 Hz nitrogen laser, using FlexControl™ software (v 3.4; Bruker Daltonik GmbH, Bremen, Germany) in a positive linear mode within a mass range from 1,960 to 22,000 dalton. According to the manufacturer's instructions, system calibration was performed using the Bruker Bacterial Test Standard (BTS, Bruker Daltonics, Germany) solution able to cover a mass range of spectra acquisition between 3,6 and 17 kDa. Data processing was performed automatically by MBT Compass 4.1.100.10 software (Bruker Daltonik GmbH, Bremen, Germany), and the mass spectra were matched against the instrument library provided by Bruker



Daltonik (MBT compass library v 11.0.0.0). The library included a list of 10,833 bacterial reference spectra, containing 86 reference spectra belonging to the *Paenibacillus* genus and 10 grasping to *P. polymyxa* species. The MSPs of *P. polymyxa* ATCC 842<sup>T</sup> (= DSM 36T 2), *P. polymyxa* DSM 365, and *P. polymyxa* DSM 292 were already present as reference spectra inside the MBT compass library.

The assessment of the spectra quality was carried out by FlexAnalysis (v 3.4; Bruker Daltonik GmbH, Bremen, Germany), a software for spectra processing (smoothing, baseline subtraction and intensity normalisation) that allows removing all flatline spectra or those with outlier peaks. Next to the quality check step, the spectra were then analysed with the MBT Compass Explorer 4.100.1 module (Bruker Daltonik GmbH, Bremen, Germany) to confirm the identification results obtained with automatic data processing and to observe the graphical representation of the match between the analysed strain and the reference MSPs. The software assigned identification results according to the (log)score value resulting from the matching degree of the unknown spectrum with the MSPs of the Bruker taxonomy. According to manufacturer interpretation, (log)score values between 2.00 and 3.00 and 1.70 - 1.99 indicated a high- and low- confidence identification, respectively [57]. Lower (log)score values meant that no microorganism identification was possible [57].

### **2.5.3 Statistical analysis of mass spectra**

The fifteen spectra of ATCC 842<sup>T</sup>, DSM 292, and DSM 365 were loaded into the Clinprotocols software (v 3.0; Bruker Daltonics, Bremen, Germany) to visualise strain-level variations and select discriminant biomarkers among the analysed classes [3158]. The raw spectra of ATCC 842<sup>T</sup>, DSM 292, and DSM 365 were fed into the software as three distinct subsets of mass data. Before loading the mass data, spectra preparation parameters were set as follows: resolution = 800; baseline subtraction by top hat baseline method; mass range (m/z) for analysis from 2,000 to 15,000; noise threshold = 2, recalibration = 1,000 ppm for maximal peak shift and 30% match to calibrant peaks. Moreover, peak calculation settings

were adjusted as follows: peak picking on the total average spectrum with a signal-to-noise threshold equal to 5.

Next, the following steps were performed for mass spectra preparation of all three classes: recalibration, average peak list calculation, and peak calculation. The first command allows reducing the mass shifts that occur during the spectra acquisition and excluding from the analysis all those spectra that do not satisfy the corresponding settings adjusted in spectra preparation parameters. After the recalibration step, a total average spectrum from the remaining individual spectra is calculated for each class. Thus, the software compared the generated average spectra for ATCC 842<sup>T</sup>, DSM 292, and DSM 365, and an average peak list table was created. The resulting peaks in such a list were used to retrieve characteristic peaks in the statistical analysis as well as for classification model generation. The analysis of characteristic peaks among ATCC 842<sup>T</sup>, DSM 292, and DSM 365 mass spectra was performed through three statistical approaches: multivariate unsupervised PCA, p-value calculation in the average peak list, and supervised algorithms generation.

All the spectra were imported into the software to observe strain clustering by means of PCA analysis. The results of the PCA were visualised in the scores and loadings plots according to the first two components (PC1 and PC2), which explain most of the variance in the dataset (PC1 = 58% and PC2 = 20%).

Characteristic peaks among ATCC 842<sup>T</sup>, DSM 292, and DSM 365 were selected and sorted through the following statistical tests: t-test, analysis of variance (ANOVA), the Wilcoxon or Kruskal-Wallis (W/KW), and the Anderson-Darling (AD) test. The P-value cut-off was set at 0.05. First, the p-value of the AD test was calculated. More in detail, if the p-value in the AD test was > 0.05, the interesting peaks were selected among those having a p-value  $\leq$  0.05 in ANOVA analysis. Whereas, if the p-value in the AD test was  $\leq$  0.05, the selection was made among those having a p-value  $\leq$  0.05 in the W/KW [59]. Then, the characteristic peaks that best described the fingerprint of each strain were identified by the log base two ( $\log_2$  times the change) of the ratio between the average peak intensities of the two strains under comparison (**Table 2.1**).

Moreover, Classification models were generated by ClinProTools software using the following algorithms: QC, SNN, and GA\_KNN to obtain systematic and objective strain discrimination. In the GA, the following parameters were set: maximal number of peaks in the model (= 30), number of generations (= 50), and number of nearest neighbors in KNN classification (= 1 for KNN1; = 3 for KNN3; = 5 KNN5). In the QC algorithm, the sort/weight mode was set according to the p-value of W/KW. Each algorithm selects a list of peaks that are the most relevant in the separation of the strains. All models were validated using independent test data sets representing the classes. The external data sets for cross-validation were composed of 21 mass spectra replicates for ATCC 842<sup>T</sup> and 20 for DSM 292 and DSM 365 selected from an independent analysis after assessing spectra quality by FlexAnalysis software (v 3.4; Bruker Daltonik GmbH, Bremen, Germany). According to the results, the model prediction capabilities were obtained by calculating the accuracy, sensitivity, and specificity.

The external data sets were also used to create the reference MSPs of DSM 292 and DSM 365 inside the *in-house* reference library. Subsequently, the identification results of the previously acquired fifteen spectra were reevaluated using the MBT Compass Explorer 4.100.1 module (Bruker Daltonik GmbH, Bremen, Germany). This reevaluation aimed to assess the impact of the library implementation with the new reference MSPs on the identification process of DSM 292 and DSM 365.

#### **2.5.4 16S rRNA sequence analysis**

The DNA was purified from an overnight culture of the strains ATCC 842<sup>T</sup>, DSM 292 and DSM 365 by means of the Wizard Genomic DNA purification Kit (Promega). The 16S rRNA gene was amplified with the primers E8F [60] and E1541R [60], and the PCR product was Sanger sequenced with the primers E27F [61] and E1492R [61]. The electropherograms were analysed and assembled by means of BioNumerics 7.6, IUPAC degenerate nucleotide codes were inserted at uncertain peaks. The obtained sequence (GenBank Acc. No. OR506150, OR506151, OR506152) was compared in the EzBioCloud database. The most related species belonging to the *P. polymixa* group in the EzBiocloud database

came from Sanger sequencing of PCR products (GenBank Acc. No. AF273740; AF391124; AJ320494; MH842737.1), except from three sequences retrieved from genomes: *P. polymyxa* ATCC 842<sup>T</sup> (GenBank Acc. No: AFOX01000032:1540-65, on contig 32) and the only non type strain in the EzBioCloud *P. polymyxa* E681 (GenBank Acc. No CP000154: 2525414-2526891) and *Paenibacillus kribbensis* AM49 (GenBank Acc. No. CP020028: 618273-619838).

### **2.5.5 Comparative genomics**

The RefSeq assembly genome sequences GCF\_903797665.1 (*P. polymyxa* ATCC 842<sup>T</sup>), GCF\_900109125.1 (*P. polymyxa* DSM 292), and GCF\_000714835.1 (*P. polymyxa* DSM 365) were used to calculate the Average Nucleotide Identity (ANI) with the OrthoANI algorithm through the OAT software, which measures the overall similarity between two genomes without gene-finding and functional annotation steps [62].

### **2.5.6 Phenotypical test and fatty acids cellular composition profiles**

Morphological characterisation, temperature optimum, salt tolerance, API gallery tests, and fatty acids cellular composition profiles were carried out by DSMZ Services, Leibniz Institut DSMZ - Deutsche Sammlung von Mikroorganismen und Zellkulturen GmbH, Braunschweig, Germany.

The fatty acids profile was analysed by gas chromatography of fatty methyl esters (GC-FAME), using minor modifications of the method of Miller [63] and Kuykendall *et al.* [64].

Biochemical characterisation, including the analysis of different substrate utilisation and enzyme production, was performed through API 50 CHB, API 20E, API 20NE, and API ZYM systems (Biomérieux) according to the manufacturer's instructions.

## References

- [1] Patowary, R., & Deka, H. (2020). *Paenibacillus Beneficial Microbes in Agro-Ecology* (pp. 339-361): Elsevier.
- [2] Grady, E. N., MacDonald, J., Liu, L., Richman, A., & Yuan, Z.-C. Current knowledge and perspectives of *Paenibacillus*: a review. *Microbial cell factories* **15**, 1-18 (2016)
- [3] Kwak, M.-J., Choi, S.-B., Ha, S.-M., Kim, E. H., Kim, B.-Y., & Chun, J. Genome-based reclassification of *Paenibacillus jamilae* Aguilera et al. 2001 as a later heterotypic synonym of *Paenibacillus polymyxa* (Prazmowski 1880) Ash et al. 1994. *International Journal of Systematic and Evolutionary Microbiology* **70**, 3134-3138 (2020)
- [4] Ash, C., Priest, F. G., & Collins, M. D. Molecular identification of rRNA group 3 bacilli (Ash, Farrow, Wallbanks and Collins) using a PCR probe test. *Antonie Van Leeuwenhoek* **64**, 253-260 (1993)
- [5] Langendries, S., & Goormachtig, S. *Paenibacillus polymyxa*, a Jack of all trades. *Environmental Microbiology* **23**, 5659-5669 (2021)
- [6] Lal, S., & Tabacchioni, S. Ecology and biotechnological potential of *Paenibacillus polymyxa*: a minireview. *Indian journal of microbiology* **49**, 2-10 (2009)
- [7] Liu, X., Li, Q., Li, Y., Guan, G., & Chen, S. *Paenibacillus* strains with nitrogen fixation and multiple beneficial properties for promoting plant growth. *PeerJ* **7**, e7445 (2019)
- [8] Coelho, M. R. R., von der Weid, I., Zahner, V., & Seldin, L. Characterization of nitrogen-fixing *Paenibacillus* species by polymerase chain reaction–restriction fragment length polymorphism analysis of part of genes encoding 16S rRNA and 23S rRNA and by multilocus enzyme electrophoresis. *FEMS Microbiology Letters* **222**, 243-250 (2003)
- [9] Lal, S., Chiarini, L., & Tabacchioni, S. (2016). New insights in plant-associated *Paenibacillus* species: biocontrol and plant growth-promoting activity *Bacilli and Agrobiotechnology* (pp. 237-279): Springer.
- [10] Raza, W., Yang, W., & Shen, Q. *Paenibacillus polymyxa*: antibiotics, hydrolytic enzymes and hazard assessment. *Journal of Plant Pathology*, 419-430 (2008)
- [11] Daud, N. S., Rosli, M. A., Azam, Z. M., Othman, N. Z., & Sarmidi, M. R. *Paenibacillus polymyxa* bioactive compounds for agricultural and biotechnological applications. *Biocatalysis and Agricultural Biotechnology* **18**, 101092 (2019)
- [12] Tinôco, D., Pateraki, C., Koutinas, A. A., & Freire, D. M. Bioprocess Development for 2, 3-Butanediol Production by *Paenibacillus* Strains. *ChemBioEng Reviews* **8**, 44-62 (2021)

- [13] Dias, B. d. C., Lima, M. E. d. N. V., Vollú, R. E., et al. 2, 3-Butanediol production by the non-pathogenic bacterium *Paenibacillus brasilensis*. *Applied Microbiology and Biotechnology* **102**, 8773-8782 (2018)
- [14] Białkowska, A. M. Strategies for efficient and economical 2, 3-butanediol production: new trends in this field. *World Journal of Microbiology and Biotechnology* **32**, 1-14 (2016)
- [15] Xie, N.-Z., Li, J.-X., Song, L.-F., et al. Genome sequence of type strain *Paenibacillus polymyxa* DSM 365, a highly efficient producer of optically active (R, R)-2, 3-butanediol. *Journal of Biotechnology* **195**, 72-73 (2015)
- [16] Kumar, S., & Ujor, V. C. Complete Genome Sequence of *Paenibacillus polymyxa* DSM 365, a Soil Bacterium of Agricultural and Industrial Importance. *Microbiology Resource Announcements*, e00329-00322 (2022)
- [17] Leibniz Institute DSMZ-German Collection of Microorganisms and Cell Cultures GmbH. (2023) Retrieved 08/31/2023, 2023, from <https://www.dsmz.de/collection/catalogue/details/culture/DSM-365>
- [18] Park, K. Y., Seo, S. Y., Oh, B.-R., Seo, J.-W., & Kim, Y. J. 2, 3-Butanediol induces systemic acquired resistance in the plant immune response. *Journal of Plant Biology* **61**, 424-434 (2018)
- [19] Heinze, S., Lagkouvardos, I., Liebl, W., Schwarz, W. H., Kornberger, P., & Zverlov, V. V. Draft Genome Sequence of *Paenibacillus polymyxa* DSM 292, a Gram-Positive, Spore-Forming Soil Bacterium with High Biotechnological Potential. *Microbiology Resource Announcements* **9**, e00071-00020 (2020)
- [20] Heinze, S., Zimmermann, K., Ludwig, C., et al. Evaluation of promoter sequences for the secretory production of a *Clostridium thermocellum* cellulase in *Paenibacillus polymyxa*. *Applied Microbiology and Biotechnology* **102**, 10147-10159 (2018)
- [21] Weis, C. V., Jutzeler, C. R., & Borgwardt, K. Machine learning for microbial identification and antimicrobial susceptibility testing on MALDI-TOF mass spectra: a systematic review. *Clinical Microbiology and Infection* **26**, 1310-1317 (2020)
- [22] Holland, J. H. (1992). *Adaptation in natural and artificial systems: an introductory analysis with applications to biology, control, and artificial intelligence*: MIT press.
- [23] Chun, J., Oren, A., Ventosa, A., et al. Proposed minimal standards for the use of genome data for the taxonomy of prokaryotes. *International Journal of Systematic and Evolutionary Microbiology* **68**, 461-466 (2018)

- [24] Qadri, S., Nichols, C., Qadri, S., & Villarreal, A. Rapid test for acetyl-methylcarbinol formation by Enterobacteriaceae. *Journal of Clinical Microbiology* **8**, 463-464 (1978)
- [25] Pérez-Sancho, M., Vela, A. I., Horcajo, P., et al. Rapid differentiation of *Staphylococcus aureus* subspecies based on MALDI-TOF MS profiles. *Journal of Veterinary Diagnostic Investigation* **30**, 813-820 (2018)
- [26] Gekenidis, M.-T., Studer, P., Wüthrich, S., Brunisholz, R., & Drissner, D. Beyond the matrix-assisted laser desorption ionization (MALDI) biotyping workflow: in search of microorganism-specific tryptic peptides enabling discrimination of subspecies. *Applied and Environmental Microbiology* **80**, 4234-4241 (2014)
- [27] Huang, C.-H., & Huang, L. Rapid species- and subspecies-specific level classification and identification of *Lactobacillus casei* group members using MALDI Biotyper combined with ClinProTools. *Journal of Dairy Science* **101**, 979-991 (2018)
- [28] Suarez, S., Ferroni, A., Lotz, A., et al. Ribosomal proteins as biomarkers for bacterial identification by mass spectrometry in the clinical microbiology laboratory. *Journal of Microbiological Methods* **94**, 390-396 (2013)
- [29] Dematheis, F., Walter, M. C., Lang, D., et al. Machine Learning Algorithms for Classification of MALDI-TOF MS Spectra from Phylogenetically Closely Related Species *Brucella melitensis*, *Brucella abortus* and *Brucella suis*. *Microorganisms* **10**, 1658 (2022)
- [30] Kann, S., Sao, S., Phoeung, C., et al. MALDI-TOF mass spectrometry for sub-typing of *Streptococcus pneumoniae*. *BMC Microbiology* **20** (2020)
- [31] Manzulli, V., Rondinone, V., Buchicchio, A., et al. Discrimination of *Bacillus cereus* group members by MALDI-TOF mass spectrometry. *Microorganisms* **9**, 1202 (2021)
- [32] Croxatto, A., Prod'hom, G., & Greub, G. Applications of MALDI-TOF mass spectrometry in clinical diagnostic microbiology. *FEMS Microbiology Reviews* **36**, 380-407 (2012)
- [33] Jeong, H., Choi, S.-K., Ryu, C.-M., & Park, S.-H. Chronicle of a soil bacterium: *Paenibacillus polymyxa* E681 as a tiny guardian of plant and human health. *Frontiers in Microbiology* **10**, 467 (2019)
- [34] Celandroni, F., Salvetti, S., Gueye, S. A., et al. Identification and pathogenic potential of clinical *Bacillus* and *Paenibacillus* isolates. *PloS one* **11**, e0152831 (2016)
- [35] Kopcakova, A., Salamunova, S., Javorsky, P., et al. The Application of MALDI-TOF MS for a Variability Study of *Paenibacillus* larvae. *Veterinary Sciences* **9**, 521 (2022)

- [36] He, Z., Kislá, D., Zhang, L., Yuan, C., Green-Church, K. B., & Yousef, A. E. Isolation and identification of a *Paenibacillus polymyxa* strain that coproduces a novel lantibiotic and polymyxin. *Applied and Environmental Microbiology* **73**, 168-178 (2007)
- [37] Qi, S. S., Cnockaert, M., Carlier, A., & Vandamme, P. A. *Paenibacillus foliorum* sp. nov., *Paenibacillus phytohabitans* sp. nov., *Paenibacillus plantarum* sp. nov., *Paenibacillus planticolens* sp. nov., *Paenibacillus phytorum* sp. nov. and *Paenibacillus germinis* sp. nov., isolated from the *Arabidopsis thaliana* phyllosphere. *International Journal of Systematic and Evolutionary Microbiology* **71**, 004781 (2021)
- [38] Tarfeen, N., Nisa, K. U., & Nisa, Q. MALDI-TOF MS: application in diagnosis, dereplication, biomolecule profiling and microbial ecology. *Proceedings of the Indian National Science Academy* **88**, 277-291 (2022)
- [39] Shu, L.-J., & Yang, Y.-L. *Bacillus* Classification Based on Matrix-Assisted Laser Desorption Ionization Time-of-Flight Mass Spectrometry—Effects of Culture Conditions. *Scientific Reports* **7** (2017)
- [40] Malviya, D., Sahu, P. K., Singh, U. B., et al. Lesson from Ecotoxicity: Revisiting the Microbial Lipopeptides for the Management of Emerging Diseases for Crop Protection. *International Journal of Environmental Research and Public Health* **17**, 1434 (2020)
- [41] Jeong, H., Park, S.-Y., Chung, W.-H., et al. Draft genome sequence of the *Paenibacillus polymyxa* type strain (ATCC 842T), a plant growth-promoting bacterium. *Journal of Bacteriology* **193** (2011)
- [42] Vater, J., Herfort, S., Doellinger, J., Weydmann, M., Borriss, R., & Lasch, P. Genome mining of the lipopeptide biosynthesis of *Paenibacillus polymyxa* E681 in combination with mass spectrometry: discovery of the lipopeptide paenilipoheptin. *ChemBioChem* **19**, 744-753 (2018)
- [43] Vater, J., Niu, B., Dietel, K., & Borriss, R. Characterization of novel fusaricidins produced by *Paenibacillus polymyxa*-M1 using MALDI-TOF mass spectrometry. *Journal of the American Society for Mass Spectrometry* **26**, 1548-1558 (2015)
- [44] Mülner, P., Schwarz, E., Dietel, K., et al. Fusaricidins, Polymyxins and Volatiles Produced by *Paenibacillus polymyxa* Strains DSM 32871 and M1. *Pathogens* **10**, 1485 (2021)
- [45] Ha, M., Jo, H.-J., Choi, E.-K., Kim, Y., Kim, J., & Cho, H.-J. Reliable identification of *Bacillus cereus* group species using low mass biomarkers by MALDI-TOF MS. *J Microbiol Biotechnol.* **29**, 887-896 (2019)



- [46] Walczak-Skierska, J., Monedeiro, F., Maślak, E., & Złoch, M. Lipidomics Characterization of the Microbiome in People with Diabetic Foot Infection Using MALDI-TOF MS. *Anal Chem* **95**, 16251-16262 (2023)
- [47] Maślak, E., Arendowski, A., Złoch, M., et al. Silver Nanoparticle Targets Fabricated Using Chemical Vapor Deposition Method for Differentiation of Bacteria Based on Lipidomic Profiles in Laser Desorption/Ionization Mass Spectrometry. *Antibiotics* **12**, 874 (2023)
- [48] Shu, L. J., & Yang, Y. L. Bacillus Classification Based on Matrix-Assisted Laser Desorption Ionization Time-of-Flight Mass Spectrometry-Effects of Culture Conditions. *Sci Rep* **7**, 15546 (2017)
- [49] Ryzhov, V., & Fenselau, C. Characterization of the protein subset desorbed by MALDI from whole bacterial cells. *Analytical chemistry* **73**, 746-750 (2001)
- [50] Wieme, A. D., Spitaels, F., Aerts, M., De Bruyne, K., Van Landschoot, A., & Vandamme, P. Effects of growth medium on matrix-assisted laser desorption-ionization time of flight mass spectra: a case study of acetic acid bacteria. *Applied and Environmental Microbiology* **80**, 1528-1538 (2014)
- [51] Suarez, S., Ferroni, A., Lotz, A., et al. Ribosomal proteins as biomarkers for bacterial identification by mass spectrometry in the clinical microbiology laboratory. *Journal of Microbiological Methods* **94**, 390-396 (2013)
- [52] Vishnoi, A., Roy, R., & Bhattacharya, A. Comparative analysis of bacterial genomes: identification of divergent regions in mycobacterial strains using an anchor-based approach. *Nucleic Acids Research* **35**, 3654-3667 (2007)
- [53] Zhou, Y., Zhang, W., Wu, H., Huang, K., & Jin, J. A high-resolution genomic composition-based method with the ability to distinguish similar bacterial organisms. *BMC Genomics* **20** (2019)
- [54] Choo, S. W., Rishik, S., & Wee, W. Y. Comparative genome analyses of *Mycobacteroides immunogenum* reveals two potential novel subspecies. *Microbial Genomics* **6** (2020)
- [55] Maasz, G., Zrínyi, Z., Fodor, I., et al. Testing the Applicability of MALDI-TOF MS as an Alternative Stock Identification Method in a Cryptic Species Complex. *Molecules* **25**, 3214 (2020)
- [56] Rahi, P., Prakash, O., & Shouche, Y. S. Matrix-assisted laser desorption/ionization time-of-flight mass-spectrometry (MALDI-TOF MS) based microbial identifications: challenges and scopes for microbial ecologists. *Frontiers in Microbiology* **7**, 1359 (2016)

- [57] Wilson, D. A., Young, S., Timm, K., et al. Multicenter Evaluation of the Bruker MALDI Biotyper CA System for the Identification of Clinically Important Bacteria and Yeasts. *American Journal of Clinical Pathology* **147**, 623-631 (2017)
- [58] Elssner, T., & Kostrzewa, M. CLINPROT-a MALDI-TOF MS based system for biomarker discovery and analysis. *Clinic Proteomics* **8**, 167 (2006)
- [59] Stephens, M. A. EDF statistics for goodness of fit and some comparisons. *Journal of the American statistical Association* **69**, 730-737 (1974)
- [60] Baker, G., Smith, J. J., & Cowan, D. A. Review and re-analysis of domain-specific 16S primers. *Journal of Microbiological Methods* **55**, 541-555 (2003)
- [61] Soergel, D. A., Dey, N., Knight, R., & Brenner, S. E. Selection of primers for optimal taxonomic classification of environmental 16S rRNA gene sequences. *The ISME journal* **6**, 1440-1444 (2012)
- [62] Lee, I., Kim, Y. O., Park, S.-C., & Chun, J. OrthoANI: an improved algorithm and software for calculating average nucleotide identity. *International Journal of Systematic and Evolutionary Microbiology* **66**, 1100-1103 (2016)
- [63] Miller, L. T. Single derivatization method for routine analysis of bacterial whole-cell fatty acid methyl esters, including hydroxy acids. *Journal of Clinical Microbiology* **16**, 584-586 (1982)
- [64] Kuykendall, L., Roy, M., O'Neill, J., & Devine, T. Fatty acids, antibiotic resistance, and deoxyribonucleic acid homology groups of *Bradyrhizobium japonicum*. *International Journal of Systematic and Evolutionary Microbiology* **38**, 358-361 (1988)

## Supplementary material

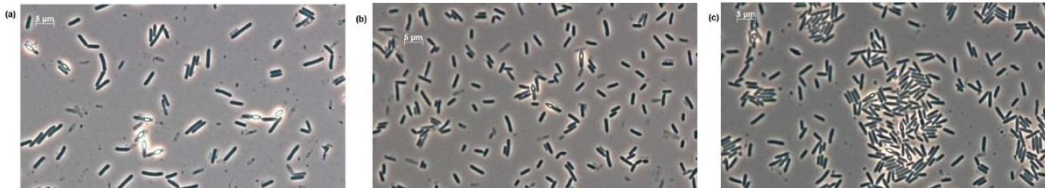


**Figure S 2.1.** Vegetative cells and endospore observation of (a) ATCC 842<sup>T</sup>, (b) DSM 292 and (c) DSM 365. The strains were grown at 28°C on M220 medium supplemented with MnSO<sub>4</sub> for 48 hours. Samples were examined by Axio Scope.A1 microscope (Zeiss) with objective oil len 100X. Pictures were made with Axio Cam MRc Zeiss using the Axiovision Rel 4.8. software. Scale bars represent 5 μm.

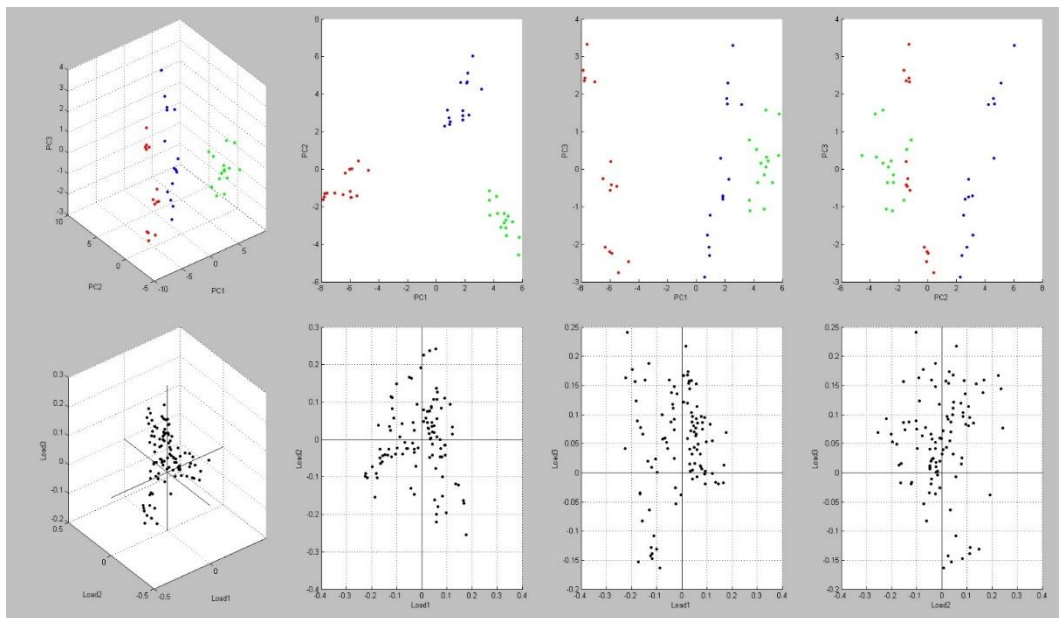


**Figure S 2.2.** Three- and two-dimensional principal component analysis and respective loadings plots of *P. polymyxa* ATCC 842<sup>T</sup> (red), DSM 292 (green), and DSM 365 (blue) strains.

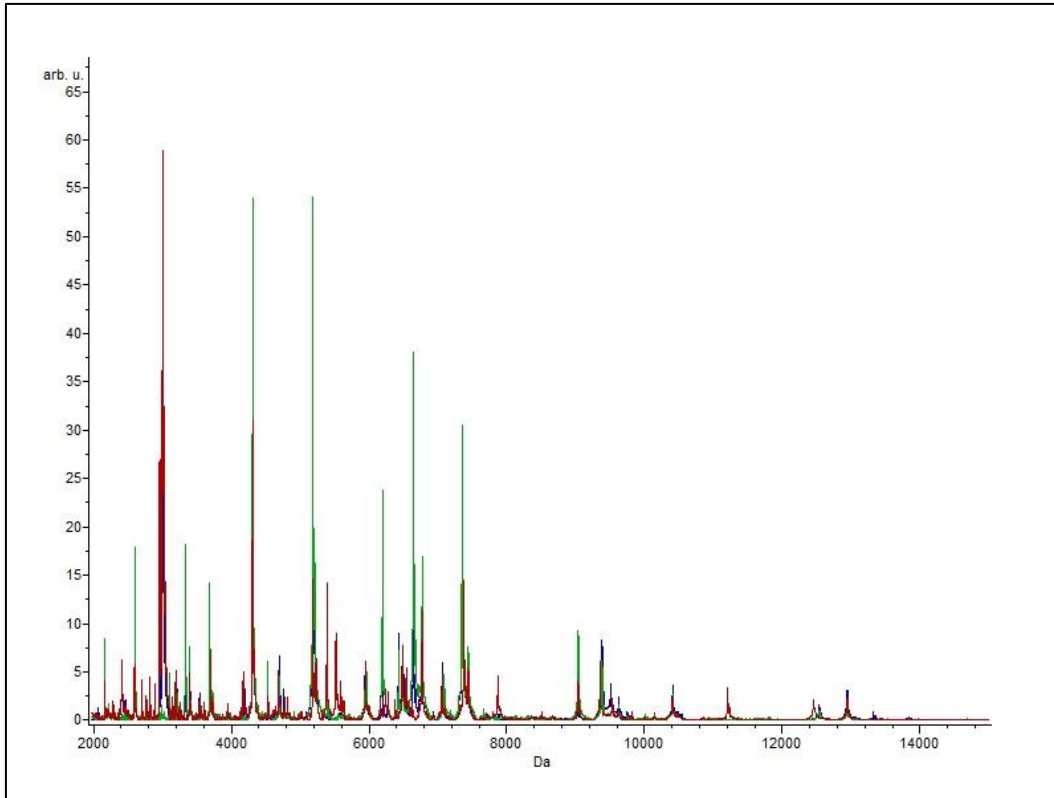


**Figure S 2.3.** Average spectra view of *P. polymyxa* ATCC 842<sup>T</sup> (red), DSM 292 (green) and DSM 365 (blue) generated through ClinProTools Software (v 3.0; Bruker Daltonics, Bremen, Germany) and processed following the standard data preparation workflow (baseline subtraction, normalisation, recalibration, average peak list calculation, and peak calculation).

**Table S 2.1.** Identification results for ATCC 842<sup>T</sup>, DSM 365, and DSM 292, using MBT Compass Library (v. 11.0.0.0). (Log)score values 2.00 - 3.00 indicate high-confidence identifications (green), 1.70 - 1.99 suggest low-confidence (yellow), and 0.00 - 1.69 (red) imply unfeasible organism identification.

Strain	No of Mass spectra	Identification	log(score)
ATCC 842 <sup>T</sup>	1	<i>P. polymyxa</i> DSM 36T DSM 2	2.14
ATCC 842 <sup>T</sup>	2	<i>P. polymyxa</i> DSM 36T DSM 2	2.03
ATCC 842 <sup>T</sup>	3	<i>P. polymyxa</i> DSM 36T DSM 2	2.25
ATCC 842 <sup>T</sup>	4	<i>P. polymyxa</i> DSM 36T DSM 2	2.2
ATCC 842 <sup>T</sup>	5	<i>P. polymyxa</i> DSM 36T DSM 2	2.14
ATCC 842 <sup>T</sup>	6	<i>P. polymyxa</i> DSM 36T DSM 2	2.01
ATCC 842 <sup>T</sup>	7	<i>P. polymyxa</i> DSM 36T DSM 2	1.85
ATCC 842 <sup>T</sup>	8	<i>P. polymyxa</i> DSM 36T DSM 2	2.07
ATCC 842 <sup>T</sup>	9	<i>P. polymyxa</i> DSM 36T DSM 2	2.16
ATCC 842 <sup>T</sup>	10	<i>P. polymyxa</i> DSM 36T DSM 2	1.98
ATCC 842 <sup>T</sup>	11	<i>P. polymyxa</i> DSM 36T DSM 2	2.22
ATCC 842 <sup>T</sup>	12	<i>P. polymyxa</i> DSM 36T DSM 2	2.21
ATCC 842 <sup>T</sup>	13	<i>P. polymyxa</i> DSM 36T DSM 2	2.22
ATCC 842 <sup>T</sup>	14	<i>P. polymyxa</i> DSM 36T DSM 2	2.18
ATCC 842 <sup>T</sup>	15	<i>P. polymyxa</i> DSM 36T DSM 2	2.14
DSM 365	1	<i>P. polymyxa</i> DSM 365 DSM	1.76
DSM 365	2	<i>P. polymyxa</i> DSM 365 DSM	1.99
DSM 365	3	<i>P. polymyxa</i> DSM 365 DSM	1.72
DSM 365	4	<i>P. polymyxa</i> DSM 365 DSM	1.87
DSM 365	5	<i>P. polymyxa</i> DSM 365 DSM	1.88
DSM 365	6	<i>P. polymyxa</i> DSM 365 DSM	1.77
DSM 365	7	<i>P. polymyxa</i> DSM 365 DSM	1.96
DSM 365	8	<i>P. polymyxa</i> DSM 365 DSM	1.78
DSM 365	9	<i>P. polymyxa</i> DSM 365 DSM	1.83
DSM 365	10	<i>P. polymyxa</i> DSM 365 DSM	1.84
DSM 365	11	<i>P. polymyxa</i> DSM 365 DSM	1.74
DSM 365	12	<i>P. polymyxa</i> DSM 365 DSM	1.82
DSM 365	13	<i>P. polymyxa</i> DSM 365 DSM	1.72
DSM 365	14	<i>P. polymyxa</i> DSM 365 DSM	1.69
DSM 365	15	<i>P. polymyxa</i> DSM 365 DSM	1.91
DSM 292	1	<i>P. polymyxa</i> DSM 292 DSM	1.84
DSM 292	2	<i>P. polymyxa</i> DSM 292 DSM	1.62
DSM 292	3	<i>P. polymyxa</i> DSM 292 DSM	1.74
DSM 292	4	<i>P. polymyxa</i> DSM 292 DSM	1.72
DSM 292	5	<i>P. polymyxa</i> DSM 292 DSM	1.42
DSM 292	6	<i>P. polymyxa</i> DSM 292 DSM	1.82
DSM 292	7	<i>P. polymyxa</i> DSM 292 DSM	1.39
DSM 292	8	<i>P. polymyxa</i> DSM 292 DSM	1.6
DSM 292	9	<i>P. polymyxa</i> DSM 292 DSM	1.67
DSM 292	10	<i>P. polymyxa</i> DSM 292 DSM	1.71
DSM 292	11	<i>P. polymyxa</i> DSM 292 DSM	1.61
DSM 292	12	<i>P. polymyxa</i> DSM 292 DSM	1.83
DSM 292	13	<i>P. polymyxa</i> DSM 292 DSM	1.72
DSM 292	14	<i>P. polymyxa</i> DSM 292 DSM	1.73
DSM 292	15	<i>P. polymyxa</i> DSM 292 DSM	1.63

**Table S 2.2.** Comparison of DSM 365 and DSM 292 mass spectra with the type strain profile *P. polymyxa* DSM 36T DSM 2 in MBT Compass Library (v. 11.0.0.0). (Log)score values 2.00 - 3.00 indicate high-confidence identifications (green), 1.70 - 1.99 suggest low-confidence (yellow), and 0.00 - 1.69 (red) imply unfeasible organism identification.

Strain	No of Mass spectra	Identification	log(score)
DSM 365	1	<i>P. polymyxa</i> DSM 36T DSM 2	1,86
DSM 365	2	<i>P. polymyxa</i> DSM 36T DSM 2	1,89
DSM 365	3	<i>P. polymyxa</i> DSM 36T DSM 2	1,7
DSM 365	4	<i>P. polymyxa</i> DSM 36T DSM 2	1,8
DSM 365	5	<i>P. polymyxa</i> DSM 36T DSM 2	1,67
DSM 365	6	<i>P. polymyxa</i> DSM 36T DSM 2	1,52
DSM 365	7	<i>P. polymyxa</i> DSM 36T DSM 2	1,7
DSM 365	8	<i>P. polymyxa</i> DSM 36T DSM 2	1,62
DSM 365	9	<i>P. polymyxa</i> DSM 36T DSM 2	1,92
DSM 365	10	<i>P. polymyxa</i> DSM 36T DSM 2	1,73
DSM 365	11	<i>P. polymyxa</i> DSM 36T DSM 2	1,64
DSM 365	12	<i>P. polymyxa</i> DSM 36T DSM 2	1,8
DSM 365	13	<i>P. polymyxa</i> DSM 36T DSM 2	1,64
DSM 365	14	<i>P. polymyxa</i> DSM 36T DSM 2	1,63
DSM 365	15	<i>P. polymyxa</i> DSM 36T DSM 2	1,61
DSM 292	1	<i>P. polymyxa</i> DSM 36T DSM 2	1,74
DSM 292	2	<i>P. polymyxa</i> DSM 36T DSM 2	1,71
DSM 292	3	<i>P. polymyxa</i> DSM 36T DSM 2	1,64
DSM 292	4	<i>P. polymyxa</i> DSM 36T DSM 2	1,47
DSM 292	5	<i>P. polymyxa</i> DSM 36T DSM 2	1,76
DSM 292	6	<i>P. polymyxa</i> DSM 36T DSM 2	1,47
DSM 292	7	<i>P. polymyxa</i> DSM 36T DSM 2	1,22
DSM 292	8	<i>P. polymyxa</i> DSM 36T DSM 2	1,05
DSM 292	9	<i>P. polymyxa</i> DSM 36T DSM 2	1,47
DSM 292	10	<i>P. polymyxa</i> DSM 36T DSM 2	1,7
DSM 292	11	<i>P. polymyxa</i> DSM 36T DSM 2	1,65
DSM 292	12	<i>P. polymyxa</i> DSM 36T DSM 2	1,85
DSM 292	13	<i>P. polymyxa</i> DSM 36T DSM 2	1,65
DSM 292	14	<i>P. polymyxa</i> DSM 36T DSM 2	1,63
DSM 292	15	<i>P. polymyxa</i> DSM 36T DSM 2	1,68

**Table S 2.3.** Identification results for DSM 365 and DSM 292 compared to their own MSPs and reference spectra in MBT Compass Library (v. 11.0.0.0). (Log)score values 2.00 - 3.00 indicate high-confidence identifications (highlighted in green), 1.70 - 1.99 suggest low-confidence (highlighted in yellow), and 0.00 - 1.69 (in red) imply unfeasible organism identification.

Strain	No of Mass spectra	Identification	log(score)
DSM 365	1	<i>P. polymyxa</i> DSM 365	2.27
		<i>P. polymyxa</i> DSM 365 DSM	1.76
DSM 365	2	<i>P. polymyxa</i> DSM 365	2.29
		<i>P. polymyxa</i> DSM 365 DSM	1.99
DSM 365	3	<i>P. polymyxa</i> DSM 365	2.26
		<i>P. polymyxa</i> DSM 365 DSM	1.72
DSM 365	4	<i>P. polymyxa</i> DSM 365	2.21
		<i>P. polymyxa</i> DSM 365 DSM	1.87
DSM 365	5	<i>P. polymyxa</i> DSM 365	2.3
		<i>P. polymyxa</i> DSM 365 DSM	1.88
DSM 365	6	<i>P. polymyxa</i> DSM 365	2.22
		<i>P. polymyxa</i> DSM 365 DSM	1.77
DSM 365	7	<i>P. polymyxa</i> DSM 365	2.28
		<i>P. polymyxa</i> DSM 365 DSM	1.96
DSM 365	8	<i>P. polymyxa</i> DSM 365	2.3
		<i>P. polymyxa</i> DSM 365 DSM	1.78
DSM 365	9	<i>P. polymyxa</i> DSM 365	2.19
		<i>P. polymyxa</i> DSM 365 DSM	1.83
DSM 365	10	<i>P. polymyxa</i> DSM 365	2.26
		<i>P. polymyxa</i> DSM 365 DSM	1.84
DSM 365	11	<i>P. polymyxa</i> DSM 365	2.28
		<i>P. polymyxa</i> DSM 365 DSM	1.74
DSM 365	12	<i>P. polymyxa</i> DSM 365	2.23
		<i>P. polymyxa</i> DSM 365 DSM	1.82
DSM 365	13	<i>P. polymyxa</i> DSM 365	2.11
		<i>P. polymyxa</i> DSM 365 DSM	1.72
DSM 365	14	<i>P. polymyxa</i> DSM 365	2.28
		<i>P. polymyxa</i> DSM 365 DSM	1.69
DSM 365	15	<i>P. polymyxa</i> DSM 365	2.26
		<i>P. polymyxa</i> DSM 365 DSM	1.91
DSM 292	1	<i>P. polymyxa</i> DSM 292	2.34
		<i>P. polymyxa</i> DSM 292 DSM	1.84
DSM 292	2	<i>P. polymyxa</i> DSM 292	2.37
		<i>P. polymyxa</i> DSM 292 DSM	1.62
DSM 292	3	<i>P. polymyxa</i> DSM 292	2.28
		<i>P. polymyxa</i> DSM 292 DSM	1.74
DSM 292	4	<i>P. polymyxa</i> DSM 292	2.34
		<i>P. polymyxa</i> DSM 292 DSM	1.72
DSM 292	5	<i>P. polymyxa</i> DSM 292	2.52
		<i>P. polymyxa</i> DSM 292 DSM	1.42
DSM 292	6	<i>P. polymyxa</i> DSM 292	2.12
		<i>P. polymyxa</i> DSM 292 DSM	1.82
DSM 292	7	<i>P. polymyxa</i> DSM 292	1.57
		<i>P. polymyxa</i> DSM 292 DSM	1.39
DSM 292	8	<i>P. polymyxa</i> DSM 292	1.78
		<i>P. polymyxa</i> DSM 292 DSM	1.6
DSM 292	9	<i>P. polymyxa</i> DSM 292	2.33

		<i>P. polymyxa</i> DSM 292 DSM	1.67
DSM 292	10	<i>P. polymyxa</i> DSM 292	2.27
		<i>P. polymyxa</i> DSM 292 DSM	1.71
DSM 292	11	<i>P. polymyxa</i> DSM 292	2.26
		<i>P. polymyxa</i> DSM 292 DSM	1.61
DSM 292	12	<i>P. polymyxa</i> DSM 292	2.23
		<i>P. polymyxa</i> DSM 292 DSM	1.83
DSM 292	13	<i>P. polymyxa</i> DSM 292	2.13
		<i>P. polymyxa</i> DSM 292 DSM	1.72
DSM 292	14	<i>P. polymyxa</i> DSM 292	2.16
		<i>P. polymyxa</i> DSM 292 DSM	1.73
DSM 292	15	<i>P. polymyxa</i> DSM 292	2.28
		<i>P. polymyxa</i> DSM 292 DSM	1.63



**Table S 2.4.** Morphological and biochemical characterization of ATCC 842<sup>T</sup>, DSM 292 and DSM 365.

<b>Feature</b>	<b>ATCC 842<sup>T</sup></b>	<b>DSM 292</b>	<b>DSM 365</b>
Cell Form	rods	rods	rods
Cell Size	4-11 x 0.8	1-3 x 0.8	2-3 x 0.8
Gram Behaviour	+	+	+
Catalase	+	+	+
Oxidase	-	-	-
Sporulation	+	+	+
Sporangium Swollen	+	+	+
Motility	+	+	+
Anaerobic Growth	+	+	+
Gas Production	+	+	+
5% NaCl	w	-	w
8% NaCl	-	-	-
PH 5	+	+	+
PH 7	+	+	+
PH 11	-	-	-
5°C	-	-	-
25°C	+	+	+
30°C	+	+	+
35°C	w	w	+
40°C	(-)	(-)	(-)
Tween 20	+	+	+
Tween 40	+	+	+
Tween 80	w	-	+
Casein	+	+	+

**Table S 2.5.** Results of API 20E system (Biomérieux) recorded after 48 hours post-incubation at 28°C.

<b>Feature</b>	<b>ATCC 842<sup>T</sup></b>	<b>DSM 292</b>	<b>DSM 365</b>
β-Galactosidase (ONPG)	+	+	+
Arginine dihydrolase (ADH)	-	-	-
Lysine decarboxylase (LDC)	-	-	-
Ornithine decarboxylase (ODC)	-	-	-
Citrate utilization	-	-	-
H <sub>2</sub> S production	-	-	-
Urease	-	-	-
Tryptophan deaminase	-	-	-
Indole	-	-	-
Voges-Proskauer (VP)	w	+	+
Gelatine hydrolysis	+	+	+
Acid from			
Glucose	-	-	-
Mannose	-	-	-
Inositol	-	-	-
Sorbitol	-	-	-
Rhamnose	-	-	-
Sucrose	-	-	-
Melibiose	-	-	-
Amygdalin	-	-	-
Arabinose	-	-	-

**Table S 2.6.** Results of API 50 CHB system (Biomérieux) recorded after 48 hours post-incubation at 28°C.

<b>Feature</b>	<b>ATCC 842<sup>T</sup></b>	<b>DSM 292</b>	<b>DSM 365</b>
Glycerol	+	+	+
Erythritol	-	-	-
D-Arabinose	-	-	-
L-Arabinose	+	+	+
Ribose	+	+	+
D-Xylose	+	+	+
L-Xylose	-	-	-
Adonitol	-	-	-
βMeDXyloside	+	+	+
Galactose	+	+	+
Glucose	+	+	+
Fructose	+	+	+
Mannose	+	+	+
Sorbose	-	-	-
Rhamnose	-	+	-
Dulcitol	-	-	-
Inositol	-	-	-
Mannitol	+	+	+
Sorbitol	-	-	-
αMeDMannoside	-	+	-
αMeGlucoside	+	+	+
N-Acetylglucosamine	-	?	-
Amygdalin	+	+	+
Arbutin	+	+	+
Esculin	+	+	+
Salicin	+	+	+
Cellobiose	+	+	+
Maltose	+	+	+
Lactose	+	+	+
Melibiose	+	+	+
Sucrose	+	+	+
Trehalose	+	+	+
Inulin	?	+	+
Melzitose	-	-	-
Raffinose	+	+	+
Starch	+	+	+
Glycogen	+	+	+
Xylitol	-	-	-
Gentibiose	+	+	+
D-Turanose	+	+	+
D-Lyxose	-	-	-
D-Tagatose	-	-	-
D-Fucose	-	-	-
L-Fucose	-	-	-
D-Arabitol	-	-	-
L-Arabitol	-	-	-
Gluconate	?	?	?
2Ketogluconate	-	-	-
5Ketogluconate	-	-	-

**Table S 2.7.** Results of API 20 NE system (Biomérieux) recorded after 48 hours post-incubation at 28°C.

<b>Feature</b>	<b>ATCC 842<sup>T</sup></b>	<b>DSM 292</b>	<b>DSM 365</b>
Nitrate reduction	+	+	+
Indole	-	-	-
Glucose fermentation	-	-	-
Arginine dihydrolase	-	-	-
Urease	-	-	-
Esculin hydrolysis	+	+	+
Gelatine hydrolysis	+	+	+
β-Galactosidase	+	+	+
Glucose assimilation	+	+	+
Arabinose assimilation	+	+	+
Mannose assimilation	+	+	+
Mannitol assimilation	+	+	+
N-Acetylglucosamine assimilation	-	-	-
Maltose assimilation	+	+	+
Gluconate assimilation	+	+	+
Caprate assimilation	-	-	-
Adipate assimilation	-	-	-
Malate assimilation	-	+	-
Citrate assimilation	-	-	-
Phenylacetate assimilation	-	-	-

**Table S 2.8.** Results of API ZYM system (Biomérieux) recorded after 6 hours post-incubation at 37°C.

<b>Feature</b>	<b>ATCC 842<sup>T</sup></b>	<b>DSM 292</b>	<b>DSM 365</b>
Alcaline Phosphatase	0.5	0.5	1
Esterase	3	3	3
Esterase Lipase	1	1	1
Lipase	0	0	0
Leucine-Arylamidase	0	1	0
Valine-Arylamidase	0.5	0.5	0.5
Cystine-Arylamidase	0	0	0
Trypsin	0	0	0
Chymotrypsin	0.5	0	0
Acid Phosphatase	0.5	0	0
Naphtol-AS-BI-Phosphohydrolase	0.5	1	0.5
α-Galactosidase	1	1	2
β-Galactosidase	3	4	5
β-Glucuronidase	0	0	0
α-Glucosidase	0	0	0
β-Glucosidase	1	0.5	0.5
N-Acetyl-β-Glucosaminidase	0	0	0
α-Mannosidase	0	0	0
α-Fucosidase	0	0	0

## **Chapter 3**

---

# **A Systematic Framework for the Selection of Plant-Growth Promoting Microbial Candidates in Biostimulant Development: from Identification to *in vitro* Evaluation**

### **3.1 Abstract**

#### **Background**

Plant biostimulants are a sustainable and environmentally friendly solution to increase crop yield, productivity, quality, and tolerance to abiotic stress. While the fascination with microbial biostimulants continues to rise, the quest to pinpoint effective and suitable microbial leads for the development of commercial products is yet to be fully defined.

This study aims to establish a systematic and methodical framework for the selection of plant-growth promoting microbial candidates showing promising and suitable traits for further plant growth efficacy assessment. This discriminating process involves the following key phases: i) accurate identification of microbial leads ii) preliminary biosafety evaluation and bio-pesticide databases assessment, and iii) *in vitro* screening and selection for plant growth-promoting traits.

#### **Results**

Seventeen bacterial strains isolated from different crops were subjected to this comprehensive approach. Among them, only three bacterial cultures were chosen based on their demonstration of promising plant growth-promoting traits and suitability as potential active ingredients for biostimulant product development.

#### **Conclusions**

In conclusion, this study presents a well-defined workflow for systematically selecting promising active ingredients in microbial biostimulant development. This methodical approach not only streamlines the screening and selection process but also ensures a rigorous evaluation, empowering researchers to make informed decisions in the pursuit of effective solutions for sustainable agriculture.

### **3.2 Introduction**

The modern agricultural landscape faces a dual challenge - the need to enhance crop productivity to feed a growing global population while minimising the environmental impact of farming practices. In the pursuit of sustainable and environmental solutions, plant biostimulants (PBS) have emerged as a powerful

innovation. They can include substances or microorganisms that promote plant growth, increase crop yield, improve quality, and enhance plants' resilience to abiotic stress factors ([Regulation (EU) 1/1009]) [1].

The microbial agents in PBS, including various bacteria and fungi, play a pivotal role in improving soil health, enhancing nutrient cycling, and mitigating the adverse effects of environmental stressors, such as drought and salinity. To delve into the specifics, these beneficial microorganisms facilitate plant growth and bolster productivity through various mechanisms. This includes the release of growth-regulating hormones (e.g., indole-3-acetic acid), solubilisation of insoluble minerals (P, Zn, K), nutrient acquisition by nitrogen fixation, iron chelation by siderophores production, hydrolytic enzymes production and even, ameliorating the plant response to abiotic (e.g. soil salinity or drought) stress [2].

As the interest in microbial biostimulants continues to grow, the challenge lies in identifying, characterising, and harnessing the most effective and suitable microbial candidates for commercial applications. This demands a multidisciplinary approach encompassing tasks such as biosafety assessments for the appropriate handling and upscaling of microbial species, alongside determining whether these species are already registered as biopesticides. To enable this assessment, the selection process of microbial candidates for biostimulant development should integrate fast and reliable technology for precise microbial identification.

Matrix-assisted laser desorption ionisation-time of flight mass spectrometry (MALDI-TOF MS) has emerged as one of the most powerful techniques for the accurate identification and classification of pure microbial cultures. It allows for obtaining a unique mass fingerprint profile for each unknown strain that is matched against the instrument database containing reference profiles to assign an identity [3]. Over the past decade, it has gained significant prominence in laboratories due to its high throughput, cost-effectiveness, speed, and reliability [4]. These distinctive features make MALDI-TOF MS an ideal technology for streamlining the identification of numerous microbial candidates during the scouting process for plant growth promoting (PGP) investigation.

While fast and accurate microbial identification is critical, other considerations must be considered when selecting promising microbial candidates for biostimulant activity, particularly the assessment of microbial biosafety. Although plant growth-promoting bacteria (PGPB) are known for providing multiple benefits in agriculture, some genera are known to cause infections in animals or humans [5].

Several microorganisms described for their plant growth-promoting activities or used as biofertilisers belong to biosafety level 2 (BSL-2) classification. This category includes microorganisms that can cause mild human disease and pose a moderate environmental hazard [6]. In addition, many of these microorganisms could be opportunistic pathogens that generally do not harm the host but can cause disease if the host's immune system falls [7]. Examples of microorganisms belonging to BSL-2 and described in several reports for plant growth promotion or biological control are *Burkholderia ambifaria* [8], *Bacillus cereus* group [9], *Enterobacter* sp. [10, 11], *Serratia marcescens* [12], *Acinetobacter* sp. [13], *Pseudomonas aeruginosa* [14], *Klebsiella* sp. [15].

Risk groups (RG) and biosafety levels (BSL) serve as distinct terms utilised for classifying and categorising microbes concerning their associated hazards [5].

According to risk groups and biosafety levels, the most harmless microorganisms typically fall under RG1 and BSL-1. These microorganisms are considered low-risk and are not known to cause disease in healthy humans or animals. They also pose minimal environmental hazards. Examples of microorganisms in RG1/BSL-1 include non-pathogenic strains like *B. subtilis* and *S. cerevisiae*, commonly used in laboratories and various applications without posing significant risks.

Nowadays, the regulatory scenario appears fragmented, and there are no clear protocols and guidelines for the safety assessment of plant growth-promoting bacteria [16].

In light of this, researchers involved in selecting microbial leads for bioinoculant development should consider isolates belonging to RG1/BSL-1, avoiding maximising risk to the environment and human health [17].

Moreover, the screening and selection of promising PGP microorganisms should also consider the complex regulatory framework of microbial biostimulants.

Indeed, according to European regulation, PBS are regulated very differently from biopesticides, which, for definition, may contain as an active ingredient a microorganism with action against pests [1].

Therefore, it's essential to ensure that microbial biostimulants do not contain active ingredients already registered in the major pesticide databases and do not possess a mode of action associated with plant protection, as this would subject them to a different regulatory framework and approval process [18].

As the last step, PGP traits characterising the mode of action of microbial candidates should be considered for the screening and selection process. Indeed, PGPB can benefit plant growth in different ways. For instance, through solubilisation and mineralisation processes, PGPB can render otherwise insoluble minerals (e.g., phosphorus, zinc, potassium) to plants. Phosphorus is one of the main elements needed for the growth and development of plant and crop quality. This element is not always promptly available for the plants since 20-80% of the total phosphorus in the soil is associated with organic matter and minerals (Ca, Fe, Al, Mg) [19].

Several beneficial soil bacteria, defined as Phosphate Solubilizing Microorganism (PSM), can solubilise insoluble P forms through a variegated pool of enzymes and organic acid and make them available to the plant [20-21]. Another important aspect to consider during the characterisation process of a microorganism is the ability to produce biofilm, which is essential during the root colonisation process. Indeed, considering the enormously complex microbial communities living in the root zone, the capacity to form biofilm confers a significant advantage to the bacterium during the competition for the colonisation process [22]. Bacteria can form biofilm and colonise the rhizosphere through a range of metabolic activities comprising synthesis and secretion of surface adhesion protein, mobility protein and exopolysaccharides [23]. A recent study shows that biofilm formation in *Bacillus velezensis* FZB42 plays a key role in colonisation compared to the exopolysaccharide non-producer mutant strain that lost this capability [24].

Indole-3-acetic acid (IAA) is an important hormone released by different PGPB genera, including *Brevibacterium*, *Bacillus*, *Pseudomonas* and *Rhizobium*. This hormone is a key regulator of root development and bacteria-root interaction [25].



In summary, our study outlines a systematic approach to identify the most promising microbial cultures for further plant-based evaluation and potential commercial product development. This multi-step process includes criteria ranging from initial identification, biosafety, regulatory compliance, evaluation of any antagonistic activity, and assessing PGP traits, setting the stage for subsequent plant-based testing.

### **3.3 Methods**

#### **3.3.1 Bacteria and culture conditions**

The bacterial cultures used in this study consisted of seventeen strains previously isolated from the soil rhizosphere of various crops by the team of the environmental microbiology laboratory of the University of Verona. Bacterial cultures were recovered from  $-80^{\circ}\text{C}$  and cultured aerobically on TSA (Sigma Aldrich, United Kingdom) at  $30^{\circ}\text{C}$  for 24 hours. Next, single colonies were streaked on fresh TSA plates, incubated at  $30^{\circ}\text{C}$  for 24 hours, and identified before further investigation studies.

#### **3.3.2 Microbial culture identification and data processing by MALDI-TOF MS**

Prior to MALDI-TOF MS measurements, bacterial samples were processed according to the manufacturer's instructions, following the extraction method. For each bacterial culture,  $\sim 0.1$  mg of cell material was transferred from a single colony to 2 ml tubes containing 300  $\mu\text{L}$  sterile water. After that, the bacterial samples were dissolved and then inactivated by adding 900  $\mu\text{L}$  of absolute ethanol solution, with thorough mixing. Briefly, individual colonies of each of the seventeen bacterial cultures were harvested and dissolved in 1.5 ml tubes containing 300  $\mu\text{L}$  of sterile water. 900  $\mu\text{L}$  of absolute ethanol solution was added and mixed thoroughly. Subsequently, bacterial pellets were collected through centrifugation at 15.000 rpm for two minutes, followed by air-drying at room temperature for one hour. To extract proteins for mass spectrometry analysis, each

pellet was treated with 25  $\mu$ L of 70% formic acid (FA) and 25  $\mu$ L of acetonitrile (ACN).

Next, one  $\mu$ L of the supernatant was applied onto a 96 polished steel target plate, air-dried, and overlaid with 1  $\mu$ L of HCCA matrix solution (10 mg/mL  $\alpha$ -cyano-4-hydroxycinnamic acid in 50% acetonitrile and 2.5% trifluoroacetic acid) to facilitate sample ionisation. After the sample dried, mass spectra for each strain were acquired using the Bruker Microflex<sup>TM</sup> LT MALDI-TOF mass spectrometer (Bruker Daltonics, Bremen, Germany) in a linear positive ion extraction mode within a mass range from 1.960 to 22.000 Da. The instrument was equipped with a 60 Hz nitrogen laser and operated using FlexControl<sup>TM</sup> software (v 3.4; Bruker Daltonik GmbH, Bremen, Germany).

Each bacterial culture was independently grown in triplicate as biological replicates. Additionally, 8 technical replicates were prepared for every bacterial culture, resulting in a total of 24 measurements per strain. Following the manufacturer's guidelines, system calibration was conducted using the Bruker Bacterial Test Standard (BTS, Bruker Daltonics, Germany) solution, which enabled coverage of a mass spectrum acquisition range between 3.6 and 17 kDa. Data processing was carried out automatically using MBT Compass 4.1.100.10 software (Bruker Daltonik GmbH, Bremen, Germany), and the mass spectra were compared to the instrument library provided by Bruker Daltonic (MBT Compass Library v 7.0.0.0).

All identifications were categorised based on the provided score values as follows: a score of less than 1.7 was considered an uncertain identification; scores between 1.7 and 2.0 indicated a likely genus identification; scores between 2.0 and 2.3 indicated a confident genus identification and a potential species identification; and scores exceeding 2.3 were indicative of a strong likelihood of species identification [65]. Moreover, a Principal Component Analysis (PCA) was performed to get more information about the relationship and clustering of the seventeen bacterial cultures. Indeed, PCA enables the creation of clustered groups of spectra that exhibit similar patterns of variation and facilitates the visualisation of distinctions among them. Data can be depicted in either a 2D or 3D coordinate

system, but typically, a 2D representation suffices, as it graphs PC1 against PC2, accounting for over 80% of the total variance among the samples [66].

In the context of PCA analysis, each of the 24 mass replicates per strain underwent analysis using ClinProTools software (version 3.0; Bruker Daltonics, Bremen, Germany). Before loading the mass data, spectra preparation parameters were set as follows: resolution = 800; baseline subtraction by top hat baseline method; mass range (m/z) for analysis from 2,000 to 15,000; noise threshold = 2, recalibration = 1,000 ppm for maximal peak shift and 30% match to calibrant peaks. Moreover, peak calculation settings were adjusted as follows: peak picking on the total average spectrum with a signal-to-noise threshold equal to 5. The data were then subjected to a standard data preparation workflow, encompassing spectra recalibration, average peak list, and peak calculation. Any spectrum with low quality, such as the presence of background noise or extreme high/low intensities, was excluded from the PCA calculation.

### **3.3.3 Identification of bacterial isolates by 16S rDNA**

Bacterial DNA was extracted using the kit Wizard Genomic DNA purification Kit (Promega) according to the manufacturer's instructions, and it was used as the template for PCR reactions. In particular, the amplification of the 16S rDNA region was conducted in a reaction containing 20 ng of genomic DNA, 1  $\mu$ M of the primer E8F (5'-AGAGTTTGATCCTGGCTCAG-3') and E1541R (5'-AAGGAGGTGATCCANCCRCA-3'), 0.25 mM dNTPs, 2 mM MgCl<sub>2</sub>, and 1 U of DNA-polymerase GoTaq (Promega) in a total volume of 25  $\mu$ l. Cycling conditions, performed on a Nexus Mastercycler® (Eppendorf), were 30 cycles of 95°C for 30 s, 59°C for 20 s, and 72°C for 90 s.

### **3.3.4 Identification with additional markers (*gapA*, *pgk*, *uvrA*, *purH*)**

To better clarify the identification of the strains, additional markers were amplified and sequenced.

In particular, in order to improve the identification of the putative *Peribacillus frigiditolerans* strain 6, the partial sequence of the gene *gapA*, *pgk* and *uvrA* were

obtained as previously described[67-68]. Moreover, the gene *purH* was amplified for *Bacillus* and *Brevibacillus* strains 7, 12 and 13 using the following primers: Bc\_sub\_GR\_purH\_70F (5'-ACAGAKCTYGGCRTYGAAGT-3') and Bc\_sub\_GR\_purH\_1186R (5'-TCGGYTCYCTTTTTGTCCG-3') for *Bacillus*, and for *Brevibacillus* Br\_baci\_purH\_166F (5'-TTCCAGAAATTTTGGACGGT-3') and Br\_baci\_purH\_720R (5'-GAAAGCTCTTTTCCTTGCAGTTG-3'). For PCR amplifications, 20 ng of genomic DNA was added to a 20 µl reaction mixture containing 1 µM of each primer, 0.20 mM dNTPs, 1.5 mM MgCl<sub>2</sub>, and 0.5 U of DNA-polymerase GoTaq (Promega). The amplification was carried out on a Nexus Mastercycler® (Eppendorf) as described above, with annealing temperatures of 56°C and 59°C, respectively.

For both 16S rDNA and genetic markers coding for proteins (*purH*, *gapA* *pgk* and *uvrA*), after visualisation of PCR products on agarose gels (1.5%), the amplicons were sequenced by Sanger.

### **3.3.5 Bioinformatic analysis of 16S rRNA and protein-coding genetic markers**

The electropherograms were analysed and assembled by means of BioNumerics 7.6, and IUPAC degenerate nucleotide codes were inserted at uncertain peaks. The obtained sequences (OR888738, OR888739, OR888740, OR888741, OR888742, OR888743, OR888745, OR888746, OR888747) were compared in the EzBioCloud database. When more than one phylogenetic marker was sequenced for the identification of the strains, the sequences of the phylogenetic markers were concatenated and aligned with those retrieved from the genome sequence available in NCBI for the type strains of the most correlated species through ClustalX software [69].

### **3.3.6 Comparative genomics**

To better clarify the intraspecific diversity of *B. brevis* species the RefSeq assembly genome sequences GCF\_000010165.1 (*B. brevis* NCTC 2611), GFC\_003385915.1\_ASM338591V1 and GFC\_00653984v1 (*B. brevis* NBRC

[31]100599) were used to calculate the Average Nucleotide Identity (ANI) with the OrthoANI algorithm through the OAT software, which measures the overall similarity between two genomes without gene-finding and functional annotation steps [32].

### **3.3.7 Biosafety evaluation and bio-pesticide databases assessment**

Two sources have been consulted for assigning the bacterial species to a risk group: TRBA 466 provided by Germany's official regulation BAuA [31], and the American Biological Safety Association database ABSA [33]. Bacterial isolates from potentially harmful species affecting either humans or animals were excluded from the screening and selection process.

For the examination of the approved biopesticides available on the market, the European (EU) Pesticide database [34], the United States Environmental Protection Agency (EPA) database [35] and the Bio-Pesticides DataBase (BPDB) [36] were consulted. Bacterial isolates belonging to the microbial species reported in the positive list for biopesticide were excluded from the examination.

### **3.3.8 Kinetic studies**

Biological screening of microbial strains focuses not only on the evaluation of their plant bio-stimulant activity but also on their fermentation performance [70]. This can be considered a marker of how easy or difficult it could be to cultivate a specific strain. This marker considers two main parameters: specific growth rate ( $\mu_{MAX}$ ) and maximum Optical Density at 600 nm (OD600 max). To determine these two parameters and thus the fermentation performance, bacterial strains were studied for the ability to grow in four different Basal Nutritive Media (BNM): Nutrient Broth (NB), Nutrient Yeast Broth (NYB), Luria Bertani (LB) and Tryptic Soy Broth (TSB). Strains were inoculated in triplicate in a 96-well microtiter plate, where each well was filled with 200  $\mu$ l of each medium. The kinetic curves were studied for 22 hours at 30°C and 110 rpm.

Cell growth was measured by optical density at 600 nm every two hours, and each microorganism's growth rate ( $\mu_{max}$ ) was calculated. The optical density values were transformed by using the Monod equation [71]:

$$\ln X = \ln X_0 + \mu t$$

Where "X" is the viable count or optical density measured at a specific time, "X<sub>0</sub>" is the viable count or optical density at time 0 (the beginning of the fermentation process), "t" is the time, and  $\mu$  is the specific growth rate. Plotting the optical density values, properly scaled using the logarithmic function, against time is possible to get a line whose slope is the specific growth rate. The fermentation performance of each strain was ultimately ascertained by adding up the values of the two parameters mentioned earlier, following the Papapetridis et al. [Papapetridis et al. 70] protocol with minor adjustments. Since those parameters have different units of measurement before summing, it is necessary to normalise the data using the following formula:

$$COMB = \frac{OD_i}{VAR(OD)} + 2 \times \frac{\mu_{max_i}}{VAR(\mu_{MAX})}$$

"OD<sub>i</sub>" is the -i value measured for that parameter, " $\mu_{max_i}$ " is the -i value measured for that parameter and "VAR" is the variance of all the sample of values considered for each parameter.

This way, it is possible to sum values referring to different units of measurement and get a unique value that describes the fermentation performance. The highest is the COMB value, and the highest is the fermentation performance.

### 3.3.9 *In vitro* bacterial antagonism evaluation

Bacterial strains were tested against a defined set of plant pathogens, such as *Xanthomonas campestris* (strain V4), *Botrytis cinerea* (strain V3), *Fusarium culmorum* (strain V2), and *Rhizoctonia solani* (strain V1) to exclude any relevant antagonistic activity. The activity of the tested bacteria against fungal and bacterial pathogens was tested by dual culture and drop method assays, respectively.

The antagonistic potential of bacterial strains was assessed against a predefined group of plant pathogens, which included *Xanthomonas campestris* (strain V4), *Botrytis cinerea* (strain V3), *Fusarium culmorum* (strain V2), and *Rhizoctonia solani* (strain V1), to exclude any substantial antagonistic effects. To evaluate the activity of these bacterial strains against both fungal and bacterial pathogens, dual culture and drop method assays were conducted, respectively [72-74].

In the dual culture method, 10 mm agar discs containing the pathogenic isolate were placed on one side of Potato Dextrose Agar (PDA) plates. Subsequently, antagonistic bacterial strains were streaked 3 cm away from the edge of the same plate, while plates containing only the pathogenic isolate served as controls. Following 6 days of incubation at 28°C, the diameters of the bacterial growth inhibition zones were measured. The percentage of growth inhibition (PGI) was calculated using the formula:

$$\text{PGI (\%)} = \frac{(\text{KR} - \text{R1})}{\text{KR} \times 100}$$

Where KR represents the diameter of the pathogenic colony on the control plate, and R1 represents the diameter of the colony on the treated plate. The PGI values were categorised on a Growth Inhibition Category (GIC) scale, as proposed by Ramírez-Olier et al. [72], ranging from 0 (denoting no growth inhibition) to 4 (corresponding to a range of 76% to 100% growth inhibition).

For the drop method assay, 20 µl of an overnight culture of the bacterial phytopathogen *X. campestris*, grown in TSB, was evenly spread on the surface of TSA plates to form an overlay, which was allowed to dry. Subsequently, 10 µl drops of an overnight culture of the bacterial isolates were spotted in triplicate on TSA plates inoculated with *X. campestris* V4, while plates containing only the pathogenic isolate were used as controls. After 48 hours of incubation at 30°C, the plates were examined for inhibition zones surrounding the drops of the tested bacterial strains, with inhibition zones classified according to the method proposed by Ismail et al. [74].

### **3.3.10 Bacterial antagonism evaluation on *S. lycopersicum***

Strains that showed the strongest inhibition activity *in vitro* were further investigated on tomato plants (*Solanum lycopersicum* variety *Optima*) against *Botrytis cinerea* strain V3 as the target pathogen. Bacterial cultures were applied by foliar spray one day before pathogen inoculation on tomato plants at BBCH 23 growth stage. More in detail, the pathogen was inoculated by placing a 5 mm mycelium-agar plug in the centre of tomato leaves. Plants were then maintained in a growth chamber under the optimal environmental conditions for the pathogen to infect the plant.

Four days after the inoculation, the grey mold symptoms were evaluated by measuring the size of the necrotic area (width measurement). The protection efficacy was calculated with the formula [75]:

$$\left(1 - \frac{\text{Disease in Treated plants}}{\text{Disease in Control plants}}\right) * 100$$

Bacterial strains were grown in TSB overnight at 30°C, 130 rpm, and applied at  $1 \times 10^7$  CFU·mL<sup>-1</sup>. Treatments (or uninoculated medium for the control) were sprayed until runoff. The biological plant protection product Serenade Max-Bayer Crop Science (*Bacillus subtilis* QST713) applied at 0.8 % was included as a positive control.

### **3.3.11 Strains characterisation for plant growth-promoting activities**

#### **3.3.11.1 Mineral solubilisation**

Bacterial cultures under the study have been investigated for the solubilisation ability of phosphate (P), zinc (Zn) and potassium (K).

Phosphate solubilisation was estimated first by a qualitative assay and then, positive strains were further investigated by a quantitative assay.

The qualitative assessment of phosphate solubilisation was conducted using Pikovskaya's agar plate with tricalcium phosphate (Ca<sub>3</sub>(PO<sub>4</sub>)<sub>2</sub>). 10 µl of each



bacterial culture at  $1 \times 10^8$  CFU·ml<sup>-1</sup> was spotted in triplicate onto the plate, left to dry and then incubated at a temperature of  $28 \pm 2^\circ\text{C}$ . After a 7-day incubation period, a clear halo surrounding the bacterial colony was considered a positive result. Phosphate solubilisation was measured as P-solubilization Index (PSI) [76], where:

$$\text{PSI} = \frac{\text{total diameter (colony + clear zone)}}{\text{diameter of colony}}$$

Quantitative estimation of tricalcium phosphate solubilisation was performed by growing the strain for 7 days in Pikovaskya's broth. The soluble phosphate concentration was subsequently assessed in the culture supernatant after filtration through a 0.2  $\mu\text{m}$  nylon filter, using ion chromatography [77]. The concentration of soluble phosphate was determined through the interpolation with a calibration curve of  $\text{P}_2\text{O}_5$  ranging from 0 to 100 mg·l<sup>-1</sup>.

Zinc and potassium solubilisation was assessed by inoculating the bacteria cultures on modified Pikovskaya's medium with insoluble zinc form (ZnO) [78] and Aleksandrov medium [79] amended with mica powder as a source of insoluble K. For both assays 10  $\mu\text{l}$  of each bacterial culture at  $1 \times 10^8$  CFU·ml<sup>-1</sup> was spotted onto the plates.

For zinc solubilisation assessment, inoculated plates were incubated at  $28^\circ\text{C}$  for five days, and a clear halo surrounding the colony was considered as positive result and measured as Zn-solubilization efficiency [79].

The ability to solubilise potassium was analysed by incubating inoculated plates at  $30^\circ\text{C}$  for four days. The results were recorded based on the capacity to form a solubilisation zone around bacterial colonies [80].

### **3.3.11.2 Carboxymethyl cellulose (CMC) degradation**

The cellulase production assay was performed by culturing all bacterial cultures on a solid medium containing carboxymethylcellulose (CMC) as the sole carbon source. Briefly, 10  $\mu\text{l}$  of each bacterial culture at a concentration of  $1 \times 10^8$  CFU·ml<sup>-1</sup> was spotted onto the plates, which were then incubated at  $30^\circ\text{C}$  for two days. After the incubation period, the hydrolysis halo zone was recorded by flooding and incubating the plates with 1% Congo Red solution for 15 minutes,

followed by destaining with a 1M NaCl solution for 20 minutes. CMC degradability was calculated as the ratio of the halo zone to the diameter of the bacterial colony [81].

### **3.3.11.3 Metabolites production: IAA, proteases and siderophores**

IAA production was determined according to Gordon and Weber's colourimetric method [82]. Briefly, 50  $\mu\text{l}$  of bacterial cultures ( $1 \times 10^8$  CFU $\cdot\text{ml}^{-1}$ ) were inoculated in triplicate in a 48-well microtiter plate, where each position contained 500  $\mu\text{l}$  of TSB medium with 0,1% of tryptophan. After the inoculum, the microtiter plate was incubated at 30°C, and supernatants recovered after 48 hours (until the log phase). For the reaction, 2 ml of Salkowski reagent and 15  $\mu\text{l}$  of orthophosphoric acid were added to 1 ml of filtered bacterial broths. After 30 minutes of incubation in the dark, samples' optical densities were determined at 540 nm using a Tecan Spark multimode microplate reader (Mannedorf, Switzerland). Values of IAA (mg/l) were obtained by interpolating OD530 nm values with the IAA calibration curve ranging from 0 to 100 mg  $\cdot\text{l}^{-1}$ . Uninoculated wells were used as a negative control.

Protease activity was detected by inoculating 10  $\mu\text{l}$  of each microbial culture ( $1 \times 10^8$  CFU $\cdot\text{ml}^{-1}$ ) onto skim milk agar [83]. The strains were then incubated at 30°C for 48 hours, and a clear zone around the colony was considered indicative of positive protease production.

Siderophore production was detected through the CAS assay. In detail, 10  $\mu\text{l}$  of each microbial culture ( $1 \times 10^8$  CFU $\cdot\text{ml}^{-1}$ ) was inoculated onto NA at 30°C for 72 hours. After the incubation period was over, plates (80 mm Petri dishes) were overlaid with 10 ml of O-CAS-agar (Chrome azurol S (CAS) 60.5 mg, hexadecyltrimethyl ammonium bromide (HDTMA) 72.9 mg, piperazine-1,4-bis(2-ethanesulfonic acid) (PIPES) 30.24 g, and 1 mM FeCl<sub>3</sub> 6H<sub>2</sub>O in 10 mM HCl 10 mL. Agarose (0.9%, w/v)) according to the Pérez-Miranda protocol [84]. After 15 minutes, a change in colour, from blue to orange, around colonies was recorded as a positive result. Moreover, siderophores were also estimated by a quantitative procedure, according to the protocol of Goswami et al. [85]. Strains were grown in NB at 30°C for 72 hours. After incubation, 0.5 ml of bacterial supernatant was

added to 0.5 CAS assay solution and mixed. After 20 minutes, a decrease in blue colour intensity meant the presence of siderophores in the sample. Siderophore production was determined as a percentage (%) of Siderophore Units following the formula:

$$\text{SU (\%)} = \left( \frac{\text{Ar} - \text{As}}{\text{Ar}} \right) \times 100$$

Where Ar represents the absorbance of the reference (NB + CAS assay solution), and As represents the absorbance of the sample (culture supernatant + CAS assay solution).

Each treatment in all PGP assays was performed in triplicate.

#### **3.3.11.4 Biofilm production**

The assessment of bacterial biofilm production involved using a static biofilm assay protocol [86] in a microtiter plate. Bacterial cultures were cultivated in TSB and SOBG, a glycerol-based medium, following Mee-Ngan et al. [87] procedure with minor adjustments. Each well received 20 µl of bacterial cell suspension ( $1 \times 10^8$  CFU·ml<sup>-1</sup>) and was incubated at 30°C for 72 hours without shaking. Uninoculated wells served as a negative control, with six replicates for each strain. Following incubation, the liquid was removed, and the plate was washed with distilled water. Then, 125 µl of 0.1% crystal violet solution was added to each well and left to stain for 10 minutes at room temperature. After staining, wells were washed three times with distilled water. To quantify the dye absorbed by adherent cells, 200 µl of 95% ethanol was added to each well and incubated for ten minutes at room temperature. The absorbance of the resolubilised dye solution was measured at 595 nm using a spectrophotometer (TECAN, Salzburg, Austria). Additionally, strains exhibiting positive aerial biofilm formation were identified by recording and quantifying the formation of a pellicle at the air-liquid interface, often measured in terms of dry weight.

#### **3.3.11.5 Growth in nitrogen free media and ammonia production**

Nitrogen-fixing ability was qualitatively studied by allowing the strains to grow in three different nitrogen-free media, namely LGI [88], SYP [89] and NFM [90].

The ability to grow without nitrogen was assessed by streaking bacterial cultures grown overnight ( $1 \times 10^8$  CFU·ml<sup>-1</sup>) onto the same N-free agar media. Strains were then incubated at 30°C for 24 hours. Bacterial growth on nitrogen-free medium was recorded as a positive result. The microbial growth assessment was repeated twice, and each treatment was performed in triplicate. The observations were recorded as a frequency distribution. The frequency distribution of microbial growth for each strain on diverse nitrogen-free media was expressed as a growth index ranging from 0 to 4. This index reflected the biomass abundance, where 0 denotes no growth, 1 indicates low growth, 2 signifies medium growth, 3 represents substantial growth, and 4 denotes excellent growth.

In addition, positive strains were further evaluated for their ability to grow and produce ammonia in LGI, SYP and NFM liquid media, measuring the maximum optical density at 600 nm (OD<sub>600nm\_MAX</sub>) after 24 hours. Ammonia production was estimated in microaerophilic conditions ( $O_2 < 0.1\%$ ) to avoid inhibiting the nitrogenase enzyme [91]. Product measurement was performed by an ammonia assay kit (Cell Biolabs', San Diego, USA) containing a chromogen reagent that produces a green-blue colour reaction in the presence of ammonia. The OD 630 nm was measured by Tecan Spark multimode microplate reader (Mannedorf, Switzerland), and ammonia (uM) was quantified after 24 hours of incubation at 30°C by interpolating samples' absorbance values with the ammonium chloride (NH<sub>4</sub>Cl) standard calibration curve ranging from 0 to 800 μM. Uninoculated wells were used as a negative control.

All treatments were performed in triplicate.

### **3.3.12 Statistical analysis**

Experiments were statistically analysed using the Statistica v 14 software (TIBCO Software Inc, Palo Alto, California, USA). All data were analysed by ANOVA, and significant differences among the treatments were determined by Fisher LSD post hoc test. Different letters indicate statistically significant differences at  $p \leq 0.05$ .

## 3.4 Results

### 3.4.1 Bacterial cultures identification by MALDI-TOF MS

Among the seventeen cultures analysed by Bruker MALDI BioTyper software, seven strains (8, 9, 14, 15, 16, and 17) were reliably identified at the species level, as indicated by a Biotyper (log)score exceeding 2.3 (**Table 3.1**). For eight other strains (1, 2, 3, 5, 6, 7, 10, and 11), the identification provided a score between 2.0 and 2.3, signifying a confident genus identification and a potential species identification. Only three strains (4, 12, and 13) received scores between 1.7 and 2.0, indicating a reliable genus identification.

Strains lacking a high-confidence species identification or supported by only a limited number of replicates to confirm this conclusion (e.g. strain 6) underwent additional scrutiny. This included detailed analysis by 16S rDNA gene examination and, where appropriate, additional marker sequence analysis to improve taxonomic resolution. This additional scrutiny was applied for most strains under study, with the exception of strains 5 and 10, which were identified within the *B. cereus* group. Despite a (log)score indicative of probable species identification (**Table 3.1**), PCA analysis (**Figure 3.1**) revealed their close clustering with securely identified *Bacillus cereus* strains 8 and 17, conclusively confirming their affiliation to the *B. cereus* group and obviating the need for further investigation. Conversely, strain 4, which exhibited the highest (log)score value of 1.99 across all mass spectra, indicative of a probable genus identification only, was subjected to genetic identification.

### 3.4.2 Bacterial culture identifications by genetic analysis

The identification of the strains in EzBioCloud by comparison of the assembled 16S rDNA obtained by Sanger sequences is reported in **Table 3.1**.

The identification of four strains, namely strains 6, 7, 12 and 13, was improved by obtaining the partial sequence of one or more genes coding for proteins (**Table 3.1**) and comparing them by multiple alignments with the sequences of the Type Strains belonging to the most related species, according to the Identification with 16S rDNA. These four strains belong to the *Peribacillus simplex* group, the

*Bacillus subtilis* group and the *Brevibacillus brevis* group, i.e. a group of closely related species that are not clearly differentiated based on the 16S rDNA sequence.

Strain 6 presented high similarity with *Peribacillus frigoritolerans*, formerly known as *Bacillus frigoritolerans* and *Brevibacterium frigoritolerans* [92], based on the 16S rDNA sequence. Three further genetic markers, namely *gapA*, *pgk* and *uvrA*, were amplified and sequenced to clarify identification at the species level. The three markers univocally indicate that strain 6 is more correlated with the type strain of the species *Brevibacterium frigoritolerans*, clarifying the taxonomic assignment at the species level. It is clear, however, the strict relationship with members of the *Peribacillus simplex* cluster [93]. The results obtained with the partial sequences of the genes *gapA* (NCBI Acc. No. OR909268), *pgk* (NCBI Acc. No. OR909269) and *uvrA* (NCBI Acc. No. OR909270) are coherent as they are in all the cases more similar to the homologous sequences from *Peribacillus frigoritolerans* FJAT2396T genome (NCBI Acc. No.: KV440950.1) than to the homologous sequences from *Peribacillus simplex* NBRC 15720T genome (NCBI Acc. No.: CP017704.1) with, respectively: 99.06 % and 97.45 % sequence similarity for *gapA*; 98.42 % and 93.23 % sequence similarity for *pgk*; 98.52 % and 96.43% sequence similarity for *uvrA*. Strain 6 can, therefore be identified as *Peribacillus frigoritolerans*.

For strains 7, 12 and 13, the partial sequence of the gene *purH* was enough to improve their identification.

More in detail, for strain 7, the partial sequence of the gene *purH* (NCBI Acc. No. OR909271) was more similar to the homologous sequence from *Bacillus spizizenii* ATCC 6633 (NCBI Acc. No.: NC-016047.1), sharing 97.42 % sequence similarity, than to the homologous sequences of *Bacillus cabrialesii* TE3T (NCBI Acc. No.: CP096889) and of *Bacillus inaquosorum* KCTC 13429T (NCBI Acc. No.: AMXN01000005.1), sharing respectively 95.47 % and 95.28 % similarity.

For the strains 12 and 13, belonging to the *B. brevis* group of species, the partial sequence of the gene *purH* (NCBI Acc. No. OR909272; OR909273) in both cases was more similar to the homologous sequence from *Brevibacillus brevis* NCTC 2611 (NCBI Acc. No.: LR134338.1) with 96.64 % sequence similarity, than to the

second hit, that is *Brevibacillus formosus* DSM 9885 (NCBI Acc. No. LDCN01000006.1) with 96.29 %. Considering strains other than only Type Strains, both strain 12 and strain 13 share higher similarity with the homologous *purH* sequences; for instance, the *purH* sequence from *Brevibacillus brevis* NBRC 100599 (NC\_012491.1) is 99.0 % similar, confirming the strains 12 and 13 are related to other strains of this species. Analysing the genome classification of *B. brevis* on the Genome Taxonomy Database (GTDB) (<https://gtdb.ecogenomic.org/>), it was observed that *B. brevis* formed two additional clusters besides the one associated with the type strain labelled as *B. brevis\_C* and *B. brevis\_D*. *B. brevis* NBRC 100599 was found to belong specifically to the *B. brevis\_D* cluster. The relatedness of the strains by means of a whole-genome approach was defined by calculating the Average Nucleotide Identity (ANI) with the OrthoANI algorithm and setting 95-96% as the threshold to propose new species [61]. The ANI values for strain *B. brevis* NBRC 100599 distinctly differentiated it from *B. brevis* NCTC 2611<sup>T</sup>, as the result was less than 95% identity. This outcome suggests that *B. brevis* NBRC 100599 is distinguishable from the type strains and could be considered a reference for a cluster of *B. brevis* strains, including 12 and 13, distinct from *B. brevis sensu stricto*, in agreement with the results suggested by the high variability of the partial sequence of the *purH* gene in comparison with the same region of *B. brevis* NCTC 2611<sup>T</sup>.

### **3.4.3 Biosafety evaluation and bio-pesticide databases assessment**

Three bacterial cultures (strains 5, 8, and 17) were not characterised further due to a preliminary risk assessment that pointed out their relation to the *Bacillus cereus* group. Microorganisms belonging to this group are spore-forming organisms commonly associated with food poisoning and intestinal infections [94].

In the evaluation of bio-pesticides databases, *Bacillus licheniformis* and *Bacillus subtilis* were found to be either approved or awaiting approval as active substances on the PPP list in the USA and Europe, respectively (**Table 3.2**). Since these findings, strains 7, 14, 15 and 16 were not carried on in the screening and selection process of microbial candidates for biostimulants.

#### **3.4.4 Kinetic performance**

Biological screening of microbial strains focuses not only on the evaluation of their plant bio-stimulant activity but also on their fermentation performance. This can be considered as a marker of how easy or difficult it could be to cultivate a specific strain. Strains 1, 2, 3, 6, 9, 11, 12, and 13 underwent evaluation for their fermentation performance across four different media. This assessment involved the calculation of the COMB value, as outlined earlier. The results for each strain in the four media are detailed in **Table 3.3**. The COMB value results (**Table 3.3**) reveal that TSB stands out as the most suitable medium for all the strains in the analysis, making it the preferred choice common to all tested strains. Furthermore, a comparison of the strains was conducted in the TSB medium, highlighting strains 12 and 9 as the top performers in terms of fermentation performance, followed by strains 13 and 11.

#### **3.4.5 *In vitro* bacterial antagonism evaluation**

The summary of *in vitro* antagonistic activity results against various pathogens is presented in **Figure 3.2 A** and **Figure 3.2 B**. Notably, Strains 12 and 13 exhibited robust inhibitory activity against most pathogens. Indeed, both strains demonstrated an antagonistic activity exceeding 80% against both *R. solani* strain V1 and *B. cinerea* strain V3. Additionally, Strain 12 exhibited a medium activity (56.5%), and strain 13 displayed a high activity (69.4%) against *F. culmorum* strain V2. Given their substantial *in vitro* inhibition, strains 12 and 13 were further investigated on tomato plants, targeting *B. cinerea* strain V3 as the pathogen of interest.

#### **3.4.6 Bacterial antagonism evaluation on *S. lycopersicum***

The grey mould symptoms were evaluated on tomato leaves of untreated control (UTC) plants and plants treated with strains 12 and 13 and the product Serenade Max- Bayer Crop Science (*Bacillus subtilis* QST713) four days after the inoculation of the pathogen. Subsequently, the protection efficacy was calculated. Plants in the UTC showed a heavy infection of the grey mold with an average necrose width of 17,54 mm. The application of Serenade Max significantly



reduced the symptoms compared to the UTC. Here the necrose was 7 mm, and protection of 60%. The application of the different bacterial strains did not provide control of grey mold symptoms. The values of necrose were like those observed in UTC. Results are represented in **Figure 3.2 C**.

### **3.4.7 Screening for PGP activities**

#### **3.4.7.1 Mineral solubilisation**

A total of eight strains were screened for P-solubilization ability. Among them, five bacteria with an evident diameter of the transparent zone surrounding the colony and an Index larger or equal to 1, meaning the release of inorganic phosphate Pi, have been selected as positive for the trait (**Figure 3.3 A**). Strains 1, 6, 9, 12, and 13 were statistically signed as positive (**Figure 3.3 A**). Only the positive strains, according to the P-solubilization plate assay results, were further tested in a liquid test to confirm the previous result and quantify the released phosphate in the form of P<sub>2</sub>O<sub>5</sub> through the Ion Chromatography methodology.

Quantitative analysis confirmed the results obtained in the plate screening for strains 1, 6, and 9, which were statistically positive for the release of inorganic phosphate in the form of P<sub>2</sub>O<sub>5</sub> with a range from 58.50 ± 9.5 to 199.85 ± 6.09 ppm. Among all, strain 6 was the best P-solubilizer (**Figure 3.3 B**).

None of the tested strains could solubilise the insoluble form of potassium and zinc (data not shown).

#### **3.4.7.2 Carboxymethyl cellulose (CMC) degradation**

The CMC-degrading ability was established for seven out of eight strains. The results showed the formation of clear zones surrounding the colonies with an Index range value of 1.17-1.53 (**Figure 3.3 C**). Strains 1, 2, 3, 6, 11, 12, and 13 resulted positive for the ability to produce extracellular cellulolytic enzyme for cellulose degradation (**Figure 3.3 C**).

#### **3.4.7.3 Metabolites production: IAA, protease and siderophores**

IAA plays a central role in modulating plant growth and development. Five strains out of eight were found to be positive for IAA production. IAA quantification has

been obtained in a range of 4.7-7.57 mg L<sup>-1</sup> concentrations. Among the positive strains, 12 and 13 resulted to be the best producer of IAA (**Figure 3.3 D**). **Figure 3.3 E** show the results of protease enzyme activity for the eight microorganisms tested. A statistically significant difference ( $p < 0.05$ ) was observed between strain 6 and all other strains. Strain 6 exhibited a proteolytic halo with an Index of  $1.10 \pm 0.06$ .

None of the tested strains was able to produce siderophores (data not shown).

#### **3.4.7.4 Biofilm production**

The assessment of biofilm production was conducted in two distinct liquid media. The results of the biofilm assay revealed that strains 12 and 13 exhibited the most promising biofilm production, both in TSB and SBOG media. Notably, when inoculated in the glycerol-based medium SBOG biofilm production reached its peak (**Figure 3.3 F**). This outcome affirms the documented role of glycerol in promoting bacterial biofilm production, as highlighted by previous studies [95-96]. Conversely, all other microorganisms tested displayed no biofilm-producing ability (**Figure 3.3 F**).

Additionally, strains 12 and 13 demonstrated the formation of an aerial pellicle in SBOG medium, representing a specific form of biofilm formation at the air-liquid interface [86]. The quantification of pellicles' dry weights for positive strains 12 and 13 was performed (**Table 3.4**). Even in the case of biofilm formation as an air film, the presence of glycerol in the medium proved advantageous compared to the glycerol-free medium (TSB) (**Table 3.4**). These results confirm that the SBOG medium, particularly with glycerol, enhances cell adhesion in pellicle formation.

#### **3.4.7.5 Growth evaluation in N-free media and ammonia production**

Growth on nitrogen-free media (NFM, SYP and LGI) results of the second streak confirmed the capability of three out of eight strains (11, 12, and 13) to grow without any nitrogen source (**Figure 3.4 A**; **Figure 3.4 B**). Strains 11, 12, and 13 were able to grow predominantly in LGI and SYP. The same strains were also able to grow on NFM but with lower growth index values (**Figure 3.4 A**; **Figure 3.4 B**).

Strains that showed the capability to grow on nitrogen-free solid media, potentially leading to the ability to fix nitrogen from the atmosphere, were further tested in the three liquid N-free media to assess their growth compared with the BNM. Bacterial growth was monitored spectrophotometrically by measuring the OD at 600<sub>nm</sub> every two hours for 24 hours, and the maximum OD at 600 nm wavelength (OD600nm\_MAX) was observed. Strains 11, 12, and 13 confirmed their ability to grow without nitrogen in all three N-free media (**Figure 3.4 C**).

Also, in the study of growth kinetics in liquid media without nitrogen, strains 12 and 13 confirmed that they perform better in LGI. In contrast, no statistical differences between growth (OD600nm\_MAX) in SYP and NFM were observed. Strain 11 grew best in SYP, with a statistical difference between the OD600nm\_MAX values and those in LGI and NFM.

All three strains were also evaluated for their ability to produce ammonia in LGI, SYP and NFM media, one of the main metabolites produced in the nitrogen fixation process. Results showed that all the strains were able to produce ammonia, and specifically, the best producers were 11 and 13 in SYP and NFM media, respectively (**Figure 3.4 D**).

### **3.5 Discussion**

In this study, we devised a stepwise screening program and validated it by selecting three PGPB candidates capable of meeting all the criteria necessary for the successful development of new and effective biostimulants.

The first stage of our systematic approach was focused on evaluating dependable methods applicable in any laboratory setting for accurately identifying microbial candidates during a screening and selection process. Indeed, prioritising such a step in the workflow is crucial for subsequent pathogenicity assessments or alignment with regulatory frameworks related to microbial biostimulants.

In alignment with these objectives, we explored the efficacy of MALDI-TOF MS, a technology that has rapidly gained traction in laboratories over the past decade, emerging as a swift and dependable technology. Various researchers have drawn comparisons between MALDI-TOF MS and molecular approaches, highlighting its efficiency and reliability. This technology has proven effective in identifying

bacterial cultures and has emerged as a solid alternative to the 16S rRNA gene approach, especially for high-throughput identification of bacterial isolates [65]. In this study, we showcased its ability to rapidly and accurately identify strains with high reliability, specifically achieving success for six of the seventeen isolates.

Furthermore, the application of Principal Component Analysis (PCA) as a statistical tool proved instrumental in enhancing the taxonomic resolution of MALDI-TOF MS. This analytical approach facilitated the grouping of strains 5 and 10, initially identified only at the genus level, conclusively placing them within the *B. cereus* group. This refinement expanded the number of strains identified with a high confidence level to eight.

The remaining strains were identified, at the very least, at the genus level, and none of the identifications were deemed unreliable. Strains with lower confidence in identification underwent additional scrutiny, which included examining the 16S rRNA gene and incorporating marker sequence analysis for strains 6, 7, 12, and 13.

The case of strain 7 was particularly unusual, as only one mass profile replicate was securely identified by MALDI-TOF MS as *B. subtilis* among the identification outputs. Genetic identification revealed that strain 6 belongs to *Bacillus spizizenii*, previously recognised as *Bacillus subtilis* subsp. *spizizenii* [97], thereby affirming the accuracy of the MALDI-TOF MS results in correctly assigning the taxonomic group. This underscores the importance of regularly enriching the database with new MSP reference profiles or consistently updating the taxonomy of those already included to ensure accuracy in identification.

Furthermore, strains 12 and 13 exhibited a limited match with the profile of the reference type strain *B. brevis* (NCBI identifier 1393) in the instrument library. Although the initial best match in the identification result was *B. brevis*, the (log)score provided confidence only at the genus level for 18 and 11 out of 24 mass replicates for strains 12 and 13, respectively (**Table S 3.1**). Genetic analysis confirmed their affiliation with this species, although with a *purH* gene similarity of only 96.64% compared to the strain *B. brevis* NCTC 2611<sup>T</sup> (NCBI Acc. No.:

LR134338.1). Notably, the *purH* gene demonstrated a 99% similarity with the non-type strain *B. brevis* NBRC 100599 (NC\_012491.1).

Analysing the genome classification of *B. brevis* by referencing the GTDB, it was observed that *B. brevis* formed two additional clusters beyond the one associated with the type strain, labelled as *B. brevis\_C* and *B. brevis\_D*. *B. brevis* NBRC 100599 was found to belong specifically to the *B. brevis\_D* cluster. The ANI values for strain *B. brevis* NBRC 100599 distinctly differentiated it from *B. brevis* NCTC 2611<sup>T</sup>, with less than 95% identity.

This outcome suggests that *B. brevis* NBRC 100599 is distinguishable from the type strains and could serve as a reference for a cluster of *B. brevis* strains, including strains 12 and 13, which are distinct from *B. brevis sensu stricto*. This underscores the utility of the proteomic approach as a predictive tool preceding genomic analyses, offering insights into microbial biodiversity and revealing notable differences among closely related strains (Chapter 1).

Furthermore, this discovery contributes new perspectives to the genomic diversity of *B. brevis* strains, laying the groundwork for a more comprehensive study involving a larger sample of *B. brevis* strains, both proteomically and genomically. The classification of *B. brevis* according to the GTDB framework can guide the selection of representative strains based on genome phylogeny and intra-specific clustering.

Strains within the *B. cereus* group (4, 5, 8, 10, 17) were promptly excluded from the selection due to their association with human infections or food poisoning highlighting their potential hazards in a biostimulant formulation. For instance, *B. thuringiensis*, already commercialised as entomopathogens in biocontrol products, falls within this group. While the biosafety of commercially available *B. thuringiensis* strains has been assessed, a few studies have reported infections in individuals with weakened immune systems [98-99].

Similarly, *Bacillus cereus*, known as an opportunistic human pathogen, depending on its production of emetic and diarrheal toxins, can cause two types of illnesses: emetic and diarrheal syndromes [99]. However, not all *Bacillus cereus* strains produce one or both toxins, and a preliminary prediction of enterotoxigenicity can be conducted through PCR and immunoassay analysis [100].

Based on the analysis of EPA and EU databases, strains belonging to microbial species registered as actives for PPPs (7, 14, 15 and 16) were removed from the selection process of potential candidates for microbial biostimulants development. Currently, the EU pesticide database comprises 124 microorganisms listed as active substances, with 3 of them currently pending approval [34]. The list includes various microbial species, including well-known PGPRs such as *B. subtilis*, *B. pumilus*, and *B. amyloliquefaciens*, which are not only recognised for their PGPR properties but also for their established biocontrol capabilities [101-103]. Similarly, according to the United States EPA, biopesticides fall in a different category than biostimulants as the first are used for pest control. In contrast, biostimulants enhance plant growth without direct pest control properties [104]. In the context of biostimulant development, it might be a more strategic approach to avoid choosing microbial species already listed in the European Union and United States biopesticide databases. The presence of these species in biopesticide databases may increase the likelihood of regulatory scrutiny or rejection when seeking biostimulant registrations due to the distinct categorisation and regulations governing biopesticides and biostimulants [105]. Therefore, adopting this strategy may be more effective in simplifying the approval process and reducing regulatory obstacles.

Similarly, in a screening and selection process for microbial biostimulant candidates, it is crucial from a regulatory perspective to meticulously outline the mode of action of the screened microorganisms, including the exclusion of any potential significant activity as a biocontrol agent [105].

In the initial *in vitro* antagonistic activity assessment, strains *B. brevis* 12 and 13 exhibited significant inhibitory effects on *R. solani* V1, *F. culmorum* V2, *B. cinerea* V3 and *X. campestris* V4. These observed *in vitro* antagonistic activities of *B. brevis* 12 and 13 are consistent with the well-documented biocontrol properties associated with *Brevibacillus* strains. *B. brevis*, in particular, has been recognised for its ability to synthesise gramicidin S, a potential peptide antibiotic that specifically targets the lipid bilayer of organisms' membranes [106]. This biocontrol prowess extends to its effectiveness against various isolates of *Fusarium*, including *F. oxysporum* f.sp. *lycopersici* on tomatoes [107], gray mold

disease in strawberries [108], and *A. alternata*-induced brown leaf spot in potatoes [106].

Furthermore, the *B. brevis* strain DZQ7, isolated from tobacco rhizosphere soil, has demonstrated broad-spectrum antimicrobial activity against soilborne pathogens such as *R. solanacearum*, *Phytophthora nicotianae*, and *Fusarium spp.* [109].

Despite the observed antagonistic inhibitory activity *in vitro*, strains *B. brevis* 12 and 13 did not confer protection against grey mold when applied on plants. In light of this outcome, strains 12 and 13 were deemed suitable to proceed to the next stages of the screening and selection process.

Among all strains analysed for PGP traits, strains 12 and 13 (*B. brevis*) showed to be positive for all traits except for protease production. They performed as strong biofilm and IAA producers and promising for nitrogen fixing activity, as strain 11 (*P. lautus*).

All these findings are in line with PGP traits described in the literature for *B. brevis* and *P. lautus*. Indeed, *B. brevis* and *P. lautus* are both producers of growth regulators, including IAA [110-113]. The role of IAA is particularly important in stimulating plant root surface area, thereby facilitating the uptake of nutrients and water from the soil. In addition, an expanded root surface increases the potential for bacterial colonisation and adhesion and provides an increased area for these microorganisms to thrive. This attachment is further facilitated by the ability of certain bacteria to form the biofilm, an exopolysaccharide matrix, on the plant surface. These biofilms serve to maximise nutrient exchange between the plant and the microorganisms, creating a protective and favourable microenvironment that promotes successful colonisation and nutrient exchange. Notably, *B. brevis* strains 12 and 13 exhibited a robust ability to produce biofilms, and this activity appeared to be enhanced in the presence of glycerol in the growth medium. The role of glycerol in biofilm formation is noteworthy, as observed in various biofilm-producing microorganisms such as *B. subtilis* [96], *P. aeruginosa* [114], *C. albicans* [115], and *M. pneumoniae* [116].

The heightened capacity for biofilm production in the presence of glycerol can be attributed to its dual role as a nutrient source and a potential stimulator of

microbial production of extracellular polymeric substances (EPS), which form the structural foundation of biofilm [95]. Based on this evidence, exploring the use of glycerol as a significant enhancer to promote plant colonisation could be a promising avenue for future research in agricultural applications. This aspect holds particular intrigue in the realm of biostimulant formulations, where the optimisation of microbial colonisation on the plant is pivotal for maximising agronomic benefits.

In the PGP assay, we also included the screening for nitrogen fixation. Nitrogen (N) is one of the key elements for plant growth, playing a fundamental role in various physiological processes. It serves as a primary nutrient essential for the synthesis of crucial components such as proteins, nucleic acids, and chlorophyll. Despite its paramount importance in fostering plant growth and productivity, the excessive use of inorganic N fertilisers has negatively impacted the ecosystem, including soil degradation, water pollution, and nutrient leaching [84]. One of the solutions to overcome this issue and reduce N inputs is the application of N-fixing microbial inoculants that can supply plants with part of the needed N in the form of ammonia through the reduction of atmospheric nitrogen [117]. Given the importance and ambition of this trait, we placed particular emphasis on strains positive for N-fixation in our selection. Specifically, strains 11, 12, and 13 were the only strains exhibiting positive traits in this regard.

While some strains of *B. brevis* have been previously described for nitrogen fixation ability [118-119], there are no previous evidence describing such an activity for *P. lautus*. That's why further investigation is necessary for the definitive assessment of the potential nitrogen fixation ability of these strains. This includes a search for *nif* genes and conducting the ethylene reduction assay (ARA) [110].

Putting together all the above described results, strains 11, 12, and 13 emerge as the most promising microbial candidates among the ones under investigation. Consequently, they will undergo further assessment in plant-based studies (Chapter 3).

In conclusion, the findings from this study underscore the reliability of the MALDI-TOF MS technology when thoroughly implemented in its database,



allowing rapid and accurate identification of microorganisms and exploration of differences between closely related microbial strains. This technology is proving to be useful in exploring the biodiversity of different groups of microorganisms involved in screening and selection processes.

The systematic approach outlined in this work provides a robust framework for identifying and selecting the most promising microbial cultures. This methodology sets the stage for subsequent plant-based evaluations and holds the potential for the development of commercial products. The comprehensive process includes criteria such as initial identification, biosafety evaluation, regulatory compliance, antagonistic activity, and plant growth-promoting traits assessment. Strains 11, 12 and 13 identified through this approach show promise in various parameters such as biofilm production, IAA synthesis and nitrogen-fixing ability. These strains will be selected for further evaluation in plant-based studies, a critical step in translating laboratory discoveries into practical applications. The goal is to determine whether the identified PGP traits benefit plants, ultimately contributing to developing effective biostimulant products for agricultural use.

**Table 3.1.** Bacterial culture identification (ID) results by MALDI-TOF MS and genetic analysis. Bacterial cultures previously identified by MALDI-TOF MS with high reliability (log score  $\geq 2.3$ ) and not further genetically investigated (NA:Not Analysed) are reported in grey.

Strain code	MALDI BioTyper™ ID (Top Score value)	Identification by 16S rDNA			Additional Markers (Acc. No.)
		Bacterial species	Identity level (%)	NCBI Acc. No.	
1	<i>Paenibacillus</i> sp. (2.29)	<i>Paenibacillus lautus</i>	99.57	OR888738	
2	<i>Paenibacillus</i> sp. (2.29)	<i>Paenibacillus lautus</i>	99.57	OR888739	
3	<i>Paenibacillus</i> sp. (2.29)	<i>Paenibacillus lautus</i>	99.57	OR888740	
4	<i>Bacillus</i> sp. (1.99)	<i>Bacillus cereus</i> group	99.79 <sup>a</sup>	OR888741	
5	<i>Bacillus cereus</i> group (2.14)		NA		
6	<i>Peribacillus</i> sp. (2.13)	<i>Peribacillus frigoritolerans</i>	100.0 <sup>b</sup>	OR888742	<i>gapA</i> (OR909268) <i>pgk</i> (OR909269) <i>uvrA</i> (OR909270)
7	<i>Bacillus subtilis</i> (2.30)	<i>Bacillus spizizenii</i>	99.86 <sup>c</sup>	OR888743	<i>purH</i> (OR909271)
8	<i>Bacillus cereus</i> (2.45)		NA		
9	<i>Lysinibacillus fusiformis</i> (2.50)		NA		
10	<i>Bacillus cereus</i> (2.21)		NA		
11	<i>Paenibacillus</i> sp. (2.24)	<i>Paenibacillus lautus</i>	99.57	OR888745	
12	<i>Brevibacillus</i> sp. (1.92)	<i>Brevibacillus brevis</i>	99.62 <sup>d</sup>	OR888746	<i>purH</i> (OR909272)
13	<i>Brevibacillus</i> sp. (1.91)	<i>Brevibacillus brevis</i>	99.62 <sup>d</sup>	OR88874	<i>purH</i> (OR909273)
14	<i>Bacillus licheniformis</i> (2.50)		NA		
15	<i>Bacillus licheniformis</i> (2.45)		NA		
16	<i>Bacillus licheniformis</i> (2.39)		NA		
17	<i>Bacillus cereus</i> (2.39)		NA		

---

<sup>a</sup>The strain belongs to the *Bacillus cereus* group, as the 16S rDNA sequence does not differentiate the closely related species *B. cereus*, *Bacillus thuringiensis*, *Bacillus anthracis*, *Bacillus toyonensis*, *Bacillus wiedmannii*, *Bacillus mycoides*, *Bacillus paramycoides*, *Bacillus paranthracis*, *Bacillus albus*, *Bacillus luti*, *Bacillus nitratireducens*, *Bacillus clarus*, *Bacillus sanguinis*, *Bacillus basilensis*, *Bacillus pseudomycoides*, *Bacillus proteolyticus*, *Bacillus tropicus*, *Bacillus fungorum*, *Bacillus arachidis*, *Bacillus pacificus*, *Bacillus mobilis*, *Bacillus bingmayongensis*, *Bacillus gaemokensis*

<sup>b</sup>The strain belongs to the *Peribacillus simplex* group, as the 16S rDNA sequence does not differentiate the closely related species *P. simplex*, *P. frigoritolerans*, *P. muralis*, *P. butanolivorans*. The partial sequences of *gapA*, *pgk* and *uvrA* genes were analysed to improve the identification.

<sup>c</sup>The strain belongs to the *Bacillus subtilis* group, as the the 16S rDNA sequence does not differentiate the closely related species *Bacillus subtilis*, *Bacillus spizizenii*, *Bacillus rugosus*, *Bacillus tequilensis*, *Bacillus halotolerans*, *Bacillus cabrialesii*, *Bacillus inaquosorum*, *Bacillus stercoris*, *Bacillus mojaviensis*, *Bacillus vallismortis*, *Bacillus nakamurai*, *Bacillus velezensis*, *Bacillus nematocida*, *Bacillus amyloliquefaciens*, *Bacillus siamensis*, *Bacillus atrophaeus*, *Bacillus glycinifermentans* The partial sequence of the *purH* gene was analysed to improve the identification.

<sup>d</sup>The strain belongs to the *Brevibacillus brevis* group, as the the 16S rDNA sequence does not differentiate the closely related species *Brevibacillus brevis*, *Brevibacillus schisleri*, *Brevibacillus formosus*, *Brevibacillus porteri*, *Brevibacillus antibioticus*, *Brevibacillus fortis*, *Brevibacillus choshinensis*, *Brevibacillus parabrevis*, *Brevibacillus reuszeri*, *Brevibacillus nitrificans*, *Brevibacillus gelatini*, *Brevibacillus agri*. The partial sequence of the *purH* gene was analysed to improve the identification.

**Table 3.2.** List of *B. licheniformis* and *B.subtilis* Plant Protection Products (PPP) active substances reported in the EU Pesticide database [120], EPA database [121] and BPDB [122]. Regulatory Status: NA: Not Approved (according to the EC Regulation 1107/200); Pe: Pending (according to the EC Regulation 1107/200).

Strain	Type of pesticide	Geographical area and Status
<i>B. licheniformis</i> strain	Fungicide and	USA, Europe (NA)
<i>B. licheniformis</i> strain	Fungicide and	USA, EU (Pe)
<i>B. subtilis</i> strain FMCH002	Fungicide and	USA, EU (Pe)
<i>B. subtilis</i> strain GB03	Fungicide and	USA, EU (NA)
<i>B. subtilis</i> strain GB34	Fungicide and	USA, EU (NA)
<i>B. subtilis</i> strain IAB/BS03	Fungicide	USA, EU
<i>B. subtilis</i> strain RTI477	Fungicide	USA, EU (Pe)
<i>B. subtilis</i> strain IBE 711	Fungicide	EU (NA)

**Table 3.3.** Kinetic performance evaluation for all strains in four media according to COMB\_value (A). Kinetic performance comparison of all strains calculated as COMB value in TSB medium (B). Data were subjected to analysis of variance (ANOVA) (n=3). Different letters indicate significant differences among treatments according to LSD's test ( $\alpha = 0.05$ ).

A					B	
COMB_value (media comparison for all strains)					COMB_value (strains comparison)	
Strain	NYB	LB	NB	TSB	Strain	TSB
1	34,09 <sup>b</sup>	74,98 <sup>a</sup>	80,95 <sup>a</sup>	78,03 <sup>a</sup>	3	75,03 <sup>c</sup>
2	34,08 <sup>c</sup>	80,75 <sup>a</sup>	48,29 <sup>b</sup>	75,19 <sup>a</sup>	2	75,19 <sup>c</sup>
3	41,91 <sup>b</sup>	87,40 <sup>a</sup>	45,34 <sup>b</sup>	75,03 <sup>a</sup>	1	78,02 <sup>c</sup>
6	80,14 <sup>ns</sup>	80,51 <sup>ns</sup>	57,57 <sup>ns</sup>	84,13 <sup>ns</sup>	6	84,12 <sup>c</sup>
9	335,21 <sup>ns</sup>	254,30 <sup>ns</sup>	245,78 <sup>ns</sup>	318,73 <sup>ns</sup>	11	88,35 <sup>c</sup>
11	43,96 <sup>b</sup>	93,39 <sup>a</sup>	90,45 <sup>a</sup>	88,36 <sup>a</sup>	13	153,75 <sup>b</sup>
12	327,93 <sup>c</sup>	362,26 <sup>c</sup>	325,12 <sup>b</sup>	398,79 <sup>a</sup>	9	318,72 <sup>a</sup>
13	158,08 <sup>ns</sup>	164,22 <sup>ns</sup>	141,18 <sup>ns</sup>	153,76 <sup>ns</sup>	12	325,11 <sup>a</sup>

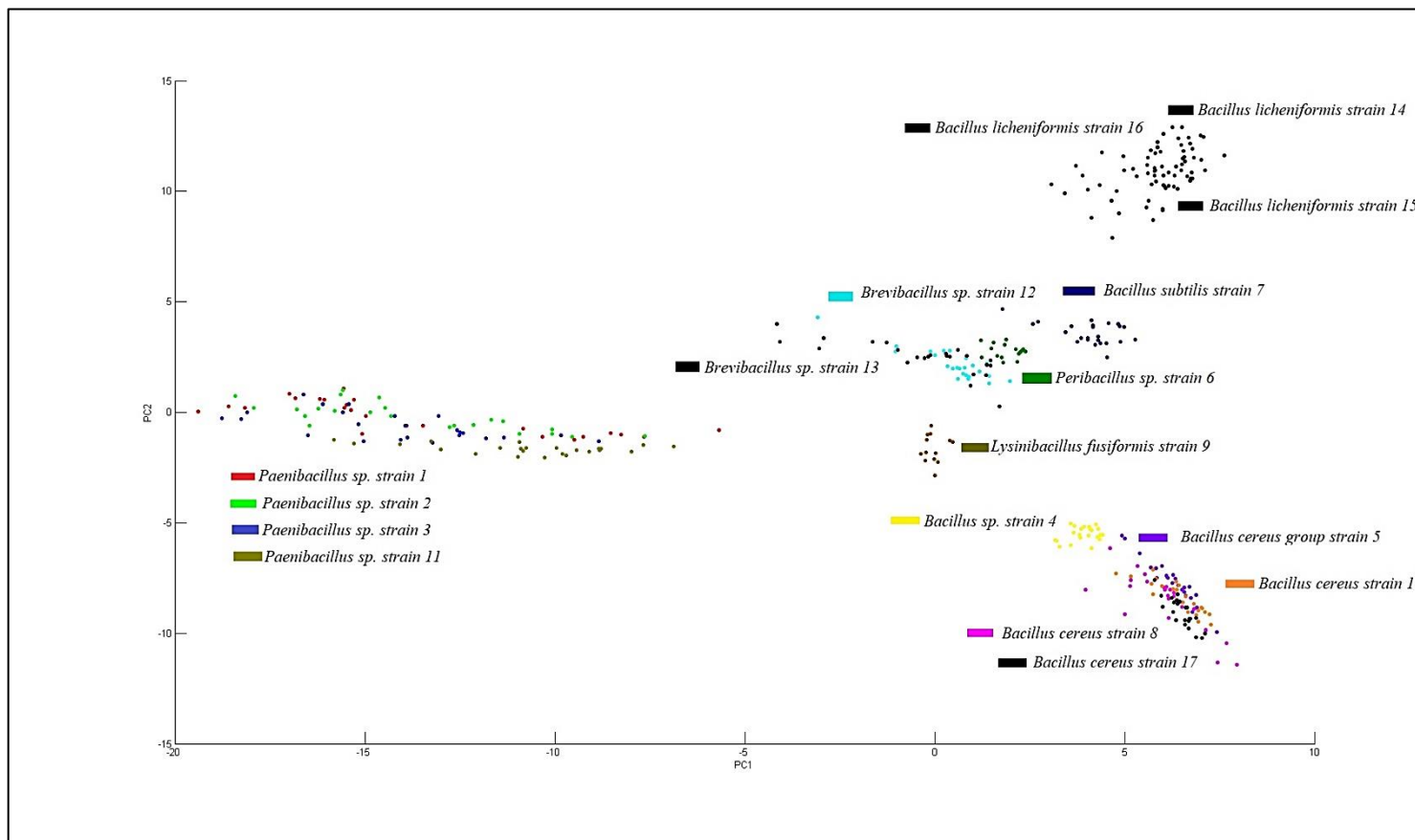


**Figure 3.1.** PCA of the seventeen bacterial cultures.

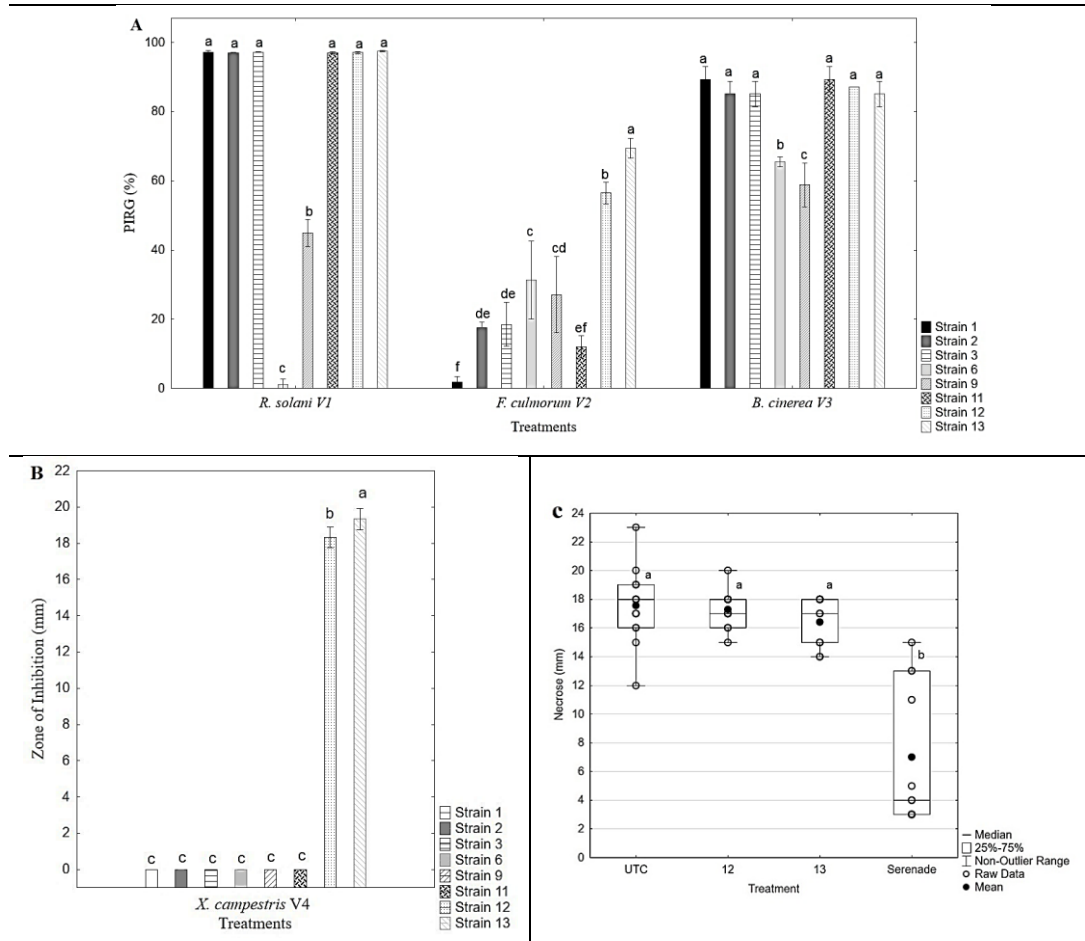


**Figure 3.2.** Antagonistic activity results of bacterial cultures against *R. solani* V1, *F. culmorum* V2, *B. cinerea* V3 (**A**) and *X. campestris* V4 (**B**) *in vitro* and PIRG (%) interpretation (**A**): PIRG  $\leq$  50%: low, 50% < PIRG  $\leq$  60%: medium, 60% < PIRG  $\leq$  75%: high, PIRG > 75%: very high. Drop method interpretation (**B**): inhibition zone > to 25 mm: very strong (++++), inhibition zone from 15 to 25 mm: strong (+++), inhibition zone from 7 to 15 mm: moderate (++) , inhibition zone < 7 mm: weak activity (+) and inhibition zone = 0: no activity (-). Error bars show standard deviation. Data were subjected to analysis of variance (ANOVA) (n=3). Different letters indicate significant differences among treatments according to LSD's test ( $\alpha = 0.05$ ).

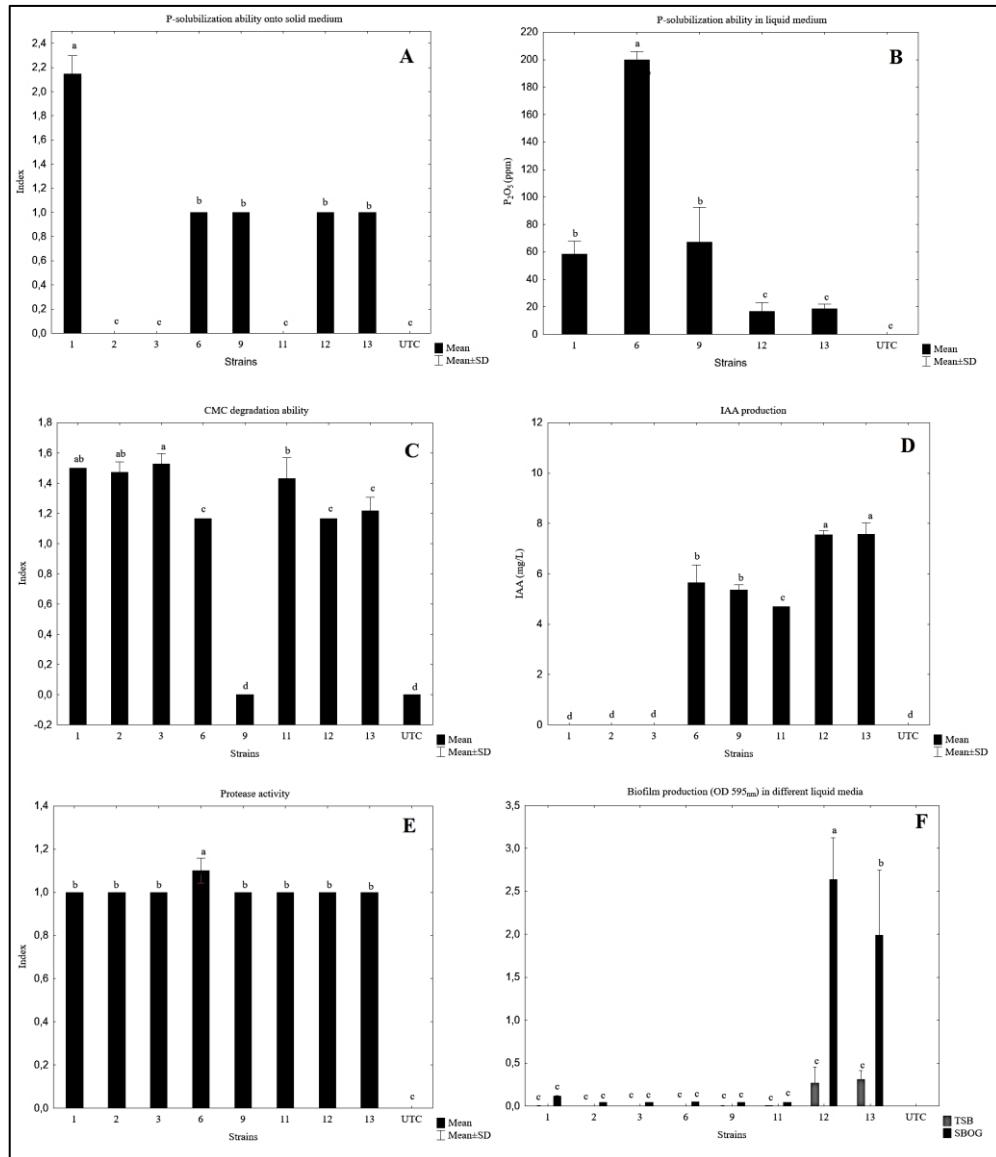


**Figure 3.3.** P-solubilization assay on solid medium (A); P-solubilization liquid assay (B); CMC degrading Index (C), IAA production (D), Protease assay (E) and Biofilm production (F) in TSB and SBOG after 48 hours at 30°C. Error bars show standard deviation. Data were subjected to analysis of variance (ANOVA) (n=3). Different letters indicate significant differences among treatments according to LSD's test ( $\alpha = 0.05$ ).

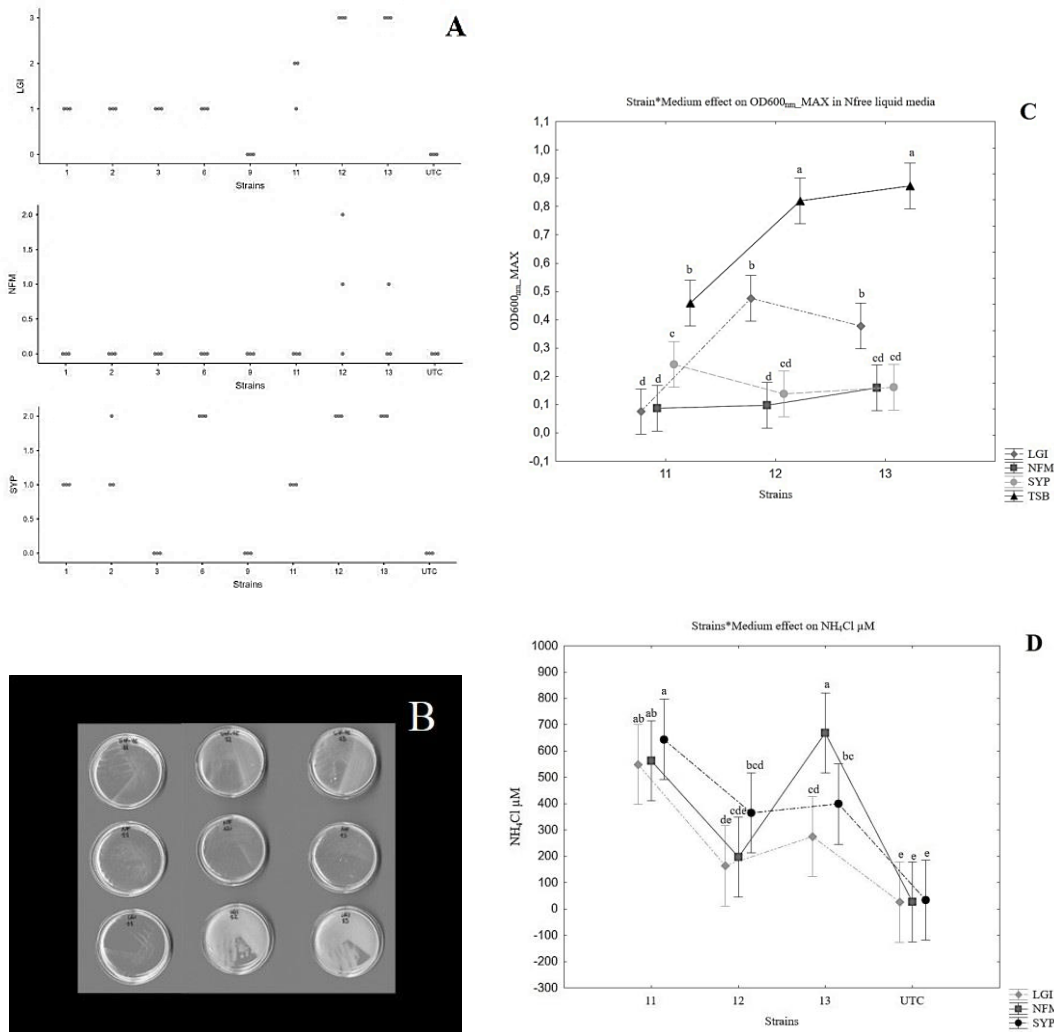


**Figure 3.4.** **A)** Frequency growth distribution of the eight strains tested in LGI, NFM ,and SYP solid media after 24 h incubation at 30°C; **B)** Strains 11, 12 and 13 growth on LGI, NFM , and SYP solid media in Petri-dish plates after 34h incubation at 30°C; **C)** Interaction of strains and media on OD600nm\_MAX in LGI, NFM, SYP, and TSB liquid media after 24 h incubation at 30°C; **D)** Ammonia production as NH<sub>4</sub>Cl (μM) release by strains 11, 12, and 13 in LGI, NFM, and SYP liquid media after 24h incubation at 30°C in a low oxygen atmosphere (O<sub>2</sub> < 0.1%). Error bars show standard deviation. Data were subjected to analysis of variance (ANOVA) (n=3). Different letters indicate significant differences among treatments according to LSD's test (α = 0.05).

**Table 3.4.** Quantification of aerial pellicle biofilm produced by strains 12 and 13 by the means of the dry weight in TSB and SBOG growth media. Data were subjected to analysis of variance (ANOVA) (n=3). Different letters indicate significant differences among treatments according to LSD's test (α = 0.05).

Strain	Medium	Weight (mg) ± SD
12	TSB	0,67 ± 0,06 <sup>c</sup>
12	SBOG	3,77 ± 0,25 <sup>b</sup>
13	TSB	0,23 ± 0,06 <sup>d</sup>
13	SBOG	4,63 ± 0,12 <sup>a</sup>



## References

- [1] Patowary, R., & Deka, H. (2020). Paenibacillus *Beneficial Microbes in Agro-Ecology* (pp. 339-361): Elsevier.
- [2] Grady, E. N., MacDonald, J., Liu, L., Richman, A., & Yuan, Z.-C. Current knowledge and perspectives of Paenibacillus: a review. *Microbial cell factories* **15**, 1-18 (2016)
- [3] Kwak, M.-J., Choi, S.-B., Ha, S.-M., Kim, E. H., Kim, B.-Y., & Chun, J. Genome-based reclassification of Paenibacillus jamilae Aguilera et al. 2001 as a later heterotypic synonym of Paenibacillus polymyxa (Prazmowski 1880) Ash et al. 1994. *International Journal of Systematic and Evolutionary Microbiology* **70**, 3134-3138 (2020)
- [4] Ash, C., Priest, F. G., & Collins, M. D. Molecular identification of rRNA group 3 bacilli (Ash, Farrow, Wallbanks and Collins) using a PCR probe test. *Antonie Van Leeuwenhoek* **64**, 253-260 (1993)
- [5] Langendries, S., & Goormachtig, S. Paenibacillus polymyxa, a Jack of all trades. *Environmental Microbiology* **23**, 5659-5669 (2021)
- [6] Lal, S., & Tabacchioni, S. Ecology and biotechnological potential of Paenibacillus polymyxa: a minireview. *Indian journal of microbiology* **49**, 2-10 (2009)
- [7] Liu, X., Li, Q., Li, Y., Guan, G., & Chen, S. Paenibacillus strains with nitrogen fixation and multiple beneficial properties for promoting plant growth. *PeerJ* **7**, e7445 (2019)
- [8] Coelho, M. R. R., von der Weid, I., Zahner, V., & Seldin, L. Characterization of nitrogen-fixing Paenibacillus species by polymerase chain reaction–restriction fragment length polymorphism analysis of part of genes encoding 16S rRNA and 23S rRNA and by multilocus enzyme electrophoresis. *FEMS Microbiology Letters* **222**, 243-250 (2003)
- [9] Lal, S., Chiarini, L., & Tabacchioni, S. (2016). New insights in plant-associated Paenibacillus species: biocontrol and plant growth-promoting activity *Bacilli and Agrobiotechnology* (pp. 237-279): Springer.
- [10] Raza, W., Yang, W., & Shen, Q. Paenibacillus polymyxa: antibiotics, hydrolytic enzymes and hazard assessment. *Journal of Plant Pathology*, 419-430 (2008)
- [11] Daud, N. S., Rosli, M. A., Azam, Z. M., Othman, N. Z., & Sarmidi, M. R. Paenibacillus polymyxa bioactive compounds for agricultural and biotechnological applications. *Biocatalysis and Agricultural Biotechnology* **18**, 101092 (2019)
- [12] Tinoco, D., Pateraki, C., Koutinas, A. A., & Freire, D. M. Bioprocess Development for 2, 3-Butanediol Production by Paenibacillus Strains. *ChemBioEng Reviews* **8**, 44-62 (2021)
- [13] Dias, B. d. C., Lima, M. E. d. N. V., Vollú, R. E., et al. 2, 3-Butanediol production by the non-pathogenic bacterium Paenibacillus brasilensis. *Applied Microbiology and Biotechnology* **102**, 8773-8782 (2018)
- [14] Białkowska, A. M. Strategies for efficient and economical 2, 3-butanediol production: new trends in this field. *World Journal of Microbiology and Biotechnology* **32**, 1-14 (2016)
- [15] Xie, N.-Z., Li, J.-X., Song, L.-F., et al. Genome sequence of type strain Paenibacillus polymyxa DSM 365, a highly efficient producer of optically active (R, R)-2, 3-butanediol. *Journal of Biotechnology* **195**, 72-73 (2015)
- [16] Kumar, S., & Ujor, V. C. Complete Genome Sequence of Paenibacillus polymyxa DSM 365, a Soil Bacterium of Agricultural and Industrial Importance. *Microbiology Resource Announcements*, e00329-00322 (2022)
- [17] Leibniz Institute DSMZ-German Collection of Microorganisms and Cell Cultures GmbH. (2023) Retrieved 08/31/2023, 2023, from <https://www.dsmz.de/collection/catalogue/details/culture/DSM-365>
- [18] Park, K. Y., Seo, S. Y., Oh, B.-R., Seo, J.-W., & Kim, Y. J. 2, 3-Butanediol induces systemic acquired resistance in the plant immune response. *Journal of Plant Biology* **61**, 424-434 (2018)
- [19] Heinze, S., Lagkouvardos, I., Liebl, W., Schwarz, W. H., Kornberger, P., & Zverlov, V. V. Draft Genome Sequence of Paenibacillus polymyxa DSM 292, a Gram-Positive, Spore-Forming Soil Bacterium with High Biotechnological Potential. *Microbiology Resource Announcements* **9**, e00071-00020 (2020)
- [20] Heinze, S., Zimmermann, K., Ludwig, C., et al. Evaluation of promoter sequences for the secretory production of a Clostridium thermocellum cellulase in Paenibacillus polymyxa. *Applied Microbiology and Biotechnology* **102**, 10147-10159 (2018)

- [21] Weis, C. V., Jutzeler, C. R., & Borgwardt, K. Machine learning for microbial identification and antimicrobial susceptibility testing on MALDI-TOF mass spectra: a systematic review. *Clinical Microbiology and Infection* **26**, 1310-1317 (2020)
- [22] Holland, J. H. (1992). *Adaptation in natural and artificial systems: an introductory analysis with applications to biology, control, and artificial intelligence*: MIT press.
- [23] Chun, J., Oren, A., Ventosa, A., et al. Proposed minimal standards for the use of genome data for the taxonomy of prokaryotes. *International Journal of Systematic and Evolutionary Microbiology* **68**, 461-466 (2018)
- [24] Qadri, S., Nichols, C., Qadri, S., & Villarreal, A. Rapid test for acetyl-methyl-carbinol formation by Enterobacteriaceae. *Journal of Clinical Microbiology* **8**, 463-464 (1978)
- [25] Pérez-Sancho, M., Vela, A. I., Horcajo, P., et al. Rapid differentiation of *Staphylococcus aureus* subspecies based on MALDI-TOF MS profiles. *Journal of Veterinary Diagnostic Investigation* **30**, 813-820 (2018)
- [26] Gekenidis, M.-T., Studer, P., Wüthrich, S., Brunisholz, R., & Drissner, D. Beyond the matrix-assisted laser desorption ionization (MALDI) biotyping workflow: in search of microorganism-specific tryptic peptides enabling discrimination of subspecies. *Applied and Environmental Microbiology* **80**, 4234-4241 (2014)
- [27] Huang, C.-H., & Huang, L. Rapid species-and subspecies-specific level classification and identification of *Lactobacillus casei* group members using MALDI Biotyper combined with ClinProTools. *Journal of Dairy Science* **101**, 979-991 (2018)
- [28] Suarez, S., Ferroni, A., Lotz, A., et al. Ribosomal proteins as biomarkers for bacterial identification by mass spectrometry in the clinical microbiology laboratory. *Journal of Microbiological Methods* **94**, 390-396 (2013)
- [29] Dematheis, F., Walter, M. C., Lang, D., et al. Machine Learning Algorithms for Classification of MALDI-TOF MS Spectra from Phylogenetically Closely Related Species *Brucella melitensis*, *Brucella abortus* and *Brucella suis*. *Microorganisms* **10**, 1658 (2022)
- [30] Kann, S., Sao, S., Phoeung, C., et al. MALDI-TOF mass spectrometry for sub-typing of *Streptococcus pneumoniae*. *BMC Microbiology* **20** (2020)
- [31] Manzulli, V., Rondinone, V., Buchicchio, A., et al. Discrimination of *Bacillus cereus* group members by MALDI-TOF mass spectrometry. *Microorganisms* **9**, 1202 (2021)
- [32] Croxatto, A., Prod'hom, G., & Greub, G. Applications of MALDI-TOF mass spectrometry in clinical diagnostic microbiology. *FEMS Microbiology Reviews* **36**, 380-407 (2012)
- [33] Jeong, H., Choi, S.-K., Ryu, C.-M., & Park, S.-H. Chronicle of a soil bacterium: *Paenibacillus polymyxa* E681 as a tiny guardian of plant and human health. *Frontiers in Microbiology* **10**, 467 (2019)
- [34] Celandroni, F., Salvetti, S., Gueye, S. A., et al. Identification and pathogenic potential of clinical *Bacillus* and *Paenibacillus* isolates. *PloS one* **11**, e0152831 (2016)
- [35] Kopcakova, A., Salamunova, S., Javorsky, P., et al. The Application of MALDI-TOF MS for a Variability Study of *Paenibacillus* larvae. *Veterinary Sciences* **9**, 521 (2022)
- [36] He, Z., Kisla, D., Zhang, L., Yuan, C., Green-Church, K. B., & Yousef, A. E. Isolation and identification of a *Paenibacillus polymyxa* strain that coproduces a novel lantibiotic and polymyxin. *Applied and Environmental Microbiology* **73**, 168-178 (2007)
- [37] Qi, S. S., Cnockaert, M., Carlier, A., & Vandamme, P. A. *Paenibacillus foliorum* sp. nov., *Paenibacillus phytohabitans* sp. nov., *Paenibacillus plantarum* sp. nov., *Paenibacillus planticolens* sp. nov., *Paenibacillus phytorum* sp. nov. and *Paenibacillus germinis* sp. nov., isolated from the *Arabidopsis thaliana* phyllosphere. *International Journal of Systematic and Evolutionary Microbiology* **71**, 004781 (2021)
- [38] Tarfeen, N., Nisa, K. U., & Nisa, Q. MALDI-TOF MS: application in diagnosis, dereplication, biomolecule profiling and microbial ecology. *Proceedings of the Indian National Science Academy* **88**, 277-291 (2022)
- [39] Shu, L.-J., & Yang, Y.-L. *Bacillus* Classification Based on Matrix-Assisted Laser Desorption Ionization Time-of-Flight Mass Spectrometry—Effects of Culture Conditions. *Scientific Reports* **7** (2017)
- [40] Malviya, D., Sahu, P. K., Singh, U. B., et al. Lesson from Ecotoxicity: Revisiting the Microbial Lipopeptides for the Management of Emerging Diseases for Crop Protection. *International Journal of Environmental Research and Public Health* **17**, 1434 (2020)

- [41] Jeong, H., Park, S.-Y., Chung, W.-H., et al. Draft genome sequence of the *Paenibacillus polymyxa* type strain (ATCC 842T), a plant growth-promoting bacterium. *Journal of Bacteriology* **193** (2011)
- [42] Vater, J., Herfort, S., Doellinger, J., Weydmann, M., Borriss, R., & Lasch, P. Genome mining of the lipopeptide biosynthesis of *Paenibacillus polymyxa* E681 in combination with mass spectrometry: discovery of the lipopeptide paenilipoheptin. *ChemBioChem* **19**, 744-753 (2018)
- [43] Vater, J., Niu, B., Dietel, K., & Borriss, R. Characterization of novel fusaricidins produced by *Paenibacillus polymyxa*-M1 using MALDI-TOF mass spectrometry. *Journal of the American Society for Mass Spectrometry* **26**, 1548-1558 (2015)
- [44] Mülner, P., Schwarz, E., Dietel, K., et al. Fusaricidins, Polymyxins and Volatiles Produced by *Paenibacillus polymyxa* Strains DSM 32871 and M1. *Pathogens* **10**, 1485 (2021)
- [45] Ha, M., Jo, H.-J., Choi, E.-K., Kim, Y., Kim, J., & Cho, H.-J. Reliable identification of *Bacillus cereus* group species using low mass biomarkers by MALDI-TOF MS. *J Microbiol Biotechnol.* **29**, 887-896 (2019)
- [46] Walczak-Skierska, J., Monedeiro, F., Maślak, E., & Złoch, M. Lipidomics Characterization of the Microbiome in People with Diabetic Foot Infection Using MALDI-TOF MS. *Anal Chem* **95**, 16251-16262 (2023)
- [47] Maślak, E., Arendowski, A., Złoch, M., et al. Silver Nanoparticle Targets Fabricated Using Chemical Vapor Deposition Method for Differentiation of Bacteria Based on Lipidomic Profiles in Laser Desorption/Ionization Mass Spectrometry. *Antibiotics* **12**, 874 (2023)
- [48] Shu, L. J., & Yang, Y. L. *Bacillus* Classification Based on Matrix-Assisted Laser Desorption Ionization Time-of-Flight Mass Spectrometry-Effects of Culture Conditions. *Sci Rep* **7**, 15546 (2017)
- [49] Ryzhov, V., & Fenselau, C. Characterization of the protein subset desorbed by MALDI from whole bacterial cells. *Analytical chemistry* **73**, 746-750 (2001)
- [50] Wieme, A. D., Spitaels, F., Aerts, M., De Bruyne, K., Van Landschoot, A., & Vandamme, P. Effects of growth medium on matrix-assisted laser desorption-ionization time of flight mass spectra: a case study of acetic acid bacteria. *Applied and Environmental Microbiology* **80**, 1528-1538 (2014)
- [51] Suarez, S., Ferroni, A., Lotz, A., et al. Ribosomal proteins as biomarkers for bacterial identification by mass spectrometry in the clinical microbiology laboratory. *Journal of Microbiological Methods* **94**, 390-396 (2013)
- [52] Vishnoi, A., Roy, R., & Bhattacharya, A. Comparative analysis of bacterial genomes: identification of divergent regions in mycobacterial strains using an anchor-based approach. *Nucleic Acids Research* **35**, 3654-3667 (2007)
- [53] Zhou, Y., Zhang, W., Wu, H., Huang, K., & Jin, J. A high-resolution genomic composition-based method with the ability to distinguish similar bacterial organisms. *BMC Genomics* **20** (2019)
- [54] Choo, S. W., Rishik, S., & Wee, W. Y. Comparative genome analyses of *Mycobacteroides immunogenum* reveals two potential novel subspecies. *Microbial Genomics* **6** (2020)
- [55] Maasz, G., Zrínyi, Z., Fodor, I., et al. Testing the Applicability of MALDI-TOF MS as an Alternative Stock Identification Method in a Cryptic Species Complex. *Molecules* **25**, 3214 (2020)
- [56] Rahi, P., Prakash, O., & Shouche, Y. S. Matrix-assisted laser desorption/ionization time-of-flight mass-spectrometry (MALDI-TOF MS) based microbial identifications: challenges and scopes for microbial ecologists. *Frontiers in Microbiology* **7**, 1359 (2016)
- [57] Wilson, D. A., Young, S., Timm, K., et al. Multicenter Evaluation of the Bruker MALDI Biotyper CA System for the Identification of Clinically Important Bacteria and Yeasts. *American Journal of Clinical Pathology* **147**, 623-631 (2017)
- [58] Elssner, T., & Kostrzewa, M. CLINPROT-a MALDI-TOF MS based system for biomarker discovery and analysis. *Clinic Proteomics* **8**, 167 (2006)
- [59] Stephens, M. A. EDF statistics for goodness of fit and some comparisons. *Journal of the American statistical Association* **69**, 730-737 (1974)
- [60] Baker, G., Smith, J. J., & Cowan, D. A. Review and re-analysis of domain-specific 16S primers. *Journal of Microbiological Methods* **55**, 541-555 (2003)

- [61] Soergel, D. A., Dey, N., Knight, R., & Brenner, S. E. Selection of primers for optimal taxonomic classification of environmental 16S rRNA gene sequences. *The ISME journal* **6**, 1440-1444 (2012)
- [62] Lee, I., Kim, Y. O., Park, S.-C., & Chun, J. OrthoANI: an improved algorithm and software for calculating average nucleotide identity. *International Journal of Systematic and Evolutionary Microbiology* **66**, 1100-1103 (2016)
- [63] Miller, L. T. Single derivatization method for routine analysis of bacterial whole-cell fatty acid methyl esters, including hydroxy acids. *Journal of Clinical Microbiology* **16**, 584-586 (1982)
- [64] Kuykendall, L., Roy, M., O'Neill, J., & Devine, T. Fatty acids, antibiotic resistance, and deoxyribonucleic acid homology groups of *Bradyrhizobium japonicum*. *International Journal of Systematic and Evolutionary Microbiology* **38**, 358-361 (1988)
- [65] Strejcek, M., Smrhova, T., Junkova, P., & Uhlik, O. Whole-Cell MALDI-TOF MS Versus 16S rRNA Gene Analysis for Identification and Dereplication of Recurrent Bacterial Isolates. *Front Microbiol* **9**, 1294 (2018)
- [66] Samad, R. A., Al Disi, Z., Ashfaq, M. Y. M., Wahib, S. M., & Zouari, N. The use of principle component analysis and MALDI-TOF MS for the differentiation of mineral forming *Virgibacillus* and *Bacillus* species isolated from sabkhas. *RSC advances* **10**, 14606-14616 (2020)
- [67] Schwartz, A. R., Ortiz, I., Maymon, M., et al. *Bacillus simplex*—a little known PGPB with anti-fungal activity—alters pea legume root architecture and nodule morphology when coinoculated with *Rhizobium leguminosarum* bv. *viciae*. *Agronomy* **3**, 595-620 (2013)
- [68] Sikorski, J., & Nevo, E. Adaptation and incipient sympatric speciation of *Bacillus simplex* under microclimatic contrast at “Evolution Canyons” I and II, Israel. *Proceedings of the National Academy of Sciences* **102**, 15924-15929 (2005)
- [69] Larkin, M. A., Blackshields, G., Brown, N. P., et al. Clustal W and Clustal X version 2.0. *Bioinformatics* **23**, 2947-2948 (2007)
- [70] Papapetridis, I., Goudriaan, M., Vázquez Vitali, M., et al. Optimizing anaerobic growth rate and fermentation kinetics in *Saccharomyces cerevisiae* strains expressing Calvin-cycle enzymes for improved ethanol yield. *Biotechnology for Biofuels* **11** (2018)
- [71] Tonso, A., Pessoa, A., & Vitolo, M. (2021). Kinetics of Cell Cultivation *Pharmaceutical Biotechnology* (pp. 147-156): CRC Press.
- [72] Ramírez-Olier, J., Trujillo-Salazar, J., Osorio-Echeverri, V., Jaramillo-Ciro, M., & Botero-Botero, L. In vitro antagonism of *Trichoderma asperellum* against *Colletotrichum gloeosporioides*, *Curvularia lunata*, and *Fusarium oxysporum*. *Revista UIS Ingenierías* **18**, 159-165 (2019)
- [73] Balouiri, M., Sadiki, M., & Ibsouda, S. K. Methods for in vitro evaluating antimicrobial activity: A review. *Journal of pharmaceutical analysis* **6**, 71-79 (2016)
- [74] Ismail, A., Ktari, L., Ahmed, M., et al. Antimicrobial activities of bacteria associated with the brown alga *Padina pavonica*. *Frontiers in Microbiology* **7**, 1072 (2016)
- [75] Abbott, W. S. A method of computing the effectiveness of an insecticide. *J. econ. Entomol* **18**, 265-267 (1925)
- [76] Sitepu, I. R., Hashidoko, Y., Santoso, E., & Tahara, S. (2007). *Potent phosphate-solubilizing bacteria isolated from dipterocarps grown in peat swamp forest in Central Kalimantan and their possible utilization for biorehabilitation of degraded peatland*. Paper presented at the Proceedings of the international symposium and workshop on tropical Peatland, Yogyakarta.
- [77] Ahmed, I., Lewis, M., & Knowles, J. Quantification of anions and cations from ternary phosphate based glasses with fixed 50 and 55 mol% P<sub>2</sub>O<sub>5</sub> using ion chromatography. *Physics and chemistry of glasses* **46**, 547-552 (2005)
- [78] RI, P. Mobilization of phosphorus in soil in connection with the vital activity of some microbial species. *Microbiologiya* **17**, 362-370 (1948)
- [79] Hu, X., Chen, J., & Guo, J. Two phosphate- and potassium-solubilizing bacteria isolated from Tianmu Mountain, Zhejiang, China. *World Journal of Microbiology and Biotechnology* **22**, 983-990 (2006)
- [80] Fatharani, R., & Rahayu, Y. (2018). *Isolation and characterization of potassium-solubilizing bacteria from paddy rhizosphere (*Oryza sativa* L.)*. Paper presented at the Journal of Physics: Conference Series.

- [81] Saini, J. K., & Lakshmi, T. Simultaneous isolation and screening of cellulolytic bacteria: selection of efficient medium. *Journal of Pure and Applied Microbiology* **6**, 1339-1344 (2012)
- [82] Gordon, S. A., & Weber, R. P. Colorimetric estimation of indoleacetic acid. *Plant Physiology* **26**, 192 (1951)
- [83] Abdelmoteleb, A., Troncoso-Rojas, R., Gonzalez-Soto, T., & González-Mendoza, D. Antifungal activity of autochthonous *Bacillus subtilis* isolated from *Prosopis juliflora* against phytopathogenic fungi. *Mycobiology* **45**, 385-391 (2017)
- [84] Pérez-Miranda, S., Cabirol, N., George-Téllez, R., Zamudio-Rivera, L. S., & Fernández, F. J. O-CAS, a fast and universal method for siderophore detection. *Journal of Microbiological Methods* **70**, 127-131 (2007)
- [85] Goswami, D., Parmar, S., Vaghela, H., Dhandhukia, P., & Thakker, J. N. Describing *Paenibacillus mucilaginosus* strain N3 as an efficient plant growth promoting rhizobacteria (PGPR). *Cogent Food & Agriculture* **1**, 1000714 (2015)
- [86] Merritt, J. H., Kadouri, D. E., & O'Toole, G. A. Growing and analyzing static biofilms. *Current protocols in microbiology* **22**, 1B. 1.1-1B. 1.18 (2011)
- [87] Yap, M. N., Yang, C. H., Barak, J. D., Jahn, C. E., & Charkowski, A. O. The *Erwinia chrysanthemi* type III secretion system is required for multicellular behavior. *Journal of Bacteriology* **187**, 639-648 (2005)
- [88] Cavalcante, V. A., & Dobereiner, J. A new acid-tolerant nitrogen-fixing bacterium associated with sugarcane. *Plant and Soil* **108**, 23-31 (1988)
- [89] Caballero-Mellado, J., & Martinez-Romero, E. Limited genetic diversity in the endophytic sugarcane bacterium *Acetobacter diazotrophicus*. *Applied and Environmental Microbiology* **60**, 1532-1537 (1994)
- [90] Okon, Y., Albrecht, S. L., & Burris, R. Methods for growing *Spirillum lipoferum* and for counting it in pure culture and in association with plants. *Applied and Environmental Microbiology* **33**, 85-88 (1977)
- [91] Soto-Urzuá, L., & Baca, B. E. [Mechanisms for protecting nitrogenase from inactivation by oxygen]. *Revista Latinoamericana de Microbiologia* **43**, 37-49 (2001)
- [92] Montecillo, J. A. V., & Bae, H. Reclassification of *Brevibacterium frigoritolerans* as *Peribacillus frigoritolerans* comb. nov. based on phylogenomics and multiple molecular synapomorphies. *International Journal of Systematic and Evolutionary Microbiology* **72**, 005389 (2022)
- [93] Liu, G.-H., Liu, B., Wang, J.-P., Che, J.-M., & Li, P.-F. Reclassification of *Brevibacterium frigoritolerans* DSM 8801T as *Bacillus frigoritolerans* comb. nov. based on genome analysis. *Current Microbiology* **77**, 1916-1923 (2020)
- [94] Bianco, A., Capozzi, L., Monno, M. R., et al. Characterization of *Bacillus cereus* Group Isolates From Human Bacteremia by Whole-Genome Sequencing. *Front Microbiol* **11**, 599524 (2020)
- [95] Scofield, J., & Silo-Suh, L. Glycerol metabolism promotes biofilm formation by *Pseudomonas aeruginosa*. *Can J Microbiol* **62**, 704-710 (2016)
- [96] Shemesh, M., & Chai, Y. A combination of glycerol and manganese promotes biofilm formation in *Bacillus subtilis* via histidine kinase KinD signaling. *Journal of Bacteriology* **195**, 2747-2754 (2013)
- [97] Dunlap, C. A., Bowman, M. J., & Zeigler, D. R. Promotion of *Bacillus subtilis* subsp. *inaquosorum*, *Bacillus subtilis* subsp. *spizizenii* and *Bacillus subtilis* subsp. *stercoris* to species status. *Antonie Van Leeuwenhoek* **113**, 1-12 (2020)
- [98] Hansen, B. M., & Salamitou, S. (2000). *Virulence of Bacillus thuringiensis*.
- [99] Ehling-Schulz, M., Lereclus, D., & Koehler, T. M. The *Bacillus cereus* Group: *Bacillus* Species with Pathogenic Potential. *Microbiol Spectr* **7** (2019)
- [100] Tallent, S. M., Hait, J. M., & Bennett, R. W. Analysis of *Bacillus cereus* toxicity using PCR, ELISA and a lateral flow device. *Journal of Applied Microbiology* **118**, 1068-1075 (2015)
- [101] Chowdhury, S. P., Uhl, J., Grosch, R., et al. Cyclic Lipopeptides of *Bacillus amyloliquefaciens* subsp. *plantarum* Colonizing the Lettuce Rhizosphere Enhance Plant Defense Responses Toward the Bottom Rot Pathogen *Rhizoctonia solani*. *Mol Plant Microbe Interact* **28**, 984-995 (2015)

- [102] Schönbichler, A., Díaz-Moreno, S. M., Srivastava, V., & McKee, L. S. Exploring the Potential for Fungal Antagonism and Cell Wall Attack by *Bacillus subtilis* natto. *Front Microbiol* **11**, 521 (2020)
- [103] Dobrzyński, J., Jakubowska, Z., Kulkova, I., Kowalczyk, P., & Kramkowski, K. Biocontrol of fungal phytopathogens by *Bacillus pumilus*. *Front Microbiol* **14**, 1194606 (2023)
- [104] EPA. (Accessed October 30, 2023). Draft Guidance for Plant Regulators and Claims, Including Plant Biostimulants. from <https://www.epa.gov/pesticides/draft-guidance-plant-regulators-and-claims-including-plant-biostimulants>
- [105] Traon, D., Amat, L., Zotz, F., & du Jardin, P. A Legal Framework for Plant Biostimulants and Agronomic Fertiliser Additives in the EU-Report to the European Commission, DG Enterprise & Industry. (2014)
- [106] Ahmed, A. Biological control of potato brown leaf spot disease caused by *Alternaria alternata* using *Brevibacillus formosus* strain DSM 9885 and *Brevibacillus brevis* strain NBRC 15304. *J Plant Pathol Microbiol* **8**, 1-8 (2017)
- [107] Chandel, S., Allan, E. J., & Woodward, S. Biological control of *Fusarium oxysporum* f. sp. *lycopersici* on tomato by *Brevibacillus brevis*. *Journal of Phytopathology* **158**, 470-478 (2010)
- [108] Wafaa, M. H., Abd El Kareem, F. K., & Shabaan, A. A. H. Bioprocessing of *Brevibacillus brevis* and *Bacillus polymyxa*: a potential biocontrol agents of gray mould disease of strawberry fruits. *Current Opinion in Biotechnology*, S45 (2013)
- [109] Hou, Q., Wang, C., Hou, X., et al. Draft Genome Sequence of *Brevibacillus brevis* DZQ7, a Plant Growth-Promoting Rhizobacterium with Broad-Spectrum Antimicrobial Activity. *Genome Announc* **3** (2015)
- [110] Nehra, V., Saharan, B. S., & Choudhary, M. Evaluation of *Brevibacillus brevis* as a potential plant growth promoting rhizobacteria for cotton (*Gossypium hirsutum*) crop. *SpringerPlus* **5**, 948 (2016)
- [111] Vivas, A., Barea, J. M., & Azcón, R. *Brevibacillus brevis* Isolated from Cadmium- or Zinc-Contaminated Soils Improves in Vitro Spore Germination and Growth of *Glomus mosseae* under High Cd or Zn Concentrations. *Microbial Ecology* **49**, 416-424 (2005)
- [112] Fouda, A., Eid, A. M., Elsaied, A., et al. Plant Growth-Promoting Endophytic Bacterial Community Inhabiting the Leaves of *Pulicaria incisa* (Lam.) DC Inherent to Arid Regions. *Plants* **10**, 76 (2021)
- [113] Ptak, A., Morańska, E., Warchoń, M., et al. Endophytic bacteria from in vitro culture of *Leucopodium aestivum* L. a new source of galanthamine and elicitor of alkaloid biosynthesis. *Sci Rep* **12**, 13700 (2022)
- [114] Scoffield, J., & Silo-Suh, L. Glycerol metabolism promotes biofilm formation by *Pseudomonas aeruginosa*. *Canadian journal of microbiology* **62**, 704-710 (2016)
- [115] Desai, J. V., Bruno, V. M., Ganguly, S., et al. Regulatory role of glycerol in *Candida albicans* biofilm formation. *mBio* **4**, e00637-00612 (2013)
- [116] Hames, C., Halbedel, S., Hoppert, M., Frey, J., & Stülke, J. Glycerol metabolism is important for cytotoxicity of *Mycoplasma pneumoniae*. *Journal of Bacteriology* **191**, 747-753 (2009)
- [117] Soumare, A., Diedhiou, A. G., Thuita, M., et al. Exploiting Biological Nitrogen Fixation: A Route Towards a Sustainable Agriculture. *Plants (Basel)* **9** (2020)
- [118] Jianguang, S. (2008).
- [119] Nehra, V., Saharan, B. S., & Choudhary, M. Evaluation of *Brevibacillus brevis* as a potential plant growth promoting rhizobacteria for cotton (*Gossypium hirsutum*) crop. *SpringerPlus* **5** (2016)
- [120] EU. Pesticides Database. (Accessed November 21, 2023) Retrieved May 2022, 2022, from [https://ec.europa.eu/food/plants/pesticides/eu-pesticides-database\\_it](https://ec.europa.eu/food/plants/pesticides/eu-pesticides-database_it)
- [121] EPA. United States Environmental Protection Agency Pesticide Database. (Accessed November 21, 2023), from <https://www.epa.gov/safepestcontrol/search-registered-pesticide-products>
- [122] BPDB. (Accessed November 21, 2023). Bio-Pesticides DataBase. from <https://sitem.herts.ac.uk/aeru/bpdb/index.htm>
- [1] Patowary, R., & Deka, H. (2020). *Paenibacillus Beneficial Microbes in Agro-Ecology* (pp. 339-361): Elsevier.

- [2] Grady, E. N., MacDonald, J., Liu, L., Richman, A., & Yuan, Z.-C. Current knowledge and perspectives of *Paenibacillus*: a review. *Microbial cell factories* **15**, 1-18 (2016)
- [3] Kwak, M.-J., Choi, S.-B., Ha, S.-M., Kim, E. H., Kim, B.-Y., & Chun, J. Genome-based reclassification of *Paenibacillus jamilae* Aguilera et al. 2001 as a later heterotypic synonym of *Paenibacillus polymyxa* (Prazmowski 1880) Ash et al. 1994. *International Journal of Systematic and Evolutionary Microbiology* **70**, 3134-3138 (2020)
- [4] Ash, C., Priest, F. G., & Collins, M. D. Molecular identification of rRNA group 3 bacilli (Ash, Farrow, Wallbanks and Collins) using a PCR probe test. *Antonie Van Leeuwenhoek* **64**, 253-260 (1993)
- [5] Langendries, S., & Goormachtig, S. *Paenibacillus polymyxa*, a Jack of all trades. *Environmental Microbiology* **23**, 5659-5669 (2021)
- [6] Lal, S., & Tabacchioni, S. Ecology and biotechnological potential of *Paenibacillus polymyxa*: a minireview. *Indian journal of microbiology* **49**, 2-10 (2009)
- [7] Liu, X., Li, Q., Li, Y., Guan, G., & Chen, S. *Paenibacillus* strains with nitrogen fixation and multiple beneficial properties for promoting plant growth. *PeerJ* **7**, e7445 (2019)
- [8] Coelho, M. R. R., von der Weid, I., Zahner, V., & Seldin, L. Characterization of nitrogen-fixing *Paenibacillus* species by polymerase chain reaction–restriction fragment length polymorphism analysis of part of genes encoding 16S rRNA and 23S rRNA and by multilocus enzyme electrophoresis. *FEMS Microbiology Letters* **222**, 243-250 (2003)
- [9] Lal, S., Chiarini, L., & Tabacchioni, S. (2016). New insights in plant-associated *Paenibacillus* species: biocontrol and plant growth-promoting activity *Bacilli and Agrobiotechnology* (pp. 237-279): Springer.
- [10] Raza, W., Yang, W., & Shen, Q. *Paenibacillus polymyxa*: antibiotics, hydrolytic enzymes and hazard assessment. *Journal of Plant Pathology*, 419-430 (2008)
- [11] Daud, N. S., Rosli, M. A., Azam, Z. M., Othman, N. Z., & Sarmidi, M. R. *Paenibacillus polymyxa* bioactive compounds for agricultural and biotechnological applications. *Biocatalysis and Agricultural Biotechnology* **18**, 101092 (2019)
- [12] Tinôco, D., Pateraki, C., Koutinas, A. A., & Freire, D. M. Bioprocess Development for 2, 3-Butanediol Production by *Paenibacillus* Strains. *ChemBioEng Reviews* **8**, 44-62 (2021)
- [13] Dias, B. d. C., Lima, M. E. d. N. V., Vollú, R. E., et al. 2, 3-Butanediol production by the non-pathogenic bacterium *Paenibacillus brasiliensis*. *Applied Microbiology and Biotechnology* **102**, 8773-8782 (2018)
- [14] Białkowska, A. M. Strategies for efficient and economical 2, 3-butanediol production: new trends in this field. *World Journal of Microbiology and Biotechnology* **32**, 1-14 (2016)
- [15] Xie, N.-Z., Li, J.-X., Song, L.-F., et al. Genome sequence of type strain *Paenibacillus polymyxa* DSM 365, a highly efficient producer of optically active (R, R)-2, 3-butanediol. *Journal of Biotechnology* **195**, 72-73 (2015)
- [16] Kumar, S., & Ujor, V. C. Complete Genome Sequence of *Paenibacillus polymyxa* DSM 365, a Soil Bacterium of Agricultural and Industrial Importance. *Microbiology Resource Announcements*, e00329-00322 (2022)
- [17] Leibniz Institute DSMZ-German Collection of Microorganisms and Cell Cultures GmbH. (2023) Retrieved 08/31/2023, 2023, from <https://www.dsmz.de/collection/catalogue/details/culture/DSM-365>
- [18] Park, K. Y., Seo, S. Y., Oh, B.-R., Seo, J.-W., & Kim, Y. J. 2, 3-Butanediol induces systemic acquired resistance in the plant immune response. *Journal of Plant Biology* **61**, 424-434 (2018)
- [19] Heinze, S., Lagkouvardos, I., Liebl, W., Schwarz, W. H., Kornberger, P., & Zverlov, V. V. Draft Genome Sequence of *Paenibacillus polymyxa* DSM 292, a Gram-Positive, Spore-Forming Soil Bacterium with High Biotechnological Potential. *Microbiology Resource Announcements* **9**, e00071-00020 (2020)
- [20] Heinze, S., Zimmermann, K., Ludwig, C., et al. Evaluation of promoter sequences for the secretory production of a *Clostridium thermocellum* cellulase in *Paenibacillus polymyxa*. *Applied Microbiology and Biotechnology* **102**, 10147-10159 (2018)
- [21] Weis, C. V., Jutzeler, C. R., & Borgwardt, K. Machine learning for microbial identification and antimicrobial susceptibility testing on MALDI-TOF mass spectra: a systematic review. *Clinical Microbiology and Infection* **26**, 1310-1317 (2020)
- [22] Holland, J. H. (1992). *Adaptation in natural and artificial systems: an introductory analysis with applications to biology, control, and artificial intelligence*: MIT press.

- [23] Chun, J., Oren, A., Ventosa, A., et al. Proposed minimal standards for the use of genome data for the taxonomy of prokaryotes. *International Journal of Systematic and Evolutionary Microbiology* **68**, 461-466 (2018)
- [24] Qadri, S., Nichols, C., Qadri, S., & Villarreal, A. Rapid test for acetyl-methyl-carbinol formation by Enterobacteriaceae. *Journal of Clinical Microbiology* **8**, 463-464 (1978)
- [25] Pérez-Sancho, M., Vela, A. I., Horcajo, P., et al. Rapid differentiation of *Staphylococcus aureus* subspecies based on MALDI-TOF MS profiles. *Journal of Veterinary Diagnostic Investigation* **30**, 813-820 (2018)
- [26] Gekenidis, M.-T., Studer, P., Wüthrich, S., Brunisholz, R., & Drissner, D. Beyond the matrix-assisted laser desorption ionization (MALDI) biotyping workflow: in search of microorganism-specific tryptic peptides enabling discrimination of subspecies. *Applied and Environmental Microbiology* **80**, 4234-4241 (2014)
- [27] Huang, C.-H., & Huang, L. Rapid species- and subspecies-specific level classification and identification of *Lactobacillus casei* group members using MALDI Biotyper combined with ClinProTools. *Journal of Dairy Science* **101**, 979-991 (2018)
- [28] Suarez, S., Ferroni, A., Lotz, A., et al. Ribosomal proteins as biomarkers for bacterial identification by mass spectrometry in the clinical microbiology laboratory. *Journal of Microbiological Methods* **94**, 390-396 (2013)
- [29] Dematheis, F., Walter, M. C., Lang, D., et al. Machine Learning Algorithms for Classification of MALDI-TOF MS Spectra from Phylogenetically Closely Related Species *Brucella melitensis*, *Brucella abortus* and *Brucella suis*. *Microorganisms* **10**, 1658 (2022)
- [30] Kann, S., Sao, S., Phoeung, C., et al. MALDI-TOF mass spectrometry for sub-typing of *Streptococcus pneumoniae*. *BMC Microbiology* **20** (2020)
- [31] Manzulli, V., Rondinone, V., Buchicchio, A., et al. Discrimination of *Bacillus cereus* group members by MALDI-TOF mass spectrometry. *Microorganisms* **9**, 1202 (2021)
- [32] Croxatto, A., Prod'hom, G., & Greub, G. Applications of MALDI-TOF mass spectrometry in clinical diagnostic microbiology. *FEMS Microbiology Reviews* **36**, 380-407 (2012)
- [33] Jeong, H., Choi, S.-K., Ryu, C.-M., & Park, S.-H. Chronicle of a soil bacterium: *Paenibacillus polymyxa* E681 as a tiny guardian of plant and human health. *Frontiers in Microbiology* **10**, 467 (2019)
- [34] Celandroni, F., Salvetti, S., Gueye, S. A., et al. Identification and pathogenic potential of clinical *Bacillus* and *Paenibacillus* isolates. *PLoS one* **11**, e0152831 (2016)
- [35] Kopcakova, A., Salamunova, S., Javorsky, P., et al. The Application of MALDI-TOF MS for a Variability Study of *Paenibacillus* larvae. *Veterinary Sciences* **9**, 521 (2022)
- [36] He, Z., Kisla, D., Zhang, L., Yuan, C., Green-Church, K. B., & Yousef, A. E. Isolation and identification of a *Paenibacillus polymyxa* strain that coproduces a novel lantibiotic and polymyxin. *Applied and Environmental Microbiology* **73**, 168-178 (2007)
- [37] Qi, S. S., Cnockaert, M., Carlier, A., & Vandamme, P. A. *Paenibacillus foliorum* sp. nov., *Paenibacillus phytohabitans* sp. nov., *Paenibacillus plantarum* sp. nov., *Paenibacillus planticolens* sp. nov., *Paenibacillus phytorum* sp. nov. and *Paenibacillus germinis* sp. nov., isolated from the Arabidopsis thaliana phyllosphere. *International Journal of Systematic and Evolutionary Microbiology* **71**, 004781 (2021)
- [38] Tarfeen, N., Nisa, K. U., & Nisa, Q. MALDI-TOF MS: application in diagnosis, dereplication, biomolecule profiling and microbial ecology. *Proceedings of the Indian National Science Academy* **88**, 277-291 (2022)
- [39] Shu, L.-J., & Yang, Y.-L. *Bacillus* Classification Based on Matrix-Assisted Laser Desorption Ionization Time-of-Flight Mass Spectrometry—Effects of Culture Conditions. *Scientific Reports* **7** (2017)
- [40] Malviya, D., Sahu, P. K., Singh, U. B., et al. Lesson from Ecotoxicity: Revisiting the Microbial Lipopeptides for the Management of Emerging Diseases for Crop Protection. *International Journal of Environmental Research and Public Health* **17**, 1434 (2020)
- [41] Jeong, H., Park, S.-Y., Chung, W.-H., et al. Draft genome sequence of the *Paenibacillus polymyxa* type strain (ATCC 842T), a plant growth-promoting bacterium. *Journal of Bacteriology* **193** (2011)
- [42] Vater, J., Herfort, S., Doellinger, J., Weydmann, M., Borriss, R., & Lasch, P. Genome mining of the lipopeptide biosynthesis of *Paenibacillus polymyxa* E681 in combination with mass spectrometry: discovery of the lipopeptide paenilipoheptin. *ChemBioChem* **19**, 744-753 (2018)



- [43] Vater, J., Niu, B., Dietel, K., & Borriss, R. Characterization of novel fusaricidins produced by *Paenibacillus polymyxa*-M1 using MALDI-TOF mass spectrometry. *Journal of the American Society for Mass Spectrometry* **26**, 1548-1558 (2015)
- [44] Mülner, P., Schwarz, E., Dietel, K., et al. Fusaricidins, Polymyxins and Volatiles Produced by *Paenibacillus polymyxa* Strains DSM 32871 and M1. *Pathogens* **10**, 1485 (2021)
- [45] Ha, M., Jo, H.-J., Choi, E.-K., Kim, Y., Kim, J., & Cho, H.-J. Reliable identification of *Bacillus cereus* group species using low mass biomarkers by MALDI-TOF MS. *J Microbiol Biotechnol.* **29**, 887-896 (2019)
- [46] Walczak-Skierska, J., Monedeiro, F., Maślak, E., & Złoch, M. Lipidomics Characterization of the Microbiome in People with Diabetic Foot Infection Using MALDI-TOF MS. *Anal Chem* **95**, 16251-16262 (2023)
- [47] Maślak, E., Arendowski, A., Złoch, M., et al. Silver Nanoparticle Targets Fabricated Using Chemical Vapor Deposition Method for Differentiation of Bacteria Based on Lipidomic Profiles in Laser Desorption/Ionization Mass Spectrometry. *Antibiotics* **12**, 874 (2023)
- [48] Shu, L. J., & Yang, Y. L. *Bacillus* Classification Based on Matrix-Assisted Laser Desorption Ionization Time-of-Flight Mass Spectrometry-Effects of Culture Conditions. *Sci Rep* **7**, 15546 (2017)
- [49] Ryzhov, V., & Fenselau, C. Characterization of the protein subset desorbed by MALDI from whole bacterial cells. *Analytical chemistry* **73**, 746-750 (2001)
- [50] Wieme, A. D., Spitaels, F., Aerts, M., De Bruyne, K., Van Landschoot, A., & Vandamme, P. Effects of growth medium on matrix-assisted laser desorption-ionization time of flight mass spectra: a case study of acetic acid bacteria. *Applied and Environmental Microbiology* **80**, 1528-1538 (2014)
- [51] Suarez, S., Ferroni, A., Lotz, A., et al. Ribosomal proteins as biomarkers for bacterial identification by mass spectrometry in the clinical microbiology laboratory. *Journal of Microbiological Methods* **94**, 390-396 (2013)
- [52] Vishnoi, A., Roy, R., & Bhattacharya, A. Comparative analysis of bacterial genomes: identification of divergent regions in mycobacterial strains using an anchor-based approach. *Nucleic Acids Research* **35**, 3654-3667 (2007)
- [53] Zhou, Y., Zhang, W., Wu, H., Huang, K., & Jin, J. A high-resolution genomic composition-based method with the ability to distinguish similar bacterial organisms. *BMC Genomics* **20** (2019)
- [54] Choo, S. W., Rishik, S., & Wee, W. Y. Comparative genome analyses of *Mycobacteroides* immunogenum reveals two potential novel subspecies. *Microbial Genomics* **6** (2020)
- [55] Maasz, G., Zrínyi, Z., Fodor, I., et al. Testing the Applicability of MALDI-TOF MS as an Alternative Stock Identification Method in a Cryptic Species Complex. *Molecules* **25**, 3214 (2020)
- [56] Rahi, P., Prakash, O., & Shouche, Y. S. Matrix-assisted laser desorption/ionization time-of-flight mass-spectrometry (MALDI-TOF MS) based microbial identifications: challenges and scopes for microbial ecologists. *Frontiers in Microbiology* **7**, 1359 (2016)
- [57] Wilson, D. A., Young, S., Timm, K., et al. Multicenter Evaluation of the Bruker MALDI Biotyper CA System for the Identification of Clinically Important Bacteria and Yeasts. *American Journal of Clinical Pathology* **147**, 623-631 (2017)
- [58] Elssner, T., & Kostrzewa, M. CLINPROT-a MALDI-TOF MS based system for biomarker discovery and analysis. *Clinic Proteomics* **8**, 167 (2006)
- [59] Stephens, M. A. EDF statistics for goodness of fit and some comparisons. *Journal of the American statistical Association* **69**, 730-737 (1974)
- [60] Baker, G., Smith, J. J., & Cowan, D. A. Review and re-analysis of domain-specific 16S primers. *Journal of Microbiological Methods* **55**, 541-555 (2003)
- [61] Soergel, D. A., Dey, N., Knight, R., & Brenner, S. E. Selection of primers for optimal taxonomic classification of environmental 16S rRNA gene sequences. *The ISME journal* **6**, 1440-1444 (2012)
- [62] Lee, I., Kim, Y. O., Park, S.-C., & Chun, J. OrthoANI: an improved algorithm and software for calculating average nucleotide identity. *International Journal of Systematic and Evolutionary Microbiology* **66**, 1100-1103 (2016)
- [63] Miller, L. T. Single derivatization method for routine analysis of bacterial whole-cell fatty acid methyl esters, including hydroxy acids. *Journal of Clinical Microbiology* **16**, 584-586 (1982)

- [64] Kuykendall, L., Roy, M., O'Neill, J., & Devine, T. Fatty acids, antibiotic resistance, and deoxyribonucleic acid homology groups of *Bradyrhizobium japonicum*. *International Journal of Systematic and Evolutionary Microbiology* **38**, 358-361 (1988)
- [65] Strejcek, M., Smrhova, T., Junkova, P., & Uhlik, O. Whole-Cell MALDI-TOF MS Versus 16S rRNA Gene Analysis for Identification and Dereplication of Recurrent Bacterial Isolates. *Front Microbiol* **9**, 1294 (2018)
- [66] Samad, R. A., Al Disi, Z., Ashfaq, M. Y. M., Wahib, S. M., & Zouari, N. The use of principle component analysis and MALDI-TOF MS for the differentiation of mineral forming *Virgibacillus* and *Bacillus* species isolated from sabkhas. *RSC advances* **10**, 14606-14616 (2020)
- [67] Schwartz, A. R., Ortiz, I., Maymon, M., et al. *Bacillus simplex*—a little known PGPB with anti-fungal activity—alters pea legume root architecture and nodule morphology when coinoculated with *Rhizobium leguminosarum* bv. *viciae*. *Agronomy* **3**, 595-620 (2013)
- [68] Sikorski, J., & Nevo, E. Adaptation and incipient sympatric speciation of *Bacillus simplex* under microclimatic contrast at “Evolution Canyons” I and II, Israel. *Proceedings of the National Academy of Sciences* **102**, 15924-15929 (2005)
- [69] Larkin, M. A., Blackshields, G., Brown, N. P., et al. Clustal W and Clustal X version 2.0. *Bioinformatics* **23**, 2947-2948 (2007)
- [70] Papapetridis, I., Goudriaan, M., Vázquez Vitali, M., et al. Optimizing anaerobic growth rate and fermentation kinetics in *Saccharomyces cerevisiae* strains expressing Calvin-cycle enzymes for improved ethanol yield. *Biotechnology for Biofuels* **11** (2018)
- [71] Tonso, A., Pessoa, A., & Vitolo, M. (2021). Kinetics of Cell Cultivation *Pharmaceutical Biotechnology* (pp. 147-156): CRC Press.
- [72] Ramírez-Olier, J., Trujillo-Salazar, J., Osorio-Echeverri, V., Jaramillo-Ciro, M., & Botero-Botero, L. In vitro antagonism of *Trichoderma asperellum* against *Colletotrichum gloeosporioides*, *Curvularia lunata*, and *Fusarium oxysporum*. *Revista UIS Ingenierías* **18**, 159-165 (2019)
- [73] Balouiri, M., Sadiki, M., & Ibsouda, S. K. Methods for in vitro evaluating antimicrobial activity: A review. *Journal of pharmaceutical analysis* **6**, 71-79 (2016)
- [74] Ismail, A., Ktari, L., Ahmed, M., et al. Antimicrobial activities of bacteria associated with the brown alga *Padina pavonica*. *Frontiers in Microbiology* **7**, 1072 (2016)
- [75] Abbott, W. S. A method of computing the effectiveness of an insecticide. *J. econ. Entomol* **18**, 265-267 (1925)
- [76] Sitepu, I. R., Hashidoko, Y., Santoso, E., & Tahara, S. (2007). *Potent phosphate-solubilizing bacteria isolated from dipterocarps grown in peat swamp forest in Central Kalimantan and their possible utilization for biorehabilitation of degraded peatland*. Paper presented at the Proceedings of the international symposium and workshop on tropical Peatland, Yogyakarta.
- [77] Ahmed, I., Lewis, M., & Knowles, J. Quantification of anions and cations from ternary phosphate based glasses with fixed 50 and 55 mol% P<sub>2</sub>O<sub>5</sub> using ion chromatography. *Physics and chemistry of glasses* **46**, 547-552 (2005)
- [78] RI, P. Mobilization of phosphorus in soil in connection with the vital activity of some microbial species. *Microbiologiya* **17**, 362-370 (1948)
- [79] Hu, X., Chen, J., & Guo, J. Two phosphate-and potassium-solubilizing bacteria isolated from Tianmu Mountain, Zhejiang, China. *World Journal of Microbiology and Biotechnology* **22**, 983-990 (2006)
- [80] Fatharani, R., & Rahayu, Y. (2018). *Isolation and characterization of potassium-solubilizing bacteria from paddy rhizosphere (Oryza sativa L.)*. Paper presented at the Journal of Physics: Conference Series.
- [81] Saini, J. K., & Lakshmi, T. Simultaneous isolation and screening of cellulolytic bacteria: selection of efficient medium. *Journal of Pure and Applied Microbiology* **6**, 1339-1344 (2012)
- [82] Gordon, S. A., & Weber, R. P. Colorimetric estimation of indoleacetic acid. *Plant Physiology* **26**, 192 (1951)
- [83] Abdelmoteleb, A., Troncoso-Rojas, R., Gonzalez-Soto, T., & González-Mendoza, D. Antifungal activity of autochthonous *Bacillus subtilis* isolated from *Prosopis juliflora* against phytopathogenic fungi. *Mycobiology* **45**, 385-391 (2017)

- [84] Pérez-Miranda, S., Cabirol, N., George-Téllez, R., Zamudio-Rivera, L. S., & Fernández, F. J. O-CAS, a fast and universal method for siderophore detection. *Journal of Microbiological Methods* **70**, 127-131 (2007)
- [85] Goswami, D., Parmar, S., Vaghela, H., Dhandhukia, P., & Thakker, J. N. Describing *Paenibacillus mucilaginosus* strain N3 as an efficient plant growth promoting rhizobacteria (PGPR). *Cogent Food & Agriculture* **1**, 1000714 (2015)
- [86] Merritt, J. H., Kadouri, D. E., & O'Toole, G. A. Growing and analyzing static biofilms. *Current protocols in microbiology* **22**, 1B. 1.1-1B. 1.18 (2011)
- [87] Yap, M. N., Yang, C. H., Barak, J. D., Jahn, C. E., & Charkowski, A. O. The *Erwinia chrysanthemi* type III secretion system is required for multicellular behavior. *Journal of Bacteriology* **187**, 639-648 (2005)
- [88] Cavalcante, V. A., & Dobereiner, J. A new acid-tolerant nitrogen-fixing bacterium associated with sugarcane. *Plant and Soil* **108**, 23-31 (1988)
- [89] Caballero-Mellado, J., & Martínez-Romero, E. Limited genetic diversity in the endophytic sugarcane bacterium *Acetobacter diazotrophicus*. *Applied and Environmental Microbiology* **60**, 1532-1537 (1994)
- [90] Okon, Y., Albrecht, S. L., & Burris, R. Methods for growing *Spirillum lipoferum* and for counting it in pure culture and in association with plants. *Applied and Environmental Microbiology* **33**, 85-88 (1977)
- [91] Soto-Urzuá, L., & Baca, B. E. [Mechanisms for protecting nitrogenase from inactivation by oxygen]. *Revista Latinoamericana de Microbiología* **43**, 37-49 (2001)
- [92] Montecillo, J. A. V., & Bae, H. Reclassification of *Brevibacterium frigoritolerans* as *Peribacillus frigoritolerans* comb. nov. based on phylogenomics and multiple molecular synapomorphies. *International Journal of Systematic and Evolutionary Microbiology* **72**, 005389 (2022)
- [93] Liu, G.-H., Liu, B., Wang, J.-P., Che, J.-M., & Li, P.-F. Reclassification of *Brevibacterium frigoritolerans* DSM 8801T as *Bacillus frigoritolerans* comb. nov. based on genome analysis. *Current Microbiology* **77**, 1916-1923 (2020)
- [94] Bianco, A., Capozzi, L., Monno, M. R., et al. Characterization of *Bacillus cereus* Group Isolates From Human Bacteremia by Whole-Genome Sequencing. *Front Microbiol* **11**, 599524 (2020)
- [95] Scoffield, J., & Silo-Suh, L. Glycerol metabolism promotes biofilm formation by *Pseudomonas aeruginosa*. *Can J Microbiol* **62**, 704-710 (2016)
- [96] Shemesh, M., & Chai, Y. A combination of glycerol and manganese promotes biofilm formation in *Bacillus subtilis* via histidine kinase KinD signaling. *Journal of Bacteriology* **195**, 2747-2754 (2013)
- [97] Dunlap, C. A., Bowman, M. J., & Zeigler, D. R. Promotion of *Bacillus subtilis* subsp. *inaquosorum*, *Bacillus subtilis* subsp. *spizizenii* and *Bacillus subtilis* subsp. *stercoris* to species status. *Antonie Van Leeuwenhoek* **113**, 1-12 (2020)
- [98] Hansen, B. M., & Salamitou, S. (2000). *Virulence of Bacillus thuringiensis*.
- [99] Ehling-Schulz, M., Lereclus, D., & Koehler, T. M. The *Bacillus cereus* Group: *Bacillus* Species with Pathogenic Potential. *Microbiol Spectr* **7** (2019)
- [100] Tallent, S. M., Hait, J. M., & Bennett, R. W. Analysis of *Bacillus cereus* toxicity using PCR, ELISA and a lateral flow device. *Journal of Applied Microbiology* **118**, 1068-1075 (2015)
- [101] Chowdhury, S. P., Uhl, J., Grosch, R., et al. Cyclic Lipopeptides of *Bacillus amyloliquefaciens* subsp. *plantarum* Colonizing the Lettuce Rhizosphere Enhance Plant Defense Responses Toward the Bottom Rot Pathogen *Rhizoctonia solani*. *Mol Plant Microbe Interact* **28**, 984-995 (2015)
- [102] Schönbichler, A., Díaz-Moreno, S. M., Srivastava, V., & McKee, L. S. Exploring the Potential for Fungal Antagonism and Cell Wall Attack by *Bacillus subtilis* natto. *Front Microbiol* **11**, 521 (2020)
- [103] Dobrzyński, J., Jakubowska, Z., Kulkova, I., Kowalczyk, P., & Kramkowski, K. Biocontrol of fungal phytopathogens by *Bacillus pumilus*. *Front Microbiol* **14**, 1194606 (2023)
- [104] EPA. (Accessed October 30, 2023). Draft Guidance for Plant Regulators and Claims, Including Plant Biostimulants. from <https://www.epa.gov/pesticides/draft-guidance-plant-regulators-and-claims-including-plant-biostimulants>

- [105] Traon, D., Amat, L., Zotz, F., & du Jardin, P. A Legal Framework for Plant Biostimulants and Agronomic Fertiliser Additives in the EU-Report to the European Commission, DG Enterprise & Industry. (2014)
- [106] Ahmed, A. Biological control of potato brown leaf spot disease caused by *Alternaria alternata* using *Brevibacillus formosus* strain DSM 9885 and *Brevibacillus brevis* strain NBRC 15304. *J Plant Pathol Microbiol* **8**, 1-8 (2017)
- [107] Chandel, S., Allan, E. J., & Woodward, S. Biological control of *Fusarium oxysporum* f. sp. *lycopersici* on tomato by *Brevibacillus brevis*. *Journal of Phytopathology* **158**, 470-478 (2010)
- [108] Wafaa, M. H., Abd El Kareem, F. K., & Shabaan, A. A. H. Bioprocessing of *Brevibacillus brevis* and *Bacillus polymyxa*: a potential biocontrol agents of gray mould disease of strawberry fruits. *Current Opinion in Biotechnology*, S45 (2013)
- [109] Hou, Q., Wang, C., Hou, X., et al. Draft Genome Sequence of *Brevibacillus brevis* DZQ7, a Plant Growth-Promoting Rhizobacterium with Broad-Spectrum Antimicrobial Activity. *Genome Announc* **3** (2015)
- [110] Nehra, V., Saharan, B. S., & Choudhary, M. Evaluation of *Brevibacillus brevis* as a potential plant growth promoting rhizobacteria for cotton (*Gossypium hirsutum*) crop. *SpringerPlus* **5**, 948 (2016)
- [111] Vivas, A., Barea, J. M., & Azcón, R. *Brevibacillus brevis* Isolated from Cadmium- or Zinc-Contaminated Soils Improves in Vitro Spore Germination and Growth of *Glomus mosseae* under High Cd or Zn Concentrations. *Microbial Ecology* **49**, 416-424 (2005)
- [112] Fouda, A., Eid, A. M., Elsaied, A., et al. Plant Growth-Promoting Endophytic Bacterial Community Inhabiting the Leaves of *Pulicaria incisa* (Lam.) DC Inherent to Arid Regions. *Plants* **10**, 76 (2021)
- [113] Ptak, A., Morańska, E., Warchoń, M., et al. Endophytic bacteria from in vitro culture of *Leucojum aestivum* L. a new source of galanthamine and elicitor of alkaloid biosynthesis. *Sci Rep* **12**, 13700 (2022)
- [114] Scoffield, J., & Silo-Suh, L. Glycerol metabolism promotes biofilm formation by *Pseudomonas aeruginosa*. *Canadian journal of microbiology* **62**, 704-710 (2016)
- [115] Desai, J. V., Bruno, V. M., Ganguly, S., et al. Regulatory role of glycerol in *Candida albicans* biofilm formation. *mBio* **4**, e00637-00612 (2013)
- [116] Hames, C., Halbedel, S., Hoppert, M., Frey, J., & Stülke, J. Glycerol metabolism is important for cytotoxicity of *Mycoplasma pneumoniae*. *Journal of Bacteriology* **191**, 747-753 (2009)
- [117] Soumare, A., Diedhiou, A. G., Thuita, M., et al. Exploiting Biological Nitrogen Fixation: A Route Towards a Sustainable Agriculture. *Plants (Basel)* **9** (2020)
- [118] Jianguang, S. (2008).
- [119] Nehra, V., Saharan, B. S., & Choudhary, M. Evaluation of *Brevibacillus brevis* as a potential plant growth promoting rhizobacteria for cotton (*Gossypium hirsutum*) crop. *SpringerPlus* **5** (2016)
- [120] EU. Pesticides Database. (Accessed November 21, 2023) Retrieved May 2022, 2022, from [https://ec.europa.eu/food/plants/pesticides/eu-pesticides-database\\_it](https://ec.europa.eu/food/plants/pesticides/eu-pesticides-database_it)
- [121] EPA. United States Environmental Protection Agency Pesticide Database. (Accessed November 21, 2023), from <https://www.epa.gov/safepestcontrol/search-registered-pesticide-products>
- [122] BPDB. (Accessed November 21, 2023).Bio-Pesticides DataBase. from <https://sitem.herts.ac.uk/aeru/bpdb/index.htm>

## **Chapter 4**

---

# **Unraveling the Potential of Synergistic Interactions in Microbial Biostimulants**

## 4.1 Abstract

### Background

The pursuit of sustainable agricultural solutions to meet the growing demands of our global population has led to the emergence of plant biostimulants as a promising avenue. These products offer environmentally friendly means of enhancing crop yield, productivity and resilience to abiotic stressors.

Plant biostimulant formulations include a diverse array of biological substances (BSs) and beneficial microorganisms, commonly referred to as plant growth-promoting bacteria (PGPB). PGPB play a pivotal role in improving soil fertility, nutrient uptake and overall plant health.

BSs have not only been extensively studied for their inherent potential to enhance plant growth but have also demonstrated the ability to boost the beneficial functions of PGPB. This synergy between BSs and PGPB holds untapped potential, paving the way for formulating highly effective microbial biostimulants. Therefore, we consider that a rigorous biostimulant development process must include not only the selection of microorganisms based on their ability to stimulate plant growth but also comprehensive studies of the influence of BSs on these microorganisms. This research is essential to fully exploit the collective microbial efficacy in enhancing crop yields.

### Results

In this study, we conducted a comprehensive investigation using three microbial strains, specifically *Paenibacillus latus* strain 11, *Brevibacillus brevis* strain 12, and *Brevibacillus brevis* strain 13. These strains were carefully selected based on their *in vitro* plant growth-promoting (PGP) properties, which denoted their potential for plant biostimulant development. Our primary objective was to identify the strain with remarkable biostimulant capabilities and to confirm the consistency of these effects in two different plant systems: the model plant *A. thaliana* and pepper (*C. annuum*) as a representative crop.

Furthermore, we evaluated the compatibility of these microbial strains with three distinct BSs (a fermentation-derived compound, a humic-acid sample and an algae extract) with the aim of identifying potential synergistic effects in plants.

### Conclusions

In conclusion, this research highlights the unexplored potential of microbial biostimulants in enhancing crop yields through synergistic interactions with BSs, contributing to the advancement of sustainable agriculture.

## **4.2 Introduction**

In the search for sustainable agricultural solutions to meet the escalating needs of our global population, plant biostimulants have emerged as a most encouraging avenue. Biostimulant products represent an eco-friendly approach to enhancing crop yield, productivity and resilience in the presence of environmental stressors.

The plant biostimulant market exhibits continuous growth and is projected to achieve a robust Compound Annual Growth Rate (CAGR) of 11.8% from 2022 to 2027 [1]. This surge can be attributed to the growing recognition of their effectiveness in promoting sustainable farming practices and concurrently reducing the ecological footprint of agriculture in accordance with the objectives outlined in the United Nations Agenda for Sustainable Development 2030 [3].

Plant biostimulant formulations encompass a wide range of BSs and beneficial microorganisms that enhance various aspects of plant and rhizosphere performance. These enhancements include improved nutrient use efficiency, greater abiotic stress tolerance, enhanced quality traits, and increased nutrient availability, as defined by the New Regulation (EU) 2019/1009 [4].

Among the main components of plant biostimulant formulations, plant growth-promoting bacteria (PGPB) play a central role. They are beneficial microorganisms able to enhance soil fertility, plant growth, nutrient uptake, and overall plant health. The interaction between plants and PGPB can manifest in various ecological niches, encompassing the phyllosphere, rhizosphere, internal plant tissues, and the broader bulk soil [5].

PGPB promote plant growth through various mechanisms, including nutrient solubilization, production of growth-promoting substances, and abiotic stress alleviation through 1-aminocyclopropane-1-carboxylic acid (ACC) deaminase production [6]. They play a pivotal role in maximizing crop yield and quality while minimizing the environmental impact of agricultural practices.

Beyond PGPB, another indispensable element within plant biostimulants is BSs. These include a diverse array of components, such as humic acid, which enhances nutrient absorption and root growth [7]; algae extracts known for their ability to invigorate plant metabolism and boost stress resistance [2]; and fermentation-derived mixtures like vinasse, which provide valuable organic matter and micronutrients to sustain overall plant health and soil vitality [8].

Many studies have documented the profound benefits and synergistic action on plant growth when PGPB and BSs are applied together. For instance, a study by <sup>[9]</sup> demonstrated that the combination of humic acid and a plant-growth-promoting consortium has proven to stimulate a stronger effect in terms of shoot and root development and potassium foliar content compared to the single treatments. Humic acid, acting as an organic carbon source, creates an environment conducive to microbial growth. When combined with PGPB, this collaboration sparks a cooperative interaction, resulting in enhanced microbial efficiency and modulation of plant physiological processes [10].

Similarly, the combination of PGPB with algae extract, a source of organic matter and mineral nutrients, has been observed to trigger a notable surge in microbial growth and metabolic activity. This synergy leverages the nutrients and bioactive compounds inherent in algae extract, magnifying their advantageous impact on the microbial community [11-12]. Consequently, microorganisms thrive and exhibit heightened biological functions, such as nutrient cycling [13].

The introduction of by-products like fermentation-derived vinasse, a rich organic matter product from the sugar-alcohol industry, delivers significant advantages in agriculture as it enhances soil biological quality by promoting an increase in the overall bacterial population [14-15]. The abundant nutrient content in vinasse, including carbon, nitrogen, and minerals, provides essential support for microbial growth by serving as a primary source of nutrients for microorganisms. For instance, the application of vinasse in sugarcane has been proven to increase bacterial diversity in the soil, with a particular enrichment of species involved in the nitrogen and iron cycles, as well as an increase in Actinomycetales species, compared to soils without vinasse application [15].



Overall, this evidence highlights the pivotal role played by BSs in enhancing the beneficial functions of PGPB and the untapped potential arising from their synergistic combination for the formulation of highly effective microbial biostimulants. Therefore, we assert that a meticulous development process for microbial biostimulants must encompass not only the scrupulous selection of microorganisms based on their capacity to stimulate plant growth but also in-depth examinations of the influence exerted by these BSs on the aforementioned microorganisms. This research is essential for fully harnessing the overall microbial efficacy in crop enhancement.

In this work, we conducted a comprehensive investigation of the biostimulant potential of three different microbial strains, specifically *Paenibacillus lautus* strain 11, *Brevibacillus brevis* strain 12, and *Brevibacillus brevis* strain 13. These strains were carefully selected from a pool of seventeen cultures based on their exhibited traits that suggested them as suitable candidates for further investigation as potential candidates in the development of plant biostimulants, as discussed in detail in Chapter 2. Our overarching objective encompassed the identification of the strain with remarkable biostimulant capabilities, as well as the validation of consistency across two distinct plant systems: the model plant *A. thaliana* and pepper (*C. annuum*), one of the most agriculturally relevant crops [16].

Furthermore, an integral aspect of our study was the careful exploration of the compatibility between these selected microbial strains and three different BSs: a fermentation-derived compound, a humic acid sample and an algae extract. Our overall goal went beyond a simple assessment of compatibility; indeed, we sought to discover a potential prebiotic effect resulting from the interaction of these substances with the microbial strains under study. Based on the observed results, we, therefore, attempted to investigate whether the prebiotic response could also translate into a synergistic effect in a model plant, with the ultimate goal of uncovering the full spectrum of plant growth-enhancing benefits of effective microbial leads.

## 4.3 Methods

### 4.3.1 Strains cultivation and quantification through impedance flow cytometry

Strains 11, 12, and 13 were cultivated in 250 ml of tryptic soy broth (TSB) medium at 30°C in 0,5 L bioreactors (Applikon Biotechnology, Schiedam, Netherlands) for 24 hours. At 0, 4, 8, 10, and 24 hours, 5 ml samples were collected for optical density measurements, and 10-fold serial dilutions were performed to estimate bacterial concentration. Serial dilutions were prepared using a solution of 0.85 % (w/v) NaCl and Flow Impedance Buffer (FIB) for viable plate count and Impedance Flow Cytometry (IFC) analyses, respectively. Diluted samples from  $10^{-4}$  to  $10^{-7}$  of plate count analysis were plated on Tryptic Soy Agar (TSA) medium and incubated at 30°C for 24 hours. For IFC, according to manufacturer instructions, 1 ml of  $10^{-2}$ ,  $10^{-4}$ , and  $10^{-6}$  serial dilutions were used for the multi-frequency IFC BactoBox<sup>®</sup> device (SBT instruments, Herlev, Denmark) analysis. All the analyses were performed in triplicate.

### 4.3.2 Effects of BSs on microbial growth *in vitro*

Three BSs, fermentation-derived (BS 1), humic-acid (BS 2), and algae extract (BS 3), were tested for compatibility and growth-supporting capabilities with strains 11, 12, and 13. Bacterial cultures were inoculated with 20 µl of overnight cultures in 180 µl of TSB supplemented with BSs at 125 and 250 ppm in a 96-well microplate (Thermo Fisher Scientific, Waltham, MA, USA), achieving a final concentration of approximately  $10^6$  CFU·ml<sup>-1</sup>. Inoculated TSB without BSs (0 ppm) was used as the positive control. Cultures were grown at 30°C, with agitation at 110 rpm, and after 6 hours, microbial growth was assessed by IFC. Three replicates were prepared for each treatment.

Additionally, the combinations of BSs and bacterial strains exhibiting a significant prebiotic effect were visualized using fluorescence microscopy. This was performed with an Axio Zoom V 16 stereomicroscope (Zeiss) equipped with a PlanNeoFluar Z 1×/0.25 FWD 56 mm objective and a 25×/10foc eyepiece. In total, four treatments were prepared, each diluted 1:10 to reach a final volume of 1

mL. Subsequently, 3 µl of the LIVE/DEAD® BacLight™ Bacterial Viability Kit (Cat L7012: ThermoFisher Scientific) were added to each solution for staining and observation.

### **4.3.3 *In vitro* treatment on *A. thaliana***

#### **4.3.3.1 Treatment with BSs**

The plant growth-promoting effect of all treatments was evaluated *in vitro* using the *A. thaliana* Col-0 ecotype. *A. thaliana* seeds were sterilized according to Contreras-Cornejo et al. [17] protocol with slight modifications. Briefly, seeds were surface sterilized by immersion in sodium hypochlorite (NaClO) (1:5) + triton-100 0,05% for 10 min. After six washes with sterile deionized water 7 seedlings per plate were sown on 0,2x M&S agar medium (Murashige and Skoog basal salts mixture, Cat M5524: Sigma, St. Louis). After sowing, seeds were stratified in the darkness at 4°C for 24 hours to break their dormancy and then grown at 24°C in a grow chamber (photoperiod of 12 h of light and 12 h of darkness) in a vertical position. After seven days of germination, the seedlings were transferred to square plates (120x120 mm) containing 0,2x M&S agar medium.

To assess the effect of the BSs, seedlings were sown following the Marsell and Fröschel [18] protocol with minor modifications. In brief, 2 cm of the medium was removed from the top of the plate, and the seedlings were sown on the cut surface to enable the hypocotyls to grow freely. Stock solutions containing 250 and 125 ppm of BSs were prepared and filtered. 20 µl of each solution was dropped 4 cm below each seedling and allowed to diffuse and dry. Sterilized water (0 ppm) was used as control. After treatment, the plates were placed in a Percival growth chamber (photoperiod of 12 h of light and 12 h of darkness) for 7 days. Three independent experiments were performed, and 4 replicate plates were used for each set of conditions. The plates were arranged in a randomized design.

#### **4.3.3.2 Treatment with microbial strains**

The strains were cultured in the TSB liquid medium at 30°C and 110 rpm overnight for bacterial treatments. The bacterial cells were centrifuged at 15,000 rpm for two minutes, washed once with MgSO<sub>4</sub> 10mM, and resuspended in sterile distilled water. The cell concentration was adjusted to 1 x 10<sup>7</sup> CFU·ml<sup>-1</sup>. Treatment was performed by dropping and streaking 20 µl of bacterial culture 4 cm from the bottom of the square agar plates for each 7-d old, germinated *Arabidopsis* seedling. After treatment, the plates were placed in a Percival growth chamber under photoperiod conditions of 12 hours of light and 12 hours of darkness for 7 days. Sterilized water was used as the negative control, and 4 replicate plates were used for each set of conditions. Plates were arranged in a randomized design.

#### **4.3.3.3 Microbial and BSs Co-treatment**

Following the acquisition of the results, the strain exhibiting the most robust plant-promoting activity was singled out for further investigation. A study was conducted to evaluate the synergy in the plant by combining the selected strain with the BS, showing both a prebiotic effect and a biostimulant activity. The strain was grown as described above, and cells were resuspended in the BS solution at 125 and 250 ppm. MgSO<sub>4</sub> 10 mM was used to resuspend the cells for testing the microorganism alone (0 ppm). The cell concentration was adjusted to 1 x 10<sup>7</sup> CFU·ml<sup>-1</sup>. BS solutions (125 and 250 ppm) not inoculated were used as controls. 20 µl of each treatment were dropped at 4 cm from the bottom of the square agar plates below each 7-days old, germinated *A. thaliana* seedling. After treatment, the plates were placed in a Percival growth chamber under photoperiod conditions of 12 hours of light and 12 hours of darkness for 7 days. 4 replicate plates were used for each set of conditions and plates were arranged in a randomized design.

#### **4.3.4 Plant Assay Treatment Data Collection**

After 7 days of treatment, fresh shoot weights were measured and analyzed. In addition, the effect on plant growth was assessed by image acquisition and

analysis. Specifically, images of seedlings were taken using a scanner (EPSON Expression 11000XL, LA2400 Scanner Calibrated for Image Analysis with REGENT INSTRUMENTS software). Seedling's root length and surface area were measured and quantified using the software WinRhizo (version 2016).

#### **4.3.5 Greenhouse experiment**

The effect of the three bacteria application was also assessed on sweet pepper (*Capsicum annuum* var. Diablo) under greenhouse conditions. 35-day-old seedlings (2-leaf stage) were transplanted into 2.4-liter pots containing a customized peat and sand substrate (Vigorplant, Italy). Fertilizer was administered at a rate of 1.2 grams per plant every 12 days via drip fertigation. The fertilization regimen included Master 13.40.13 (Valagro; Atessa, Italy), Master 13.40.13 (Valagro; Atessa, Italy), YaraTera CALCINIT (Yara; Oslo, Norway), and Master 15.5.30 (Valagro; Atessa, Italy). Plants were grown in the greenhouse with an average temperature of  $22\text{ }^{\circ}\text{C} \pm 2$  at night and  $28\text{ }^{\circ}\text{C} \pm 3$  during the day.

The bacterial cultures were dissolved in water to achieve three concentrations: 10 ml/l (D1), 25 ml/l (D2), and 50 ml/l (D3). Each plant received 100 ml of the bacterial solution, resulting in final concentrations of  $1.2 \times 10^9$  CFU/pot (D1),  $3 \times 10^9$  CFU/pot (D2), and  $6 \times 10^9$  CFU/pot (D3).

In 2,4 L pots, the final bacterial suspension concentrations were  $5 \times 10^5$  CFU·g<sup>-1</sup> (D1),  $1,25 \times 10^6$  CFU·g<sup>-1</sup> (D2), and  $2.5 \times 10^6$  CFU·g<sup>-1</sup> (D3). The untreated control received only water, and B3-2642, a plant biostimulant, was a positive control. The first application occurred two weeks after transplantation, and two subsequent applications at 10-day intervals. After 14 days from the last application, shoot and root biomass, shoot length as well as the number and weight of fruits were evaluated. Each treatment had fifteen replicates (pepper plants).

#### **4.3.6 Statistical analyses**

Experiments were statistically analyzed using the Statistica v 14 software (TIBCO Software Inc, Palo Alto, California, USA). All data were analyzed by ANOVA, and significant differences among the treatments were determined by Fisher LSD

or Student-Newman-Keuls (SNK) post hoc test. Different letters indicate statistically significant differences at  $p \leq 0.05$ .

## 4.4 Results

### 4.4.1 Microbial growth assessment through impedance flow cytometry

*In vitro* compatibility between the microbial cultures and BSs was assessed by measuring microbial viability. In addition to the conventional viable plate count, other approaches can be used to measure cell vitality, such as optical density (OD), live-dead fluorescence staining, metabolic activity based on cell reduction-oxidation status (e.g., BIOLOG), and IFC. In recent years, microfluidic sensors based on such technology have become increasingly popular as label-free and culture-independent tools. They enable the detection and enumeration of living bacteria cells in a liquid sample through a change in the electric field generated by intact cells as they pass between the electrodes of a measuring channel.

In our study, the BactoBox® microfluidic sensor was used to measure the growth of strains 11, 12 and 13 at each time point of their kinetic curves. To validate this method, the intact cell concentration (ICC) results obtained by IFC at 0, 4, 8 and 10 hours were compared by regression analysis with those obtained by quantification of viable plate counts (CFU/ml), considered the "gold standard" for cell enumeration in microbiology.

A good linear correlation between ICC and the expected results from the viable plate count analysis was observed (strain 11:  $R^2 = 0.995$ , P-value  $< 0.0001$ ; strain 12:  $R^2 = 0.967$ , P-value  $< 0.0001$  and strain 13:  $R^2 = 0.989$ , P-value  $< 0.0001$ ). These findings showed that IFC was a suitable and reliable method that can be used to measure cell viability and growth. Indeed, the kinetic curve detected by IFC in the culture broths followed a similar trend to that observed with the plate count method (**Figure 3.1**). In detail, for both strains 12 and 13, the exponential phase took place between 4 and 10 hours, with a maximum growth rate of 0.31 and 0.32 (1/h), respectively. Otherwise, the curve corresponding to strain 11 revealed a distinct kinetic pattern compared to 12 and 13. For instance, a closer inspection revealed a diauxic growth curve showing two growth peaks at 0 and 4

hours and at 8 and 10 hours (maximum growth rate of 0.63 for the phase 0 to 4 hours and 0.18 for the phase 8 to 10 hours).

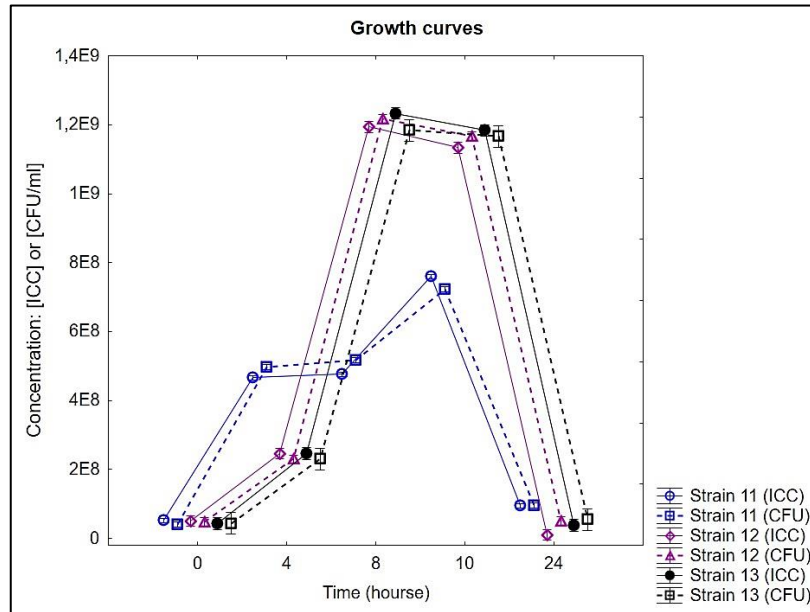


**Figure 4.1.** Kinetic curves of strains 11, 12, and 13 in TSB medium for 24 hours. Cell viability at each time point (0, 4, 8, and 24 hours) was determined by plate counts (CFU/ml) and by IFC (ICC) using the BactoBox® device.

#### 4.4.2 *In vitro* compatibility with BSs

Selecting suitable BSs that are compatible with a microbial strain is a critical step in formulating a plant biostimulant based on both active ingredients. More specifically, such a selection process can provide valuable information on their compatibility and even whether the BS can support microbial survival in the plant rhizosphere.

In the present study, a set of fermentation-derived (BS 1), humic-acid (BS 2), and algae extract (BS 3) substances were tested with strains 11, 12, and 13 to assess their compatibility and whether they could support strain growth. The results revealed that BS 1 at 250 ppm significantly enhanced the growth of strain 11, while BS 3 at 250 ppm notably promoted the growth of strains 12 and 13 (**Figure 3.2**).

The substances that significantly enhanced microbial growth were observed under a fluorescence microscope after staining. This observation confirmed the growth

trend seen in the *in vitro* data, demonstrating an increase in viable cells in solutions containing BSs at 250 ppm.



### 4.4.3 *In vitro* treatment on *A. thaliana*

#### 4.4.3.1 Treatment with BSs

In the present study, BS 1, BS 2 and BS 3 were *in vitro* tested on *A. thaliana* to assess whether they had a physiological promoting effect on plants by measuring parameters such as shoot biomass, root length and root surface area.

BS 1 (250 ppm), BS 2 (250 ppm), and BS 3 (125, 250 ppm) improved the shoot fresh weight (SFW, mg) and the total root length (RL, cm). In addition, the root surface area (RSA, cm<sup>2</sup>) increased significantly in BS 1 (250 ppm), BS 2 (125, 250 ppm), and BS 3 (125, 250 ppm) compared to the untreated plants (**Figure 3.3 A; Figure 3.3 B; Figure 3.3 C**). The effect of BS 1 on plants resulted in being correlated to the treatment dosages for all the values measured, whereas BS 2 showed a dose-dependent effect only on FSW and RL. Otherwise, BS3 showed no dose-dependent effect, and plant parameters did not significantly differ between 250 ppm and 125 ppm (**Figure 3.3 A; Figure 3.3 B; Figure 3.3 C**).

#### 4.4.3.2 Treatment with microbial strains

In this study, strains 11, 12, and 13 were tested to assess their potential effect on plant growth in *A. thaliana* by measuring plant parameters such as shoot biomass, root length and surface area.

The growth of the plants was positively affected by the inoculation of all bacteria (**Figure 3.3 D; Figure 3.3 E; Figure 3.3 F**). A significant increase in the SFW was observed in plants inoculated with strains 12 and 13. Moreover, the root system increased significantly for seedlings treated with strain 13. Indeed, a higher RL and RSA can be observed compared to the untreated plants.

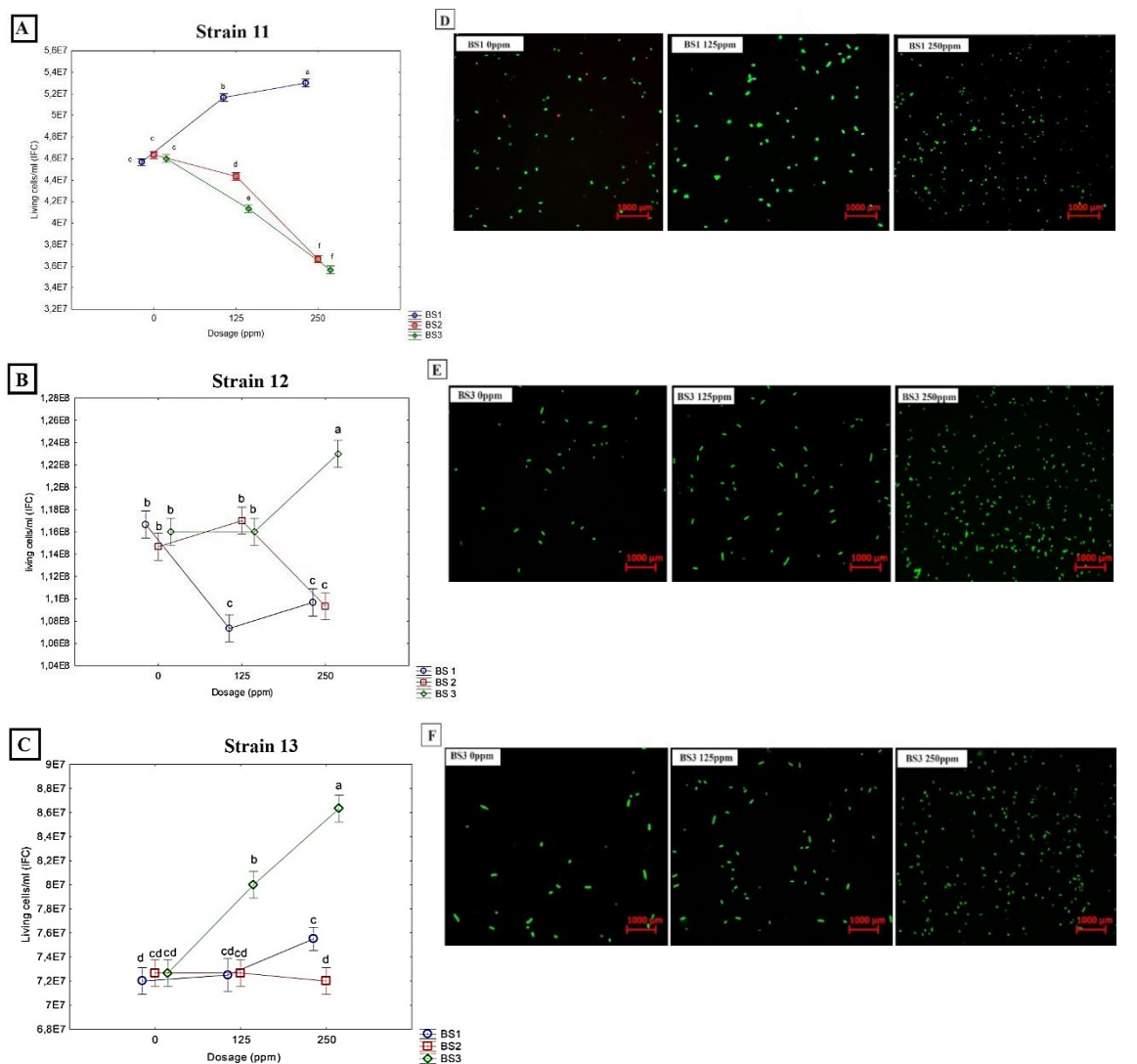
Based on the plant results, strain 13 was selected for further study in *A. thaliana* in combination with BS 3 at 250 ppm, which showed a simultaneous prebiotic effect and plant growth promotion. When the mixed solution containing strain 13 ( $\approx 10^7$  CFU·ml<sup>-1</sup>) and BS 3 at 250 ppm was applied simultaneously, it significantly enhanced the growth and development of the plants compared to untreated ones or those treated with the two individual components (**Figure 3.3 D; Figure 3.3 E; Figure 3.3 F**).

#### **4.4.3.3 Microbial and BS co-treatment**

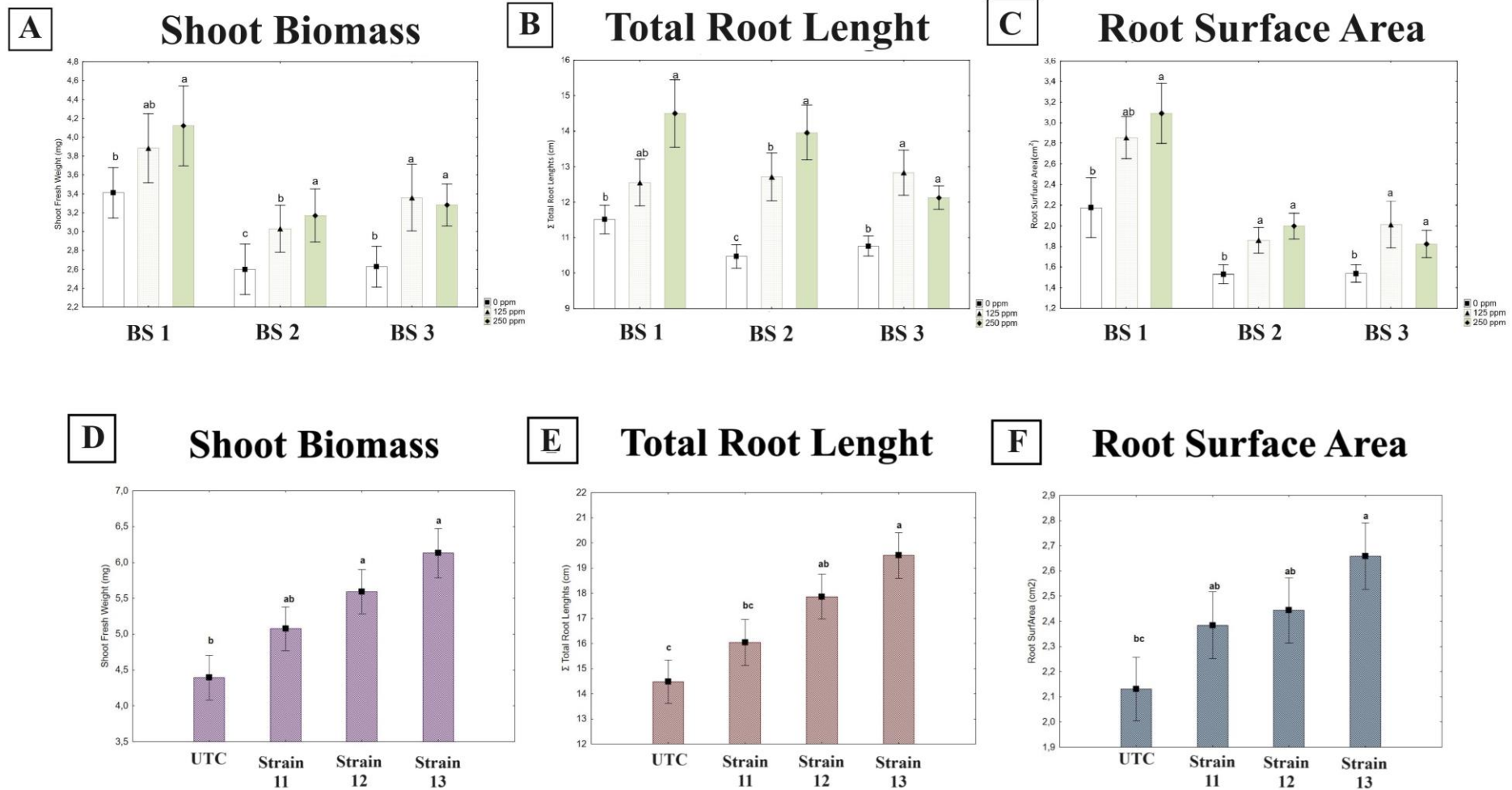
Based on the plant results, strain 13 was selected for further study in *A. thaliana* in combination with BS 3 at 250 ppm, which showed a simultaneous prebiotic effect and plant growth promotion. When the mixed solution containing strain 13 ( $\approx 10^7$  CFU·ml<sup>-1</sup>) and BS 3 at 250 ppm was applied simultaneously, it significantly enhanced the growth and development of the plants compared to untreated ones or those treated with the two individual components (**Figure 3.4**).

#### **4.4.4 Greenhouse experiment on pepper**

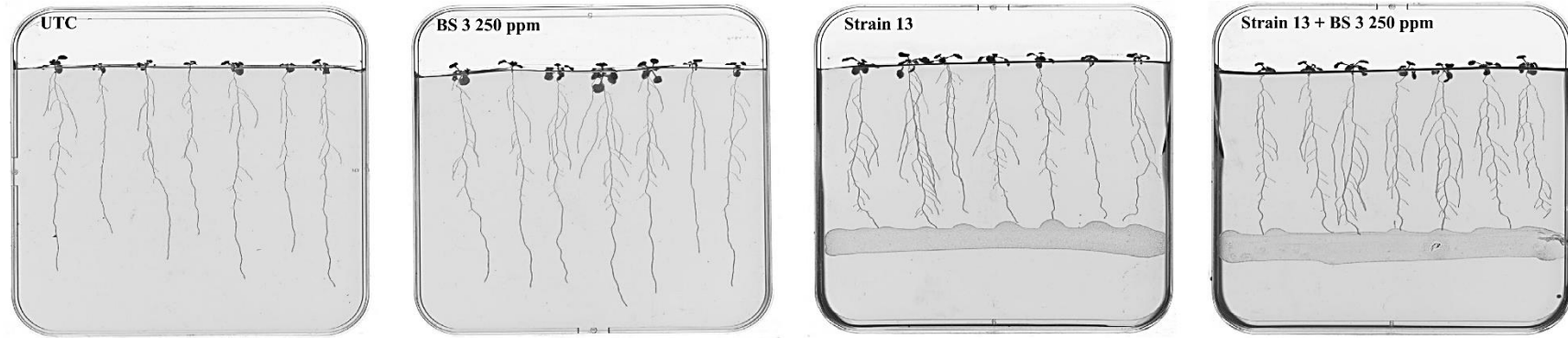
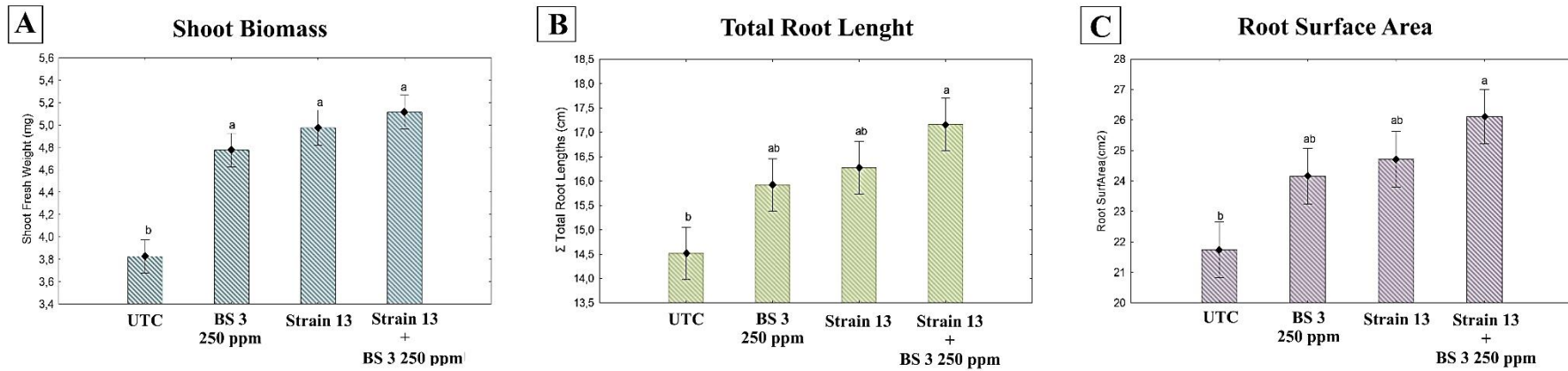
The results indicated that strain 13 at the lowest concentration (D1) was the most promising microbial candidate for improving plant height and biomass. Otherwise, plants treated with strain 13 (D1), as well as B3-2642, exhibited reduced root development compared to untreated plants, as the ample availability of soil nutrients facilitated convenient access to essential elements necessary for their growth, eliminating the need for extensive root exploration [19] (**Figure 3.5**). Fruit number and weight did not exhibit any significant differences among the treatment groups (data not shown).



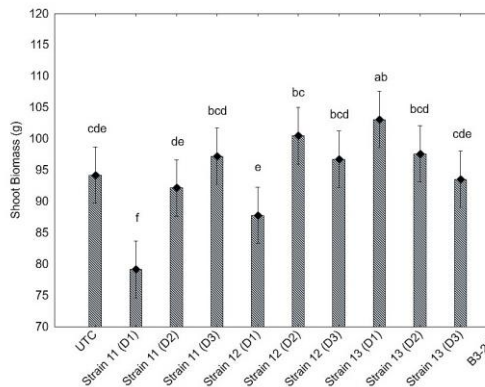
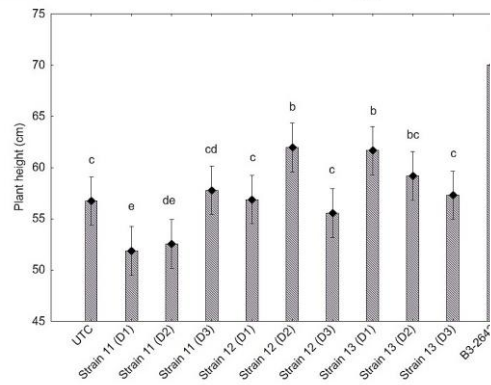
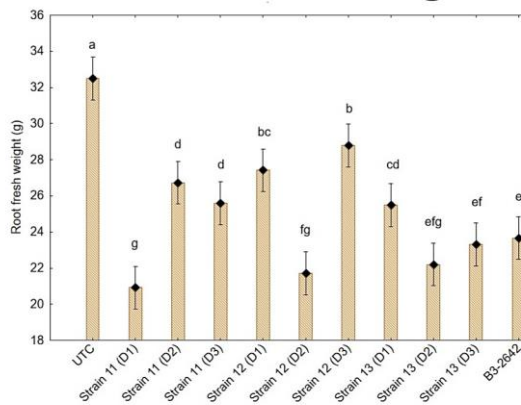
**Figure 4.2.** Effect of BSs 1, 2, and 3 on the growth of strains 11 (A), 12 (B), and 13 (C) after 6 h of incubation. Positive control: inoculated TSB without BSs (0 ppm). Vertical bars denote 0.95 confidence intervals. Two-way ANOVA with Fisher's LSD test was performed for data analysis. Different letters represent significant differences between treatments ( $p < 0.05$ ). Fluorescence microscopy of strain 11 inoculated with BS 1 (D) and strains 12 (E) and 13 (F) inoculated with BS 3. Green cells indicate living cells. Scale bar  $\mu\text{m}$ .



**Figure 4.3.** Effect of BSs 1, 2, and 3 (A, B, C) and strains 11, 12 and 13 (D, E, F) on *A. thaliana*. Shoot biomass (A; D), total root length (B; E), and root area (C; F) were evaluated 7 days after treatments. Mean and standard error values from 20 replicates are represented for each treatment. Different letters represent significant differences between treatments according to the Student-Newman-Keuls (SNK) test ( $p < 0.05$ ).

**I)****II)**

**Figure 4.4.** Effect of combination of strain 13 with BS 3 on *A. thaliana*. Image acquisition took by EPSON scanner 14 days post-inoculation (I). Shoot biomass (II, A), total root length (II, B), and root surface area (II, C) were evaluated 7 days after treatments. Mean and standard error values from 20 replicates are represented for each treatment. Different letters represent significant differences between treatments according to Student-Newman-Keuls (SNK) test ( $p < 0.05$ ).

**A****Shoot Biomass****B****Plant Height****C****Root Fresh Weight**

**Figure 4.5.** Plant growth-promoting effects of strains 11, 12, and 13 under greenhouse conditions (positive control: plant biostimulant B3-2642). Shoot biomass (A), shoot height (B), and root weight (C) were evaluated 14 days after the third treatment. Mean and standard error values for fifteen replicates are represented for each treatment. Different letters indicate significant differences according to Duncan's test ( $p < 0.05$ ).

## 4.5 Discussion

Several strains within the *Brevibacillus* bacterial genus have been recognized as plant growth-promoting bacteria (PGPB). This study provides concrete evidence of the efficacy of *Brevibacillus brevis* strain 13, showcasing its remarkable ability to promote plant growth in *A.thaliana* and pepper.

Inoculated *A. thaliana* plants with strain 13 exhibited notable increases in shoot development and, notably, a more robust expansion of root surface area compared to the other treatments and the untreated control. We hypothesized that the primary factor stimulating root development is likely related to the strain's ability to release indole acetic acid, as reported in Chapter 2. IAA plays a pivotal role in cell division, elongation, and root development [20]. Bacteria that produce auxins play a crucial role in shaping root architecture by promoting lateral root development, thus enabling the plant to access more nutrients in the soil. For example, the application of auxin-producing plant growth-promoting rhizobacteria (PGPR) such as *Pseudomonas extremaustralis* IB-κ13-1A and *Paenibacillus illinoisensis* IB 1087 to wheat plants resulted in increased root biomass and elevated root auxin levels [21-22].

The importance of bacterial IAA in fostering host plant root system development is further substantiated by experiments with IAA-deficient mutants. For instance, inoculating canola seedlings with the IAA-deficient mutant *Pseudomonas putida* GR12-2 led to a reduction in root growth [23]. A similar effect was observed when inoculating *Arabidopsis* with an auxin-impaired mutant, *A. brasilense* strain FAJ0009, which lost its ability to modify root architecture and increase root hair elongation compared to the wild-type treatment [24].

Various strains within the *B. brevis* species have been described for their capacity to produce IAA [25-27]. The synthesis of IAA by *B. brevis* holds significant importance, particularly in the context of its role as a plant growth-promoting bacterium engaged in phytoremediation of heavy metal-contaminated soils. IAA production by *B. brevis* plays a pivotal role in facilitating the accumulation of heavy metals within bacterial cells, thereby reducing soil toxicity levels. This mechanism also fosters the proliferation of mycorrhizae, such as *G. mossae*, in soils contaminated by cadmium [25].

Furthermore, in this study, we noticed that the growth of *B. brevis* strain 13 was positively influenced by the presence of algae extract (specifically, BS 3 at the optimal concentration of 250 ppm), significantly increasing the growth of the strain after six hours compared to the other BSs and the untreated control, indicating that BS 3 at 250 ppm acted as a prebiotic for this particular strain.

Interestingly, it was found that the observed prebiotic effect was species-dependent, implying that different strains within the same species respond similarly to the same BS, but the response may differ when involving different bacterial species.

Specifically, both *B. brevis* strain 12 and strain 13 exhibited a similar response to the maximum dosage of BS 3, indicating consistency in their reaction to this particular prebiotic compound. On the other hand, *P. lautus* strain 11 displayed a unique response by showing significantly greater growth when exposed to the fermentation-derived sample, BS 1, as opposed to BS 3.

These findings underscore the importance of considering the bacterial species and strain specificity when investigating BSs acting as prebiotics. It suggests that the response to prebiotic substances may not be universally applicable across all bacterial species, and the outcomes can vary depending on the specific microorganisms involved. This information can have implications for selecting targeted BSs and designing more effective microbial biostimulant solutions in agriculture.

The specific microbial response to different natural substances can be mostly related to the microbial nutritional profile. For example, we hypothesized that, in the case of BS 3, both *B. brevis* strain 12 and 13 might harbour relevant enzymes capable of converting complex polysaccharides from algae, such as starch, cellulose, agar, carrageenan, and alginates, into simpler sugars like glucose, fructose, and other monosaccharides. These simple sugars serve as valuable energy and carbon sources for microbial cells, supporting their growth and metabolic functions. This was observed in *A. thaliana* when the combined treatment of strain 13 and BS 3 at 250 ppm was administered.

Indeed, this combined treatment exhibited a synergistic effect that outperformed the individual components.



This synergistic effect aligns with various studies highlighting the favourable outcomes of simultaneously applying PGPB and algae extracts to diverse crops. For instance, the co-treatment of the PGPB *B. licheniformis* and a biostimulant derived from seaweed to onion (*Allium cepa*) resulted in higher leaf carbohydrate content, longer leaf and root lengths [28]. Moreover, the substantial impact of this combined treatment on plants was also confirmed in *A. hybridus*, where a higher leaf carbohydrate content was observed when both *B. licheniformis* and seaweed extract were used in combination [29]. Promising results were also observed in cowpea (*Vigna unguiculata*) when a co-treatment involving rhizobia and a seaweed extract was employed, leading to improved plant growth and nutrient uptake [30]. The authors suggested that the active ingredients in seaweed, including auxins, cytokinins, macronutrients, and micronutrients, combined with the plant growth-promoting capabilities of rhizobia, may partially elucidate the interactive mechanism behind the observed synergistic treatment in plants.

Furthermore, the ability of algae extracts to stimulate PGPB growth emerges as another key factor contributing to the synergy in co-treatment, as these extracts can bolster microbial metabolic activity and vitality [31-32].

To gain a deeper understanding of the mechanisms driving the enhanced plant growth-promoting effects resulting from the co-treatment of BS 3 and strain 13, a transcriptomic analysis would be valuable. Indeed, it would be possible to identify the specific genes and pathways that are upregulated or downregulated in response to the treatment. This knowledge can reveal the molecular basis of the synergistic interactions between strain 13 and BS 3, providing crucial information on how the combination enhances plant growth.

Furthermore, extending the evaluation of the synergistic activity between BS 3 and strain 13 to an industrial crop, such as pepper, under greenhouse conditions would provide further insights. In this study, the experimentation in greenhouse not only validated the consistency of results across two distinct plant systems – the model plant *A. thaliana* and an industrial crop – but also provided compelling evidence that strain 13, when applied to pepper, emerges as the most promising microbial candidate for improving shoot height and biomass. This result confirms the strong PGP potential of *B. brevis* as also observed in other crops [33,34].

However, further studies involving a wider variety of agronomic crops, different environmental conditions and soil types would be valuable to fully explore the potential and adaptability of the promising synergy observed for strain 13 and BS 3.

In conclusion, the meticulous identification and selection of specific microbial strains with plant growth-promoting characteristics are pivotal for the development of effective biostimulants. This result reinforces the notion that a well-structured microbial screening process, encompassing studies on both model plants and agriculturally significant crops, can lead to the discovery of beneficial microbes with a great potential for effective biostimulant development in agriculture. By illustrating the positive effects of strain 13 and its synergistic interaction with BS 3, this research paves the way for future studies seeking to identify and harness the potential of other beneficial microbial strains and their interactions with different biostimulant components. This work not only enriches our understanding of plant-microbe interactions but also brings us closer to realizing the full potential of biostimulants for sustainable agriculture and food production. Ongoing efforts in this field hold promise for innovative strategies to enhance crop productivity while reducing dependence on traditional chemical inputs.

## References

- [1] Market, B. (2021). Biostimulants Market by Active Ingredient (Humic substances, Amino Acids, Seaweed Extracts, and Microbial Amendements), Mode of Application (Foliar, Soil Treatment, and Seed Treatment), Form (Liquid and Dry), Crop Type and Region - Global Forecast to 2027. . Retrieved 24 October 2023, from <http://www.marketsandmarkets.com/Market-Reports/biostimulant-market-1081.html>
- [2] Van Oosten, M. J., Pepe, O., De Pascale, S., Silletti, S., & Maggio, A. The role of biostimulants and bioeffectors as alleviators of abiotic stress in crop plants. *Chemical and Biological Technologies in Agriculture* **4**, 1-12 (2017)
- [3] Lee, B. X., Kjaerulf, F., Turner, S., et al. Transforming Our World: Implementing the 2030 Agenda Through Sustainable Development Goal Indicators. *Journal of Public Health Policy* **37 Suppl 1**, 13-31 (2016)
- [4] Commission, E. Commission Implementing Regulation (EU) No. 540/2011 of 25 May 2011 implementing Regulation (EC) No. 1107/2009 of the European Parliament and of the Council as regards the list of approved active substances. *Official Journal of the Europe Union* **153**, 1-186 (2011)
- [5] Ajjiah, N., Fiodor, A., Pandey, A. K., Rana, A., & Pranaw, K. Plant Growth-Promoting Bacteria (PGPB) with Biofilm-Forming Ability: A Multifaceted Agent for Sustainable Agriculture. *Diversity* **15**, 112 (2023)
- [6] Souza, R., Ambrosini, A., & Passaglia, L. M. Plant growth-promoting bacteria as inoculants in agricultural soils. *Genetics and Molecular Biology* **38**, 401-419 (2015)
- [7] Fahramand, M., Moradi, H., Noori, M., et al. Influence of humic acid on increase yield of plants and soil properties. *International Journal of Farming and Allied Sciences* **3**, 339-341 (2014)
- [8] Senatore, D., Queirolo, A., Monza, J., & Bajsa, N. Using sugar cane vinasse as a biofertilizer: effects on soil microbial community due to periodical application. *Environmental Sustainability*, 1-10 (2023)
- [9] Schoebitz, M., López, M., Serrí, H., Martínez, O., & Zagal, E. Combined application of microbial consortium and humic substances to improve the growth performance of blueberry seedlings. *Journal of soil science and plant nutrition* **16**, 1010-1023 (2016)
- [10] Tavares, O. C. H., Ribeiro, T. G., García-Mina, J. M., et al. Humic acids enrich the plant microbiota with bacterial candidates for the suppression of pathogens. *Applied Soil Ecology* **168**, 104146 (2021)

- [11] Alam, M. Z., Braun, G., Norrie, J., & Hodges, D. M. Effect of Ascophyllum extract application on plant growth, fruit yield and soil microbial communities of strawberry. *Canadian Journal of Plant Science* **93**, 23-36 (2013)
- [12] Renaut, S., Masse, J., Norrie, J. P., Blal, B., & Hijri, M. A commercial seaweed extract structured microbial communities associated with tomato and pepper roots and significantly increased crop yield. *Microbial biotechnology* **12**, 1346-1358 (2019)
- [13] Chen, C.-L., Song, W.-L., Sun, L., et al. Effect of seaweed extract supplement on rice rhizosphere bacterial community in tillering and heading stages. *Agronomy* **12**, 342 (2022)
- [14] Prado, R. d. M., Caione, G., & Campos, C. N. S. Filter cake and vinasse as fertilizers contributing to conservation agriculture. *Applied and Environmental Soil Science* **2013**, 1-8 (2013)
- [15] Omori, W. P., Camargo, A. F. d., Goulart, K. C. S., Lemos, E. G. d. M., & Souza, J. A. M. d. Influence of Vinasse Application in the Structure and Composition of the Bacterial Community of the Soil under Sugarcane Cultivation. *International Journal of Microbiology* **2016**, 2349514 (2016)
- [16] Kumar, S., Kumar, R., & Singh, J. (2006). Cayenne/American pepper *Handbook of herbs and spices* (pp. 299-312): Elsevier.
- [17] Contreras-Cornejo, H. A., Macías-Rodríguez, L., Beltrán-Peña, E., Herrera-Estrella, A., & López-Bucio, J. Trichoderma-induced plant immunity likely involves both hormonal-and camalexin-dependent mechanisms in Arabidopsis thaliana and confers resistance against necrotrophic fungi Botrytis cinerea. *Plant signaling & behavior* **6**, 1554-1563 (2011)
- [18] Marsell, A., & Fröschel, C. Inoculation Strategies to Infect Plant Roots with Soil-Borne Microorganisms. *JoVE (Journal of Visualized Experiments)*, e63446 (2022)
- [19] Lynch, J., Marschner, P., & Rengel, Z. (2012). Effect of internal and external factors on root growth and development *Marschner's mineral nutrition of higher plants* (pp. 331-346): Elsevier.
- [20] Overvoorde, P., Fukaki, H., & Beeckman, T. Auxin control of root development. *Cold Spring Harb Perspect Biol* **2**, a001537 (2010)
- [21] Kudoyarova, G., Vysotskaya, L., Arkhipova, T., et al. Veselov YuS (2017) Effect of auxin producing and phosphate solubilizing bacteria on mobility of soil phosphorus, growth rate, and P acquisition by wheat plants. *Acta Physiologiae* **39**, 253

- [22] Grover, M., Bodhankar, S., Sharma, A., Sharma, P., Singh, J., & Nain, L. PGPR mediated alterations in root traits: way toward sustainable crop production. *Frontiers in Sustainable Food Systems* **4**, 618230 (2021)
- [23] Patten, C. L., & Glick, B. R. Role of *Pseudomonas putida* indoleacetic acid in development of the host plant root system. *Applied and Environmental Microbiology* **68**, 3795-3801 (2002)
- [24] Averkina, I. O., Paponov, I. A., Sánchez-Serrano, J. J., & Lillo, C. Specific PP2A Catalytic Subunits Are a Prerequisite for Positive Growth Effects in Arabidopsis Co-Cultivated with *Azospirillum brasilense* and *Pseudomonas simiae*. *Plants* **10**, 66 (2020)
- [25] Vivas, A., Barea, J. M., & Azcón, R. *Brevibacillus brevis* Isolated from Cadmium- or Zinc-Contaminated Soils Improves in Vitro Spore Germination and Growth of *Glomus mosseae* under High Cd or Zn Concentrations. *Microbial Ecology* **49**, 416-424 (2005)
- [26] Nehra, V., Saharan, B. S., & Choudhary, M. Evaluation of *Brevibacillus brevis* as a potential plant growth promoting rhizobacteria for cotton (*Gossypium hirsutum*) crop. *SpringerPlus* **5** (2016)
- [27] Fouda, A., Eid, A. M., Elsaied, A., et al. Plant Growth-Promoting Endophytic Bacterial Community Inhabiting the Leaves of *Pulicaria incisa* (Lam.) DC Inherent to Arid Regions. *Plants* **10**, 76 (2021)
- [28] Gupta, S., Stirk, W. A., Plačková, L., Kulkarni, M. G., Doležal, K., & Van Staden, J. Interactive effects of plant growth-promoting rhizobacteria and a seaweed extract on the growth and physiology of *Allium cepa* L.(onion). *Journal of Plant Physiology* **262**, 153437 (2021)
- [29] Ngoroyemoto, N., Kulkarni, M. G., Stirk, W. A., Gupta, S., Finnie, J. F., & van Staden, J. Interactions Between Microorganisms and a Seaweed-Derived Biostimulant on the Growth and Biochemical Composition of *Amaranthus hybridus* L. *Natural Product Communications* **15**, 1934578X20934228 (2020)
- [30] Gyogluu Wardjomto, C., Mohammed, M., Ngmenzuma, T. Y., & Mohale, K. C. Effect of rhizobia inoculation and seaweed extract (*Ecklonia maxima*) application on the growth, symbiotic performance and nutritional content of cowpea (*Vigna unguiculata* (L.) Walp.). *Frontiers in Agronomy* **5**, 1138263 (2023)
- [31] ABDALLAH, R. A. B., Ammar, N., Ayed, F., Jabnoun-Khiareddine, H., & Daami-Remadi, M. Single and combined effects of *Bacillus* spp. and brown seaweed (*Sargassum vulgare*) extracts as bio-stimulants of eggplant (*Solanum melongena* L.) growth: *Bacillus* spp. and *Sargassum vulgare* extracts as biostimulants of eggplant growth. *Advances in Horticultural Science* **35** (2021)

- [32] Crocker, T. W. (2018). *Evaluation of synergy between PGPR and seaweed extracts for growth promotion and biocontrol of Rhizoctonia solani on soybean*. Auburn University.
- [33] Nehra, V., Saharan, B. S., & Choudhary, M. Evaluation of *Brevibacillus brevis* as a potential plant growth promoting rhizobacteria for cotton (*Gossypium hirsutum*) crop. *SpringerPlus* **5**, 948 (2016)
- [34] Girish, N., & Umesha, S. Effect of plant growth promoting rhizobacteria on bacterial canker of tomato. *Archives of Phytopathology and Plant Protection* **38**, 235-243 (2005)

## **Chapter 5**

---

### **Conclusions**

The comprehensive findings of this study unveil valuable insights and intriguing possibilities for future research and application, notably in refining processes within microbial collections and expediting decision-making, thereby fostering the development of new and more effective biostimulant products.

The adoption of MALDI-TOF MS technology for rapid and accurate identification of unknown microbial strains marks a significant milestone. Its demonstrated success in reliably identifying strains not only accelerates screening processes but also identifies promising candidates for biostimulant development. As this technology progresses, bolstered by enhanced taxonomic resolution through statistical tools and enriched databases, its efficacy in exploring microbial biodiversity and taxonomic accuracy is poised for further enhancement.

Integrating MALDI-TOF MS proteomic analysis into microbial research workflows streamlines screening processes, hastens the discovery of new microbial-based products, and deepens our understanding of microbial biodiversity. Particularly noteworthy is the technology's ability to distinguish between closely related microbial strains, providing crucial insights into market diversification and facilitating research and development activities, prompt decision-making, and the formulation of targeted strategies.

Furthermore, the proposed screening and selection workflow proved to be an efficient approach for identifying promising PGPB for product development. The observed synergistic effects on plant growth promotion resulting from the combined application of microbial leads with algae extract underscore the diverse benefits of harnessing specific microbial strains and natural substances in biostimulant formulations.

The species-specific response of microbial leads to biostimulants emphasizes the importance of considering microbial specificity in formulation design. Future studies should delve deeper into understanding the metabolic pathways and genetic determinants influencing microbial responses to prebiotic compounds, facilitating the tailored selection of prebiotics for specific microbial strains. Additionally, extending the evaluation of synergistic interactions between promising microbial leads and natural substances to a broader range of crops, soil



types, and environmental conditions would provide valuable insights for optimizing biostimulant formulations across diverse agricultural contexts.

In conclusion, the integration of innovative technologies, such as MALDI-TOF MS, with targeted screening approaches and in-depth characterization of microbial strains holds immense promise for advancing the development of effective biostimulants.